Identification of α- Glucosidase Inhibiting Natural Products From *Macaranga capensis* and *Sapium integerrimum*

BY

AISHA MAJEED

A thesis submitted to the Faculty of Graduate Studies of

The University of Manitoba

In partial fulfillment of the requirements of the degree of

MASTER OF SCIENCE

Department of Chemistry

The University of Manitoba

Winnipeg, Manitoba

Canada

THE UNIVERSITY OF MANITOBA

FACULTY OF GRADUATE STUDIES

*****

COPYRIGHT PERMISSION

Identification of α- Glucosidase Inhibiting Natural Products From *Macaranga capensis* and *Sapium integerrimum*

BY

AISHA MAJEED

A thesis submitted to the Faculty of Graduate Studies of The University of Manitoba in partial fulfillment of the requirement of the degree

MASTER OF SCIENCE

Abstract

This thesis describes the results obtained from the phytochemical studies of *Macaranga capensis* and *Sapium integerrimum* as summarized below.

Chemical investigation on the α-glucosidase inhibiting crude methanolic extract of *Macaranga capensis* resulted in the isolation of two natural products: 3α-hydroxyaleuritolic acid 2-*p*-hydroxybenzoate (**86**) and 3-acetoxyoleanolic acid (**87**) which are related to the class of triterpenoids. Both natural products were isolated for the first time from this plant. The structures of these compounds were elucidated with the aid of NMR spectroscopic data. Both compounds were assayed against α-glucosidase inhibition. Compound (**86**) exhibited moderate activity in this bioassay with the IC_{50} value of 2.17mM. Whereas, compound (**87**) could not be tested as it was only soluble in chloroform and precipitated out in buffer solution. Phytochemical investigation on the ethyl acetate extract of *Sapium integerrimum* resulted in the isolation of three known compounds; phorbol ester 12-(2'-*N*-methylaminobenzoyl)-4*β*,5,20- trideoxyphorbol-13-acetate (**113**), Quercetin-3-*O*-α-rhamnopyranoside (**114**) and scopoletin (**115**). Compounds **113**, **114** and **115** showed good to moderate α-glucosidase inhibitory activity with the IC_{50} values of 0.57, 0.74 and 1.12 mM, respectively.

Acknowledgements

First of all, I would like to express my gratefulness to my Gracious Creator Allah (SWT) who gave me the wisdom to explore His creation. I am also very thankful to my graduate supervisor, Dr. Athar Ata for his continuous support and helped me to acquire a wealth of knowledge he has imparted onto me to be successful to complete this project. I would like to thank my committee members for evaluating me on yearly basis and reading my thesis for the final opinion about my work. I would also like to thank all the members of the Department of Chemistry at the University of Winnipeg, and University of Manitoba for their assistance. I appreciate the technical support provided by Mr. Ramin Vakili. I am indebted to all my past and present lab mates I had the opportunity to work with. Last but not least, I thank my mother whose sacrifices made me to achieve my goal, my husband; Farooq Shahzad and all of my kids, who understand me and letting me to complete this project.

TABLE OF CONTENTS

		Page
Abstract		iii
Acknowledgements		iv
List of Tables		viii
List of Figures		ix
List of Schemes		x
Glossary		xi
CHAPTER 1: Natural Products Chemistry		
1.1	Introduction	1
1.2	Natural Products in Drug Discovery and Their Pharmaceutical Applications	8
1.3	Classification of Natural products and Their Biosynthetic Pathways	10
1.3.1	Shikimic Acid Derived Natural Products	11
1.3.2	Biosynthetic Pathway of Flavanoids	12
1.3.3	Triterpenoid Natural Products	14
1.3.4	Bioactive Isolated Triterpenes	16
1.4	α-Glucosidase as a Potential Target in Type II Diabetes	17
1.4.1	α-Glucosidase, Mechanism of Action	22
1.5	Molecular Docking	24
1.6	References	25

CHAPTER 2: Phytochemical Investigation of *Macaranga capensis*

2.1 Introduction 30

2.2 Results and Discussion 37

2.2.1 Structure Elucidation of Compounds (**86** and **87**) 38

2.2.1.1 3α-Hydroxyaleuritolic acid 2-*p*-hydroxybenzoate (**86**) 39

2.2.1.2 3-Acetoxyoleanolic acid (**87**) 42

2.2.1.3 α-Glucosidase Inhibitory Activity of Compound (**86**) 45

2.2.1.4 Molecular Docking 46

2.3 Experimental 47

2.3.1 General Experimental Conditions 47

2.3.1.1 Spectroscopy 47

2.3.1.2 Chromatographic Supplies 47

2.3.1.3 Bioassay Supplies 47

2.3.2 Plant Material 48

2.3.3 Extraction and Isolation 48

2.3.4 Assay for α-Glucosidase Inhibition 50

2.3.5 Molecular Docking 51

2.4 References 51

CHAPTER 3: Phytochemical investigation of *Sapium integerrimum*

3.1 Introduction 54

3.2 Results and Discussion 61

3.2.1 Structure Elucidation of Compounds **(113-115)** 62

3.2.1.1 12-(2'-*N*-methylaminobenzoyl)-4*β*,5,20-trideoxyphorbol-13-acetate (**113)** 62

3.2.1.2 Quercetin-3-*O*-α-rhamnopyranoside (**114**) 66

3.2.1.3 Scopoletin (**115**) 69

3.2.1.4 α-Glucosidase Inhibitory Activity of Compounds (**113-115**) 71

3.2.1.5 Molecular Docking 72

3.3 Experimental 75

3.3.1 General Experimental Conditions 75

3.3.2 Plant Material 75

3.3.3 Extraction and Isolation 75

3.3.4 Assay for α-Glucosidase Inhibition 77

3.3.5 Molecular Docking 77

3.4 References 78

4 Conclusion 81

Appendix 82

LIST OF TABLES

Page

Table 2.1. Anti α-glucosidase, anti xanthine oxidase and antimicrobial activities against *E. caratovora* of compounds **60-64**. 30

Table 2.2. ^{1}H and ^{13}C NMR spectroscopic data for **86** and $^{1}H/^{13}C$ one-bond shift correlations, as determined by HSQC. 40

Table 2.3 ^{1}H and ^{13}C NMR chemical shift assignments for **87** and $^{1}H/^{13}C$ one-bond shift correlations of hydrogen bearing carbons, as determined by HSQC. 43

Table 3.1 Cytotoxicity and anti-mycobacterial inhibitory activities of compounds (**108-112**). 58

Table 3.2 ^{1}H and ^{13}C NMR data for **113** and $^{1}H/^{13}C$ one-bond shift correlations as determined by HSQC. 62

Table 3.3 ^{1}H and ^{13}C NMR data for **114** and $^{1}H/^{13}C$ one-bond shift correlations as determined by HSQC. 65

Table 3.4 ^{1}H and ^{13}C NMR data for **115** and $^{1}H/^{13}C$ one-bond shift correlations as determined by HSQC. 68

Table 3.5 Docking scores (kcal/mol) and key interactions of compound **113-115** and acarbose in the α-glucosidase enzyme. 69

Table 4.1. Results of the α-glucosidase inhibition assay on compounds **86** and **113-115** isolated from *M. capensis* and *S. integerrimum*, respectively. 77

LIST OF FIGURES

	Page
Figure: 2.1% Inhibitory activity of compound (**86**) and acarbose.	44
Figure: 2.2 Binding of compounds **86** in the binding sites of α-glucosidase enzyme.	45
Figure: 3.1 % Inhibitory activity of compounds **113-115** and acarbose.	69
Figure: 3.1 Binding interactions of compound **113** (**A**), **114** (**B**), **115** (**C**) and acarbose (**D**) in α-glucosidase enzyme.	70

LIST OF SCHEMES

Page

Scheme 1.1 Biosynthesis of shikimic acid and scopoletin (**115**) 12

Scheme 1.2 Biosynthesis of Quercetin-3-*O*-α-rhamnopyranoside (**114**) 13

Scheme 1.3 Biosynthesis of triterpene and 3-acetoxyoleanolic acid (**87**) 16

Scheme 1.4 A Configuration retaining enzyme-mediated glycosidase hydrolysis 23

Scheme 1.4 B Configuration inverting enzyme-mediated glycosidase hydrolysis 23

GLOSSARY

α-Glucosidase enzyme	Alpha glucosidase enzyme presents in the brush border of small intestine and is responsible for the hydrolysis of polysaccharides.
^{1}H-NMR spectrum	Proton Nuclear Magnetic Resonance: Depicts the electronic environment of proton atom in a molecule.
^{13}C-NMR spectrum	Carbon Nuclear Magnetic Resonance: Depicts the electronic environment of carbon atoms in a molecule.
COSY spectrum	Proton-Proton Correlation Spectroscopy: Provides geminal and vicinal couplings of protons
DEPT spectrum	Distortionless Enhancement by Polarization Transfer: Helps to differentiate between, methyl, methylene, and methine and quaternary carbons.
APT spectrum	Attached Proton Test: Used to differentiate between methyl, methylene, and quaternary carbons.
EIMS	Electron Impact Mass Spectrum: high energy electrons are used to form a radical cation of the molecular species.
TOCSY spectrum	The Correlation Spectroscopy: Provides long-range proton couplings
HMBC spectrum	The Heteronuclear Multiple-Bond Correlation Spectroscopy: Displays J_2, J_3 and occasional J_4 proton-the heteronuclear correlations

	over 2–4 bonds.
IC_{50}	The concentration required to inhibit 50% of the activity of enzyme function.
TLC	Thin layer chromatography
NOESY spectrum	Nuclear Overhauser Effect Spectroscopy: Displays proton-proton correlation through space.
$CDCl_3$	Deuterated Chloroform: Solvent used for NMR spectroscopy.
IR spectrum	Infrared Spectroscopy: Used to determine the functional groups of the compounds based on their absorption.
ROESY spectrum	Rotating-frame Overhauser Effect Spectroscopy:Depicts 2D proton-proton correlations through-space proximity.
UV spectrum	Ultraviolet Spectroscopy: Provides information about chromospheres
HSQC spectrum	The Heteronuclear Single Quantum Coherence: Provides ^{1}H/ ^{13}C one bond correlation of proton bearing carbons.

CHAPTER 1

Natural Products Chemistry

1.1 Introduction

Natural products are organic compounds, produced by living organisms including plants, marine organisms, insects and microorganisms. These compounds are classified as primary and secondary metabolites.[1] Primary metabolites are the building blocks of a living system. The representative examples include amino acids, carbohydrates, fatty acids, deoxy ribose nucleic acid (DNA), ribose nucleic acid (RNA) etc. While, the secondary metabolites are produced using primary metabolites as precursors and help the living system to survive in the competitive environment. These living organisms including plants, marine organisms and microorganisms use them for their defence from predators and pathogens. Secondary metabolites, also known as natural products, have diverse structures that are difficult to achieve through chemical synthesis. These compounds exhibit various biological activities; including, anti-diabetic, anti-hypertensive, anti-fungal, anti-oxidant, anti-cancer etc.[2] Due to these properties natural products are considered as important source for providing lead bioactive compounds in drug discovery programs.

Ever since mankind started to live on earth, they have been challenged to cure different kinds of diseases, like snakebites, fever and pain etc. Therefore, they started to use different herbs, animals and mineral products to relieve pain. For instance, palaeoanthropological studies at the cave site of Shanidar, located in the Zagros Mountains of Kurdistan in Iraq suggested that more than 60,000 years ago, Neanderthals might have been aware of the medicinal properties of various plants, as evidenced by

pollen deposits in one of the graves at the site.[3] Similarly, the Chinese have been using these products either a single agent or their combinations for health related problems for more than 4000 years.[4] This is evidenced from the records in Chinese Materia Medica. This publication documented 52 prescriptions dating as far back as 1100 BCE. Hippocrates (460-377 BC) and Aristotle (38-322 BC) are considered to have developed the European healing system; from the imprints of ancient Indian and Egyptian health core systems.[5-6] In 100 AD, a Greek physician Dioscorides wrote a world famous book "De-Materia Medica", in which he recorded the collection, storage and use of medicinal herbs. This became the base and standard reference in European herbal system for more than 1000 years.[7]

These health related remedies were not only limited to China and European countries, but were practiced in Egypt as well. One Egyptian medical papyrus of herbal knowledge is the “Eber Papyrus” which contains over 700 prescriptions mostly derived from plants, and is dated back approximately 1500 BCE.[8] Similarly, the ancient Indian ayurvedic medicinal system is recorded earlier than 1000 BCE. It is believed that the origin of this ayurvedic medicinal system was developed by a religious and ritualistic person, Brahma,[9] and then it was transferred directly to Daksha Prajapati in the form of shloka sung.[10] In ayurvedic medicinal system, *Azadirachta indica* (neem), *Centella asiatica* (gotu kola), *Cinnamomum camphora* (camphor) and *Withania somnifera* (aswargandha) were the commonly used plants.[11] It is also reported that during 1900 to 400 B.C Assyrian, and Sumerians described hundreds of herbal formulations on nearly 660 clay tablets for thousands of medicinal plants.[12-13]

Plants have long lasting history in the health care system. The three main reasons for selecting plants for health care are: (**1**) the abundance and easy access to plants that reduces the discovery time period. (**2**) Reduced level of collection risk and (**3**) no professional training required to collect plant samples as opposed to oceanic products. Plant based pharmaceuticals started during 3rd century. Theophrastus; the philosopher and natural scientist, disclosed that opium poppy juice had analgesic property, and later in 10th century A.D. Rhazes (Persia) introduced opium pills for cough, aches, mental disorders and pains. The potent ingredients in opium poppy, *Papaver somniferu,* are morphine (**1**) and codeine (**2**). These compounds are still used as pain killers. Morphine (**1**) was isolated for the first time by a German pharmacist F. W. A. Serturner in 1816.[14-15] Then it was synthesized and made commercially available by M. Gates, and G. Tschudiin in 1952.[16] Similarly, East Asians and the Greek communities were using *Hyoscyamus niger*, commonly known as henbane or stinking night shade which contains scopolamine (**3**), as a tranquilizer. It is also reported that the Andean Mountain natives chewed coca leaves, containing cocaine (**4**) as an active stimulant and euphoric ingredient. Moreover, ancient Indians extracted an antihypertensive drug, reserpine (**5**), from Indian snakeroot or devil pepper, *Rauwolfia serpentine* plant, and were using it to treat vigilance, hysteria and hypertension.[13]

After the discovery of morphine one of the most important drug aspirine (**6**) was structurally modified in 1897 by A. Eichengrun and F. Hoffman at Bayerin Germany based on the natural product salicin found in meadowsweet flower and willow leaf tea.[10,16] All these discoveries and syntheses introduced a new branch of organic chemistry named as natural product chemistry. This branch is still playing an active role

in producing pharmaceutical candidate molecules to the drug discovery industry.

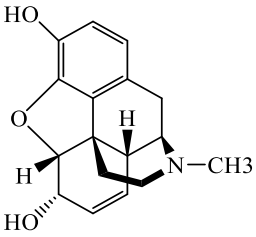

(**1**)

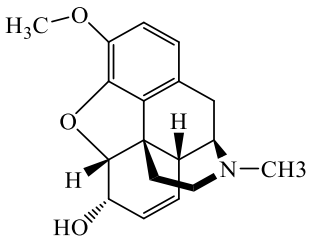

(**2**)

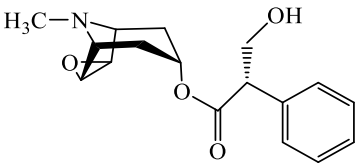

(**3**)

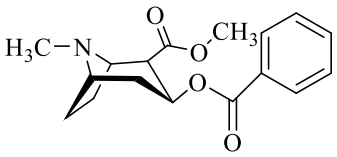

(**4**)

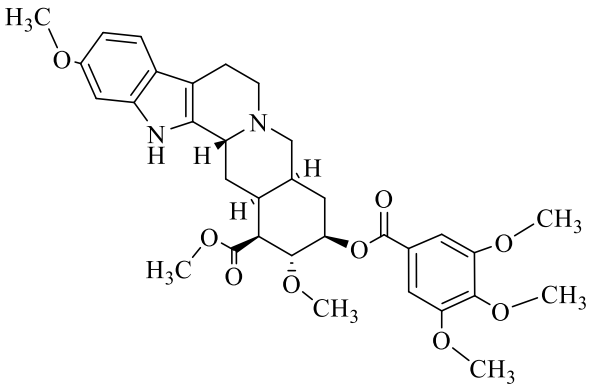

(**5**)

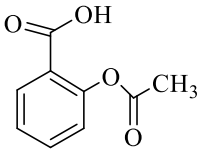

(**6**)

Researchers have isolated lead bioactive compounds from various natural sources including animals, microbes and marine organisms. Currently, over 50% of pharmaceuticals available in the market are of natural products and 25% of these pharmaceuticals are of plant origin. It is mainly due to the reason that higher plants

produce a wide variety of different bioactive compounds. These compounds are responsible for various medicinal properties. These plants play a pivotal role in primary health care of 80% of the world's population.[10] About 25% of U.S. prescriptions dispensed presently contain active ingredients derived from plants, while 13.3% and 2.7% are derived from microbial and animal sources, respectively.[17-19] Recent studies indicates that only 5% of plants have been investigated, but Business Communications Company (BCC) research report indicated that the global plant-derived drug market was valued at US$ 22.1 billion in 2012, and it is projected to grow to US$ 39.6 billion by 2022.[9]

These reports includes that a large portion of plants is still unexplored. There are a number of plant-derived drugs that are available in the market for curing different diseases. For example, artemisinin (qinghaosu) (**7**) was isolated from the aerial portion of *Artemisia annua* commonly known as sweet worm wood in 1972 by a Chinese scientist Tu Youyou and the structure was established in 1979 as a sesquiterpenoid. This herb actually is a Chinese folk medicine which has been in use thousands of years for treating malaria like symptoms.[20-22] For this discovery Nobel Prize was awarded for the first time in the area of natural products. It has been estimated that more than 2000 malaria patients has been cured by using this antimalarial agent, as this drug has the efficacy against *Plasmodium vivax, Plasmodium falciparum* and chloroquine-resistant.[22-23] Among the artemisinin derivatives, aretemether (**8**), artesunate (**9**) , dihydroartemisinin (**10**) are the most frequently used drugs in clinical practices. [24]

Another Chinese herb *Ephedra sinica,* (ma huang) based on ethnomedicine was explored for the pharmaceutically active compounds. It has the major bio-active

component (-) ephedrine (**11**) and (+) pseudoephedrine (**12**) which were isolated in 1887.[24-25] Both of these compounds became the basis for the synthesis of anti-asthma agents (beta agonists) salbutamol and salmeterol.[14] Researchers and chemists have established that *Galbulimima belgraveana*, a member of the Himantandraceae family contains a number of alkaloids: himbacine (**13**), himbeline (**14**), himandravine (**15**), himgravine (**16**), himbosine (**17**), himandrine (**18**) and himgaline (**19**). Among of these, himbacine (**13**) has been approved by the US Food and Drug Administration (FDA) [26-27] as antithrombotic and antispasmodic candidate for cardiovascular diseases.[24] Cobbin and Thorp in 1957 suggested that himandrine (**18**) is responsible for suppressing the sympathetic centers of the hypothalamus. However, when Smith, Kline and French (SKF) pharmaceutical company extended the research on himandrine and other alkaloids they found that among all of those, himbacine (**13**) is the most active, and the most significant activities of himbacine are the cardiovascular and the antispasmodic. As an antispasmodic it is similar to atropine (**20**) but is less potent.[26] Once the lead compounds are isolated and approved for clinical benefits researchers try to find the way for getting those compounds to fulfill the envisioned roles. So, synthetic chemistry is used to design and develop the lead compound. Based on the molecular template of natural product himbacine (**13**) vorapaxar (**21**) was synthesized which is a PAR-1 thrombin receptor and is currently undergoing phase- III clinical trials for Acute Coronary Syndrome (ACS) and Coronary Artery Disease (CAD) events. Patients with ACS and CAD also suffer from hypertension, angina and type II diabetes.[28-29]

Scientists not only develop one kind of analogue; instead they formulate a number of analogues to see which has the better efficacy. For example, in developing himbicine

analogues, chemists not only synthesized vorapaxar (**21**), but also synthesized a series of analogues, which showed excellent antithrombic activity. But when those were given in vivo during clinical trial it was observed that these had poor water solubility (<2 μM).[30]

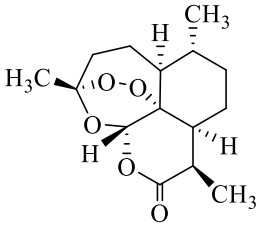

(**7**)

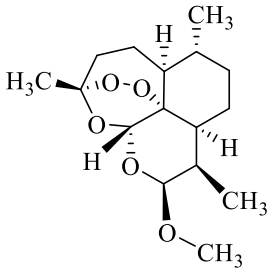

(**8**)

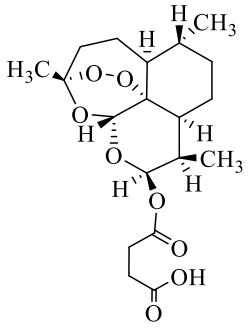

(**9**)

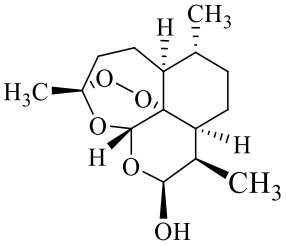

(**10**)

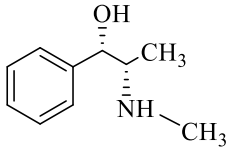

(**11**)

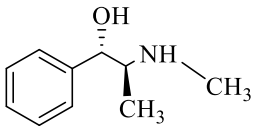

(**12**)

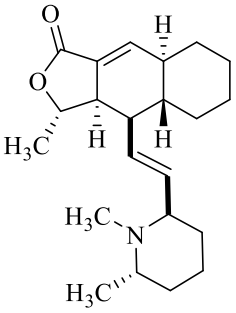

(**13**)

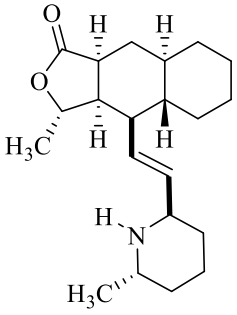

(**14**)

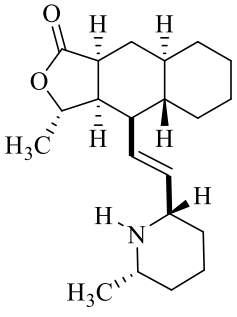

(**15**)

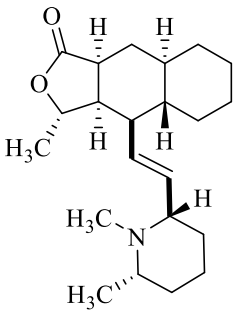

(**16**)

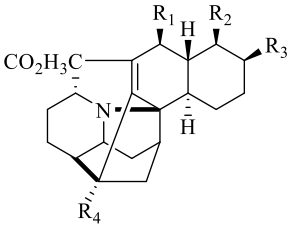

	R1	R2	R3	R4
(**17**)	OAc	OCOPh	OAc	OAc
(**18**)	OBz	OCH3	H	OH
(**19**)	OH	H	H	OH

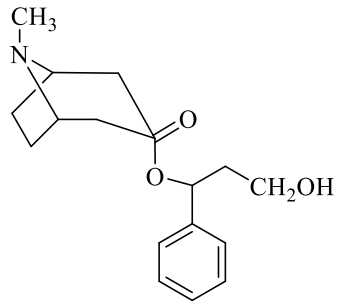

(**20**)

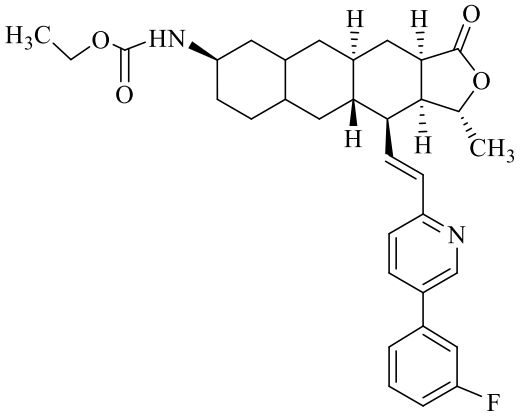

(**21**)

1.2 Natural Products in Drug Discovery and Their Pharmaceutical Applications

Natural products have played a significant role in providing lead compounds for drug discovery. Until 2013, the US food and drug administration (FDA) had approved nearly 1453 new chemical entities out of which 40 % were either natural products or natural products-inspired (semi-synthetic natural products derivatives, synthetic compounds based on NP pharmacophores, or NP mimics).[31] Moreover, 74% of the 119 currently most important drugs in USA contain active ingredients from ethnomedicinally

important plants, while 25% of all prescriptions dispensed presently contain an active ingredient derived from plants. In the last two-decades, records of natural products show that 16.4% of newly launched drugs are derived directly from natural products, and 12% have been designed based on natural products.[24] It is also reported that 87% of all human ailments including cancer, bacterial and viral infections, influenza, brain tumour, kidney and liver infections etc., have been treated by natural product based drugs.[32]

In the 20th century, natural products had to scale back in the drug discovery screening program due to the introduction of combinatorial chemistry; initially focusing on the synthesis of peptide and oligo-nucleotide libraries, but then shifting to synthesis of small drug-like molecules. As a result, many pharmaceutical companies have deemphasized natural products research in favor of high-throughput screening of mass-produced combinatorial libraries for the identification of new lead compounds. Compared to natural products screening and isolation, where fewer compounds could be isolated over a long time of period, combinatorial chemistry can provide thousands of compounds in a short period of time.[33] It was developed in 1980s with Geysen's multi-pin technology and Houghten's tea-bag technology to produce thousands of compounds.[34-35] Although combinatorial chemistry is easy and fast to provide the molecules with high chemical structural diversity, and specific biological activities this method was not successful in some of the therapeutic areas such as anti-infective, immunosuppressive and metabolic ailments.[33] Through this strategy until now only one *de novo* compound has been discovered as a drug, sorafenib (**22**) whose trade name is Nexavar 1. In 1994, with the collaboration of Bayer and Onyx pharmaceuticals, sorafenib (**22**) was discovered. It has tumour growth-inhibitory effects which could be

attributed to inhibition of angiogenesis and tumorigenesis. In December 2005, sorafenib (**22**) was approved as a renal cell carcinoma (RCC) treatment as well by FDA, and it is also in trial for approval against thyroid cancer.[31]

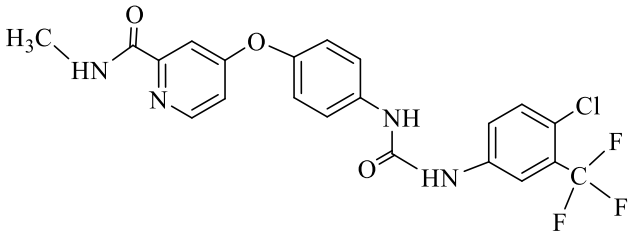

(**22**)

1.3 Classification of Natural products and Their Biosynthetic Pathways

Natural products can be derived from different sources such as plants, microorganisms, fungi, animals and even insects. These compounds can be classified into different classes based on their structural features and biosynthetic origins. The origin of natural products can be traced to key intermediates of primary metabolism. These intermediates include acetyl–CoA (**23**), shikimic acid (**24**) and mevalonic acid (**25**).[36]

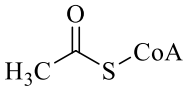

(**23**)

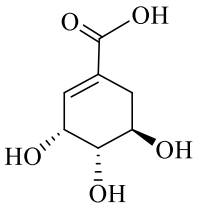

(**24**)

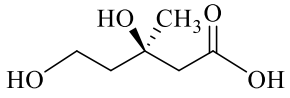

(**25**)

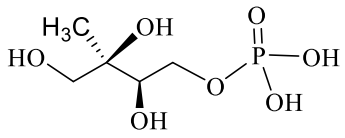

(**26**)

Acetyl CoA is a precursor for polyketide type of molecules, whereas shikimic acid (**24**) is responsible for the production of aromatic secondary metabolites, e.g. lignens and flavonoids. Mevalonic acid (**25**) is a key molecule for the biosynthesis of terpenoids and steroids; and can be derived from either acetyl CoA (**23)** or methylerythritol phosphate (MEP) (**26**). MEP itself is derived from the decarboxylation of pyruvic acid in the prescence of co-factor thiamine pyrophosphate. Subsequent attack on glyceraldehydes 3-phosphate will generate the co-factor and produce MEP.[37] This thesis will demonstrate the isolation of flavonoids and terpenoids. So the biosynthesis of the relevant secondary metabolites will be focused

1.3.1 Shikimic Acid Derived Natural Products

Shikimic acid is a precursor of aromatic compounds i.e. flavonoids and lignins. Shikimic acid is produced by the coupling of phosphoenolpyruvate (PEP) (**27**) and D-erythrose 4-Phosphate (**28**) to form an intermediate 3-deoxy-D-arabino-heptulosonic acid 7-phosphate (**29**), which leads to the synthesis of shikimic acid (**30**).[36]

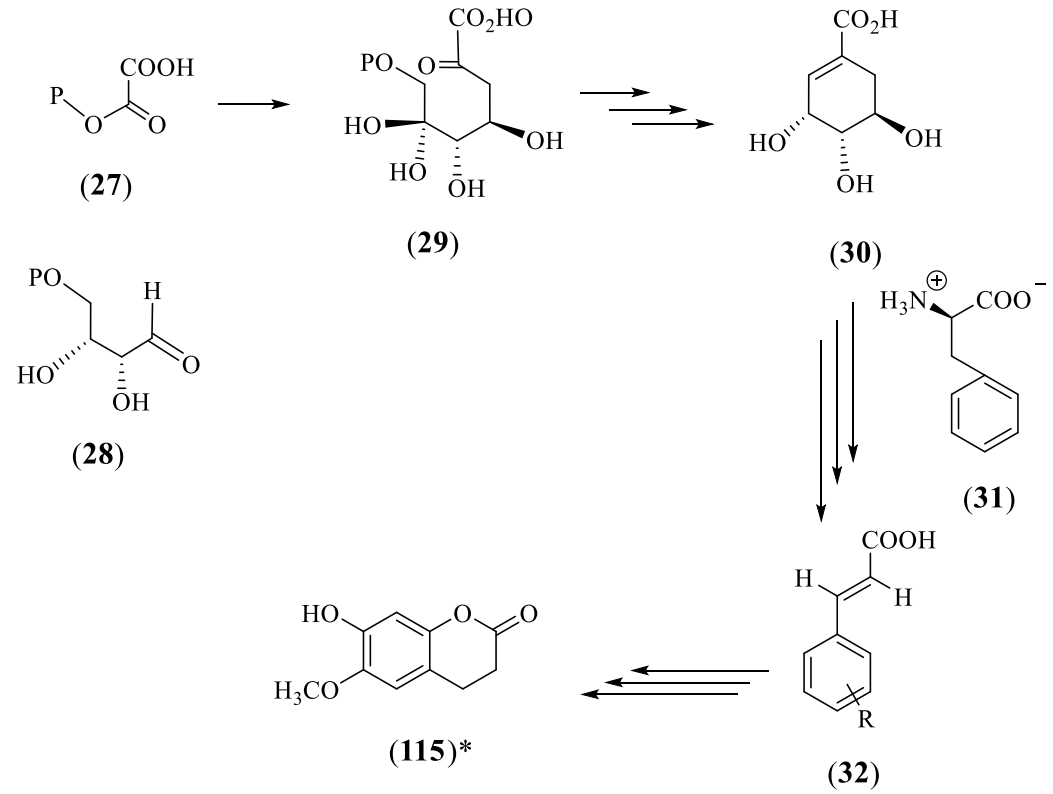

* This compound was isolated from *S. integerrimum.*

Scheme 1.1 Biosynthesis of shikimic acid and scopoletin (**115**)

The biosynthesis of scopoletin is complex and is not well understood. Shikimic acid (**30**) is converted into E-cinnamate (**32**) in the prescence of L- phyneylalanin (**31**). This (**32**) is converted into scopoletin (**115**). The process is shown in **scheme 1.1**.[38]

1.3.2 Biosynthetic Pathway of Flavanoids

In the presence of acetyl Co-A, E-cinnamate (**32**) is converted into chalcone (**35**), which in the presence of chalcone isomerase converts chalcone into quercitin (**36**). In the presence of UDP- rhamose, quercitin (**36**) is converted into quercetin-3-*O*-α-rhamnopyranoside (**114**).[39] Scheme **1.2** shows the process below.

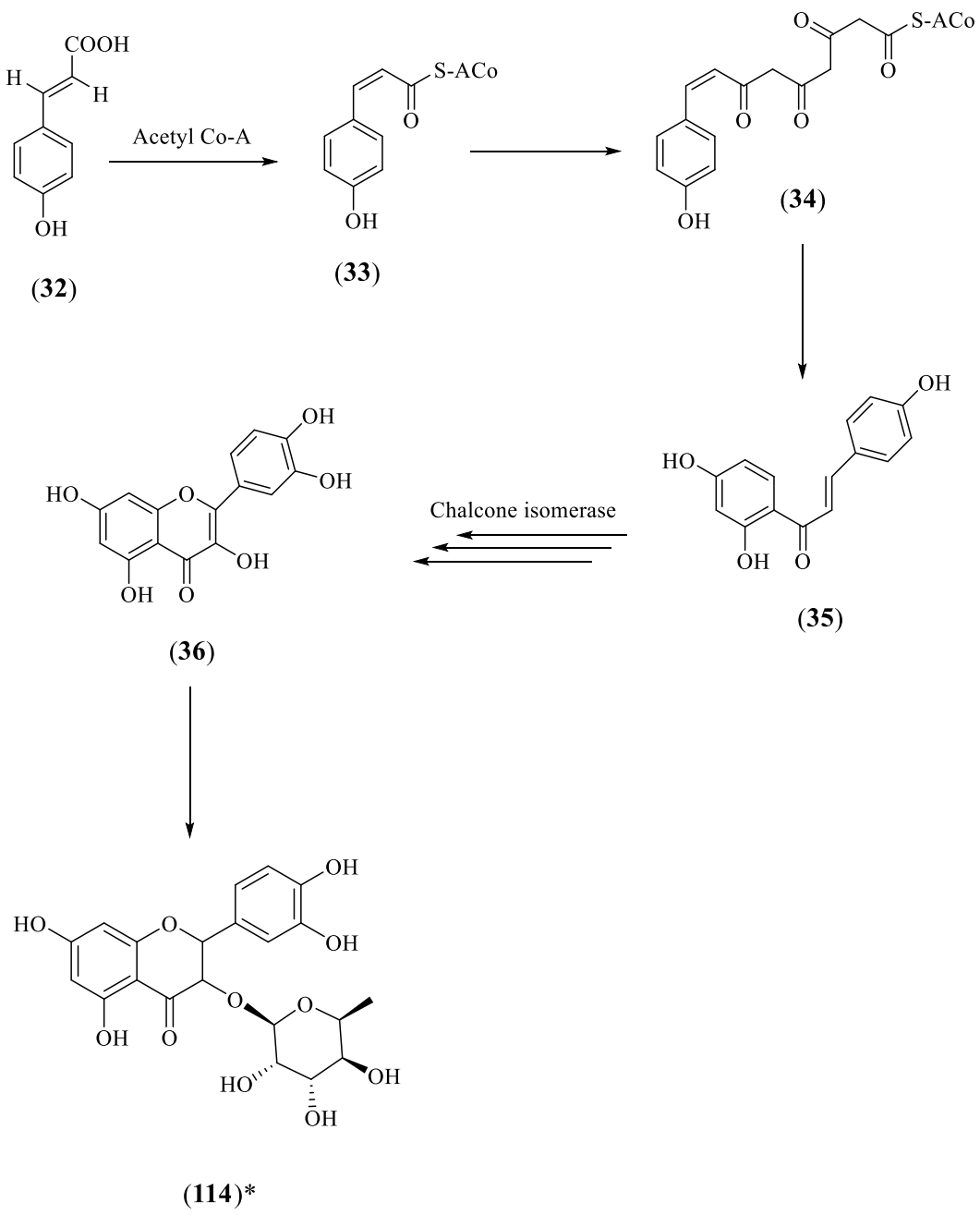

(**32**) (**33**) (**34**) (**35**) (**36**) (**114**)*

* This compound was isolated from *S. integerrimum*

Scheme 1.2 Biosynthesis of Quercetin-3-*O*-α-rhamnopyranoside (**114**)

1.3.3 Triterpenoid Natural Products

For the biosynthesis of triterpenoids, two isoprene units, dimethyl allyl PP (DMAPP) (**37**) and isopentyl PP (IPP) (**38**) are the basic units of the terpene family. They could be biosynthesized either by the de-oxyxylulose pathway, or by the mevalonate pathway as represented in **Scheme 1.2** when these two isoprene units joint in a head to tail fashion giving farnesyl pyrophosphate (FPP) (**39**), which on joining with another FPP molecule in a tail to tail fashion gives squalene (**40**). It further oxidises into 2,3- squalene (**41**), which undergoes successive Wagner-Meerwein 1,2- hydride and methyl shifts to yield lanosterol (**42**) in animals and fungi and *β*-amyrin (**43**) in plants. *β*-amyrin (**43**) undergo further oxidation to produce 3-acetoxyoleanolic acid, as shown in **scheme 1.3**.[40]

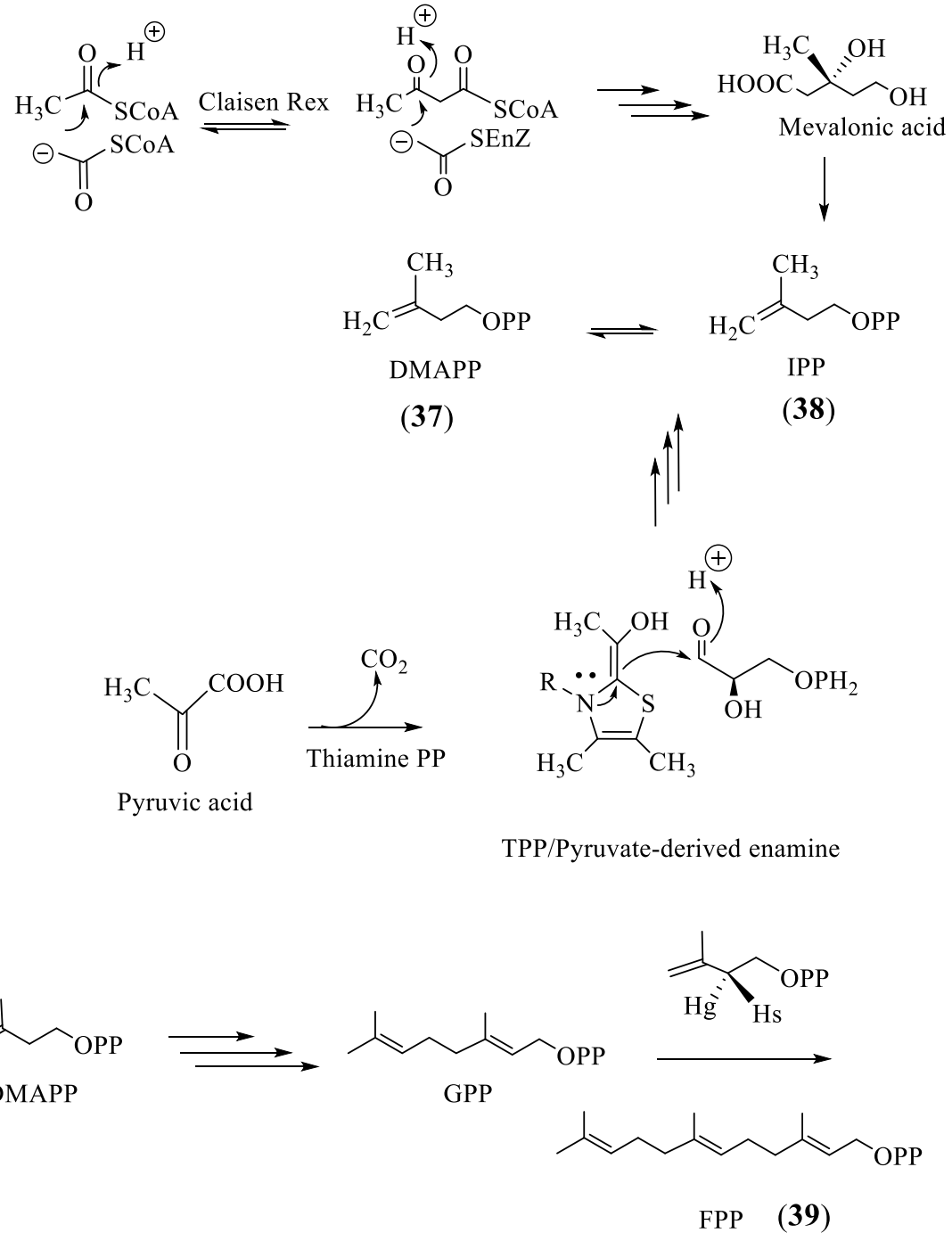
Claisen Rex
Mevalonic acid
DMAPP
(37)
IPP
(38)
Pyruvic acid
Thiamine PP
TPP/Pyruvate-derived enamine
DMAPP
GPP
FPP (39)

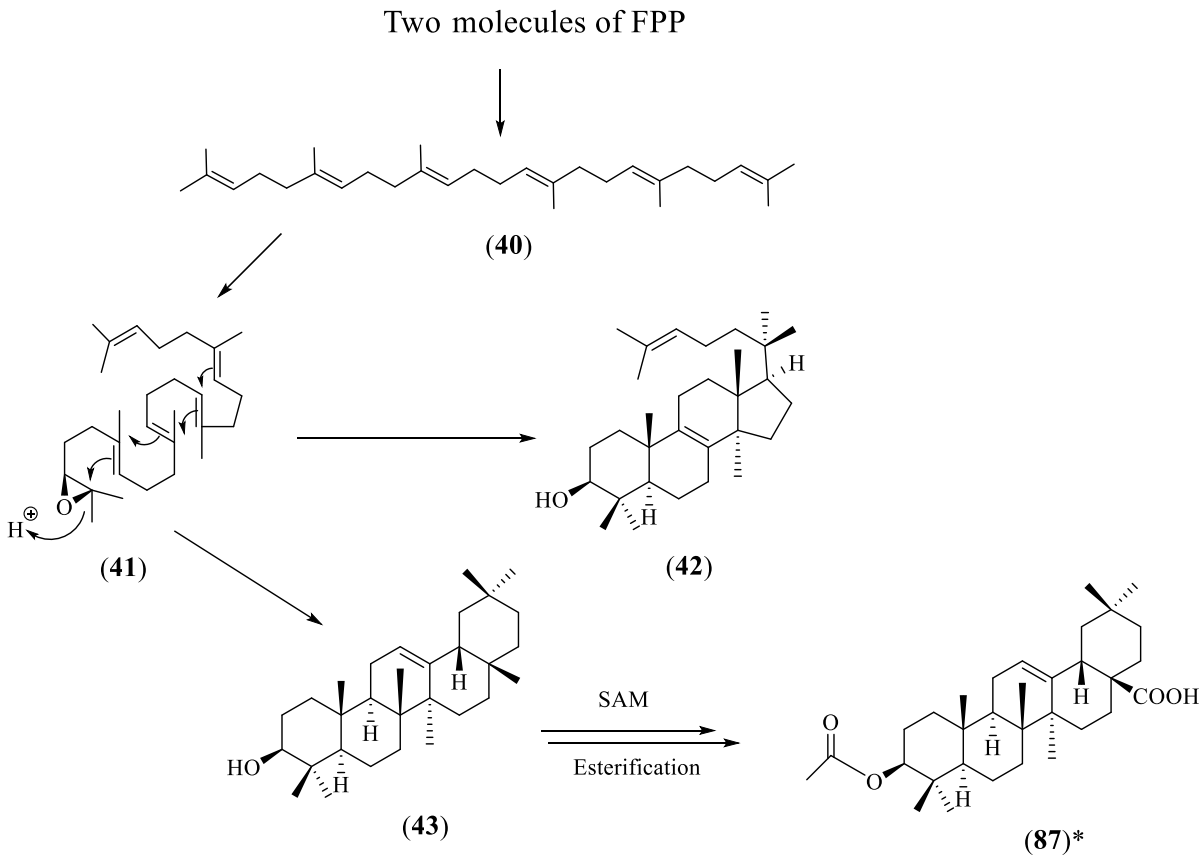

* This compound was isolated from *M. capensis*

Scheme 1.3 Biosynthesis of triterpene and 3-acetoxyoleanolic acid (**87**)

1.3.4 Bioactive Isolated Triterpenes

Phytochemical investigation on *Rhododendron latoucheae* led to the isolation of 2*α*,3*α*,24-trihydroxy-urs-12,18-diene-28-oic acid (**44**), 19*α*,30-dihydroxy-2,3-seco-urs-12-ene-2,3,28-trioic acid 3-methyl ester (**45**),[41] Rhodoterpenoid A (**46**), Rhodoterpenoid B (**47**) and Rhodoterpenoid D (**48**)[42] by hyphenated technique HPLC–MS–SPE–NMR. These showed potent activity against herpes simplex virus-1 (HSV-1 F strain VR 733)

with the IC_{50} values of 8.62 ± 0.5, 33.33 ± 2.5, 14.62 ± 1.3, 8.62, >33.33 and 6.87 μM, respectively. Acyclovir was used as a positive control with the IC_{50} of 0.41 μM.

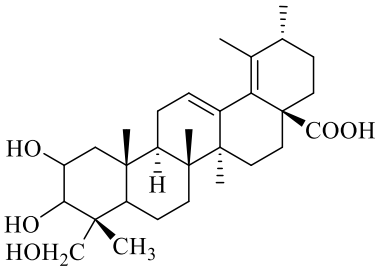

(**44**)

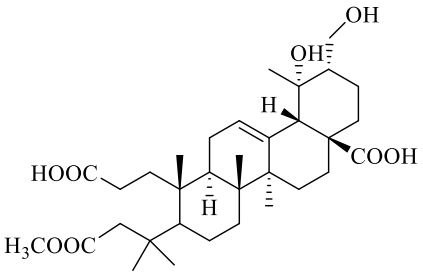

(**45**)

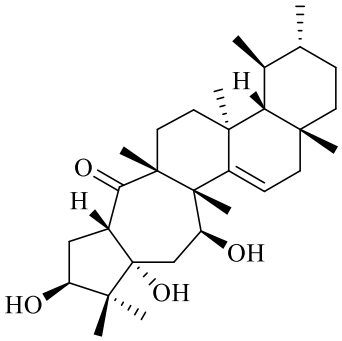

(**46**)

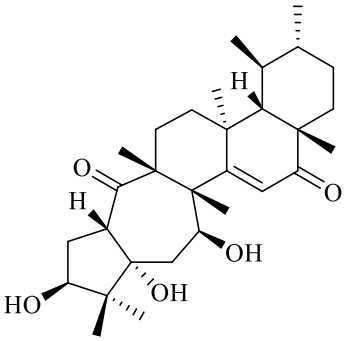

(**47**)

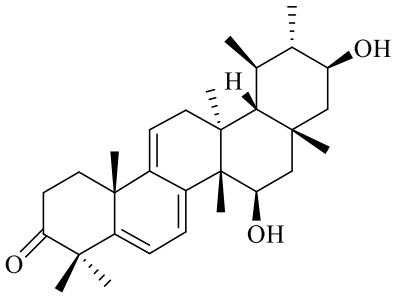

(**48**)

1.4 *α*- Glucosidase as a Potential Target in Type II Diabetes

Diabetes mellitus is a complex metabolic disorder in the endocrine system characterized as type I and type II diabetes. These are based on the abnormalities in

insulin secretion (type I diabetes) or insulin action (type II diabetes). Type I diabetes can be cured by injecting insulin artificially; whereas type II diabetes is somewhat complicated to cure. This disease is a major public health problem worldwide and is rapidly becoming more common**.** It is documented that there are nearly 350 million adults suffering from diabetes, among which 90% of the patients have type II diabetes. [43] In 2017, it was estimated by the International Diabetes Federation (IDF) that nearly 4 million deaths happened because of type II diabetes, and it is growing with the years passing. The World health Organization (WHO) estimates that the affected number of people will increase up to the limit of 470 million by 2030 mostly in low to middle income countries.[43] The main cause of type II diabetes is the over expression of α-glucosidase activity and hydrolyzing polysaccharides into monomers, which causes the hyperglycemia. One of the therapeutic approaches for decreasing postprandial hyperglycemia (PPHG) is to minimize the absorption of glucose via reducing the activity of α-glucosidase. This enzyme is located in the brush border of the small intestine and is required for breaking down of carbohydrates to the monomeric form of saccharides such as glucose, fructose etc.[44-46] As a result, the blood glucose level increases and causing postprandial hyperglycaemia.

One of the methods for avoiding type II diabetes is minimizing the activity of α-glucosidase by using different kinds of inhibitors. These inhibitors delay the absorption of ingested carbohydrates, thereby reducing the postprandial hyperglycemia. Therapy of type II diabetes relies on different approaches intended to reduce hyperglycemia. These include **1**) sulfonylureas (SU), which increase insulin release from pancreatic islets. **2**) metformin, which acts to reduce hepatic glucose production. **3**) thiazolidinediones

(TZD), which enhance insulin action. **4**) glucagon-like peptide-1 (GLP-1) receptor agonists, which slow down gastric emptying, and reduction of postprandial glucagon and of food intake. **5**) α-glucosidase inhibitors, which interfere with gut glucose absorption. Our study is limited to α-glucosidase inhibitors; so only those inhibitors will be discussed. Currently, there are only three recognized drugs available in the market that belong to the class of α-glucosidase inhibitors (AGI); acarbose (**49**), miglitol, (**50**) and voglibose (**51**) recognized as the trade names glucobay, diastabol and basen respectively. These are used in the market for the treatment of type II diabetes.[47]

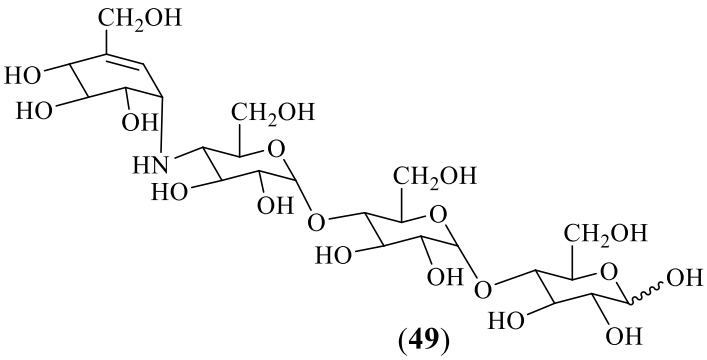

(**49**)

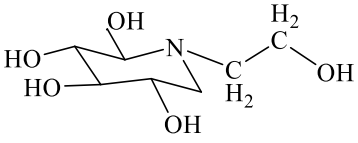

(**50**)

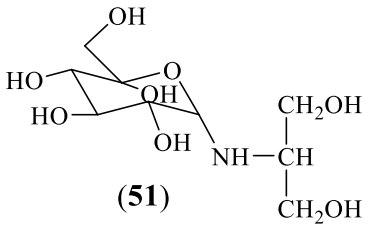

(**51**)

As a class all of the above mentioned drugs of AG inhibitors have the same mechanism of action with differences in their enzyme inhibitory profile. For instance, the inhibitory activity of miglitol and voglibose on pancreatic α-amylase is much weaker

than that of acarbose. However, the inhibitory effect of voglibose on maltase and sucrase is 190 to 270 times greater than that of acarbose, whereas acarbose has 65% inhibitory effect on sucrase and maltase 60% inhibitory effect.[48] There are a number of side effects of these AGIs, out of which gastrointestinal effects including flatulence, diarrhea, and abdominal discomfort are the major problems.[47] Due to aforementioned side effects of AGIs research efforts have been intensified to isolate and synthesize different molecules with higher efficacy and lower side effects. The search has led the researchers to identify a number of compounds belonging to different classes that could be the candidates for α-glucosidase inhibition. For example, compounds kaempferol (**52**), kaempferol-3-*O*-β-D-glucopyranoside (**53**), kaempferol-3-*O*-rutinoside (**54**) and 3,5-dicaffeoylquinic acid methyl ester (**55**), were isolated from *Gynura medica* Leaves.[49] Their α-glucosidase inhibitory activities (IC_{50}) are 1.67± 0.03 mg/ml, 1.46± 0.03 mg/ml, 0.38± 0.03 mg/ml and 0.53 ± 0.02 mg/ml of (**52**), (**53**), (**54**) and (**55**), respectively. Similarly, *Morus alba*commonly known as Mulberry showed a potent activity against α-glucosidase. The prenylated compounds isolated from this plant namely chalcomoracin (**56**), moracin C (**57**)**,** moracin D (**58**) and moracin N (**59**) exhibited a significant degree of α-glucosidase inhibitory activity with IC_{50} of 2.59 ± 0.24, 4.04± 0.84, 2.54± 0.40 and 2.76± 0.35 μM, respectively.[45]

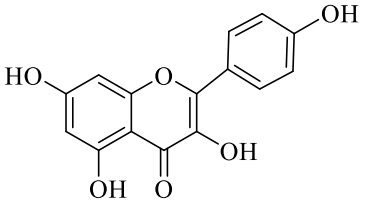

(**52**)

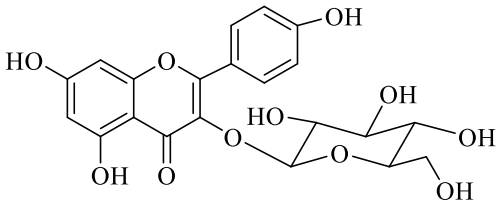

(**53**)

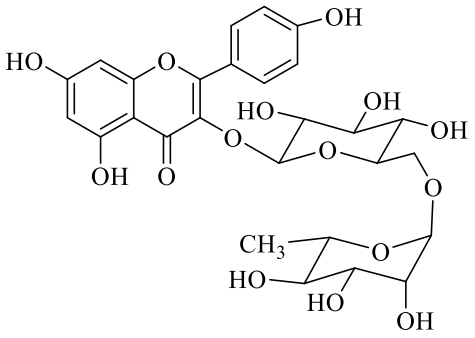

(**54**)

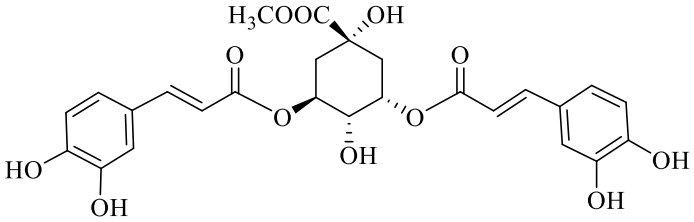

(**55**)

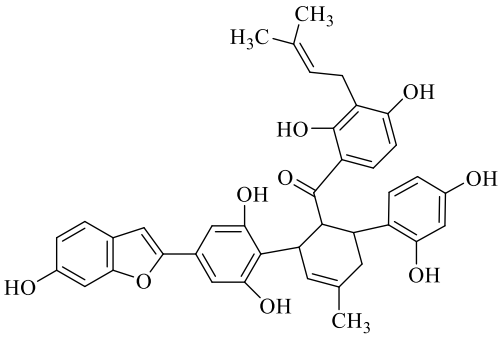

(**56**)

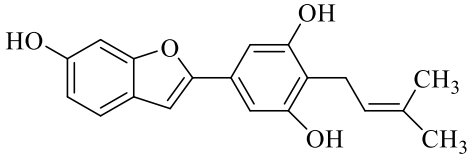

(**57**)

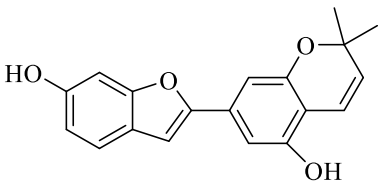

(**58**)

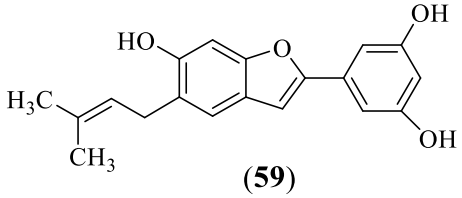

(**59**)

1.4.1 α- Glucosidase, Mechanism of Action

α-Glucosidase enzyme catalyzes the removal of the terminal glucose residue from the non-reducing end from their respective substrates.[50] In course of carbohydrate metabolism it catalyzes the hydrolysis of the α (1,4) glycosidic bonds found in oligosaccharides, resulting the removal of individual glucose residues from the chain and the individual glucose residue get absorbed into the bloodstream.[51-52] This enzyme is of particular interest because it's over expression of activity plays a main role in type II diabetes. The inhibition of this enzyme can reduce the rate at which oligosaccharides are broken down, resulting in a lower rate of glucose absorption by the small intestine, to produce an overall lower blood glucose concentration and avoidance of hyperglycemia. This control of hyperglycemia does not require supplementation of insulin.

The mechanism of α-glucosidase can be subdivided into two classes: configuration-retaining or configuration-inverting, based on the stereochemistry at the anomeric center of the hydrolyzed glucose residue. The active site of α-glucosidase contains two carboxylate groups in the form of aspartic acid or glutamic acid residues. In configuration-retaining α-glucosidases, the carboxylate groups mediate a double-displacement, occurring through an enzyme-glycosyl intermediate.[53] Specifically, the first step of the catalyzed reaction involves one carboxylate group acting as an acid catalyst, protonating the glycosidic oxygen. The other carboxylate group acts as a nucleophile that attacks the anomeric center of the glucose residue, producing the enzyme-glycosyl intermediate. The second step of the reaction involves the de-protonation of a water molecule by an enzyme carboxylate group, which then attacks the

anomeric center and displaces the enzyme carboxylate group as shown in **Scheme 1.4 A**. On the other hand, in configuration-inverting α-glucosidases, the carboxylate residues simultaneously bind water and the oligosaccharide substrate that undergo a single-step displacement.[53] One carboxylate group is deprotonated and acts as a base by deprotonating the water molecule while it attacks the anomeric carbon, resulting in the formation of a transition state with significant oxocarbenium ion character as shown in **Scheme 1.4 B**.

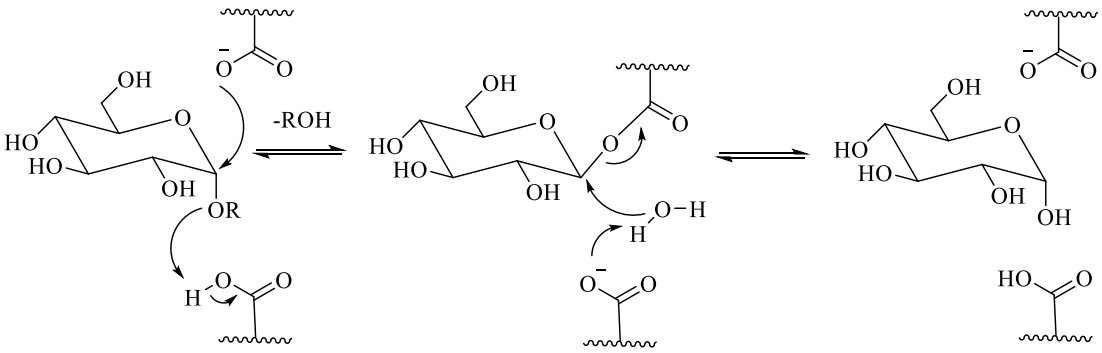

Scheme 1.4 A Configuration retaining enzyme-mediated glycosidase hydrolysis

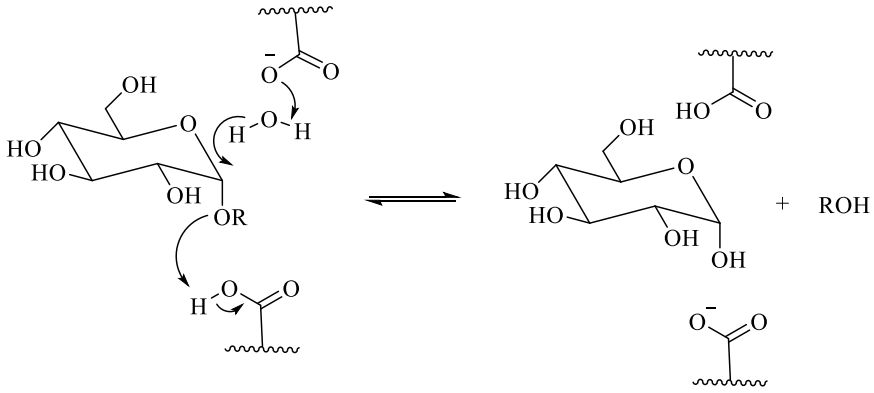

Scheme 1.4 B Configuration inverting enzyme-mediated glycosidase hydrolysis

1.5 Molecular Docking

Protein plays a crucial role in living organisms. These are the sequences of twenty different kinds of amino acids called residues. Protein folds into different spatial arrangements depending on their biological functions. These conformations are driven by different non-covalent forces such as hydrogen bonding, Van der Waal's forces.[54] Proteins cannot live alone; they have interactions with other protein molecules, DNA, RNA or other small molecules. Such interactions are very important in structure based drug discovery.

In order to understand and verify the inhibitory activity of the isolated compounds with α-glucosidase, molecular docking was performed. This showed the binding mode of the isolated compounds with the enzyme to further confirm the inhibitory activity of the compounds.

In summary, literature presented indicates that the natural product chemistry is an important branch of chemistry for the drug discovery program. It is not only important for pharmaceuticals but also for agricultural industry. These features make this branch interesting to the researcher to investigate novel chemical structures.

Based on the aforementioned importance of plant natural products, the present project was designed to perform bioassay directed phytochemical studies on *M. capensis and S. integerrimum* for the identification of natural products exhibiting α-glucosidase inhibitory activity. It was also included in the plan to study the mode of action of bioactive natural products with the aid of molecular docking studies. The results are summarized in chapter **2** and **3.**

1.6 References

1. Clark; A.M. *Pharm. Res*., 1996,13,1133
2. Javed Intekhab; M. Islam, *Pharma. Sci*., 2009,7,8
3. Solecki; R.S. Shanidar; *Sci.*, 1975, 190, 880-881
4. De-Xin Kong; Xue-Juan Li; Hong-Yu Zhang, *Drug Disc. Today*, 2009,14, 115-119
5. Cragg G. M.; Newman, D. *Pharma. Biol*., 2001, 39, 8-17.
6. Cragg G. M.; Newman, D. *Nature's Bounty. Chem. Br*., 2001, 37, 22-26.
7. M. Goerig;J. Schulte am Esch; *Thieme*, 1991, 26, 492-498
8. Christoffel Jos van Boxtel; Budiono Santoso; I. Ralph Edwards Drug Benefits and Risks: International Textbook of Clinical Pharmacology; IOS Netherland, 2008; pp 28-29
9. Ashraf A. Khalil; Marwa M.S. Diab; Kamal D. Moudgil; *J.Pharma. Sci*., 2016, 11, 297–300
10. Robert P. Borris; Joseph T. Baker; Brad Carte, *J. Nat. Prod*., 1995, 58, 132-1357
11. Schmidt B.; Ribnicky D.M.; Poulev A.; Logendra S.; Cefalu W.T.; Raskin I. *Metabolism*, 2008, 57, S3-S9
12. Nakanishi; K. In comprehensive Natural Product Chemistry, Barton, D. Nakanishi, K.; Eds; Elsevier, Amsterdam and New York, 1999, p 115
13. Richard B. Silverman and Mark W. Holladay; The Organic Chemistry of Drug Design and Drug Action. Elsevier Amsterdam, and London, 2004, pp 2-3
14. M. Goerig; J. Schulte am Esch, *J. Thieme*, 1991, 26, 492-498
15. Newman, D.; Cragg, G.; Snaderb, *J. Nat. Prod. Rep.*,2000, *17*, 215- 216

16. Marshall Gates; and Gilg Tschudi, *J. Am. Chem. Soc.*, 1952, *74*, 1109–1110

17. Gordon M. Cragg; David J. Newman; Kenneth M. Snader, *J. Nat. Prod.*,1997, 60, 52-60

18. Harvey, A., *Drug Disc. Today*, 2000, 5, 294

19. David J. Newman; Gordon M. Cragg, *J. Nat. Prod.*, 2016, *79*, 629–661

20. Schmidt B.; Ribnicky D. M.; Poulev A.; Logendra S.; Cefalu W. T.; Raskin I.,*Metabolism: clinical and exp.*, 2008, 57, S3-S9

21. Manuel F. Balandrin1; A. Douglas Kinghorn, Norman R. Farnswort, ACS Symposium Series; Washington, DC, 1993

22. Daniel L. Klayman; AiJ. Lin; Nancy Acton; John P. Scovill; James M. Hoch; Wilbur K. Milhous; Anthony D. Theoharides, *J. Nat. Prod.* 1984, 47, 715-717

23. Geoffrey C. Kirby; *Trop. Doc.*, 1997, 27, 7-11

24. Spizek, Jaroslav; Natural Product Analysis; Havlicek, Vladimir; Eds; john Wiley & Sons, Inc. Hoboken, New Jersey, 2014; pp-43-48

25. Xiangchao Dong; Wei Wang; Shujuan Ma; Hui Sun; Yan Li; Jingqiang Guo, *J. Chrom.*, 2005,1070, 125-130

26. Benjamin Thomas; Grad. Dip. *J. Psycho. drugs*, 2005, 37, 109-111

27. Uwe Rinner; Christoph Lentsch; Christian Aichinger, *J. Syn.*,2010, 22, 3763–3784

28. Leonard Katz; Richard H. Baltz; *J. Indus. Micro. & Biotech.*, 2016, 43, 155-176

29. Hong-Fnag Ji; Xue-Jaun Li; Hong Yu Zhang, *European Mol. Bio. Org.*, 2009, 10, 194-200

30. Mariappan V. Chelliah; Keith Eagen; Zhuyan Guo; Samuel Chackalamannil; Yan Xia; Hsingan Tsai; William J. Greenlee; Ho-Sam Ahn; Stan Kurowski; George Boykow; Yunsheng Hsieh; Madhu Chintala, *ACS Med. Chem. Lett.*, 2014, 5, 561−565

31. Newman, D. J.; Cragg G. M. *J. Nat. Prod.*, 2007, 70, 461-477

32. Newman, D.; Cragg, G.; Snader, K. *J. Nat. Prod*., 2003, 66, 1022

33. Koehn, F.; Carter, G. *Nat. Rev. Drug. Disc.*, 2005, 4, 206.

34. Butler; M. *J. Nat. Prod.*, 2004, 67, 2141.

35. Ruiwu Liu; K. S. Lam, *Current Opinion in Chem. Biol.*, 2017, 38, 117–126

36. Staforth; S. P. Natural Product Chemistry at a glance. Blackwell Publishing Ltd: Malden, MA. 2006; pp 2-6

37. Victor Kuete; Louis P. Sandjo; Doriane E. Djeussi; Maen Zeino; Guy M. N. Kwamou; Bonaventure Ngadjui; Thomas Efferth, *J. Invest. New Drugs*, 2014, 32, 1053–1062

38. Na Li; Jian-lin Wu; Toshiaki Hasegawa; Jun-ichi Sakai; Li-yan Wang; Saori Kakuta; Yumiko Furuya; Akihiro Tomida; Takashi Tsuruo; Masayoshi Ando, *J. Nat. Prod*., 2006, 69, 234-239

39. Dewick; P. M. Medicinal Natural Products: A Biosynthetic Approach. 3rd Ed.; John Wiley and Sons: New York. 2009; p 8.

40. Fei Liu; Ya-Nan Wang; Yong Li; Shuang-Gang Ma; Jing Qu; Yun-Bao Liu; Chang-Shan Niu; Zhong-Hai Tang; Tian-Tai Zhang; Yu-Huan Li; Li Li; Shi-Shan Yu, *Sci. Rep*., 2017, 7, 7944-7953

41. Fei Liu; Ya-Nan Wang; Yong Li; Shuang-Gang Ma; Jing Qu; Yun-Bao Liu; Chang-Shan Niu; Zhong-Hai Tang; Tian-Tai Zhang; Yu-Huan Li; Li Li; Shi-Shan Yu, *Tetrahed.,* 2019, 75, 296-307

42. Andrew J. Krentz. Drug Therapy for Type 2 Diabetes, Henry Ling Ltd, Dorchester, UK. 2012; p-9

43. H.-B. Chang; S.-H. Kim; Y.-I. Kwon; D.-H. Choung; W.-K. Choi; T.-W. Kang; *J. Antibiotics*, 2002, 55, 467–471

44. Maria D.P.T. Gunawan-Puteri; JunKawabata, *Food Chem.,* 2010, 123, 384-389

45. Abbas Mollataghi; Emilie Coudiere;A. Hamid A. Hadi; Mat Ropi Mukhtar; Khalijah Awang; Marc Litaudon; AtharAta, Fitoterapia, 2012, 83, 298-302

46. Young-In kwon; Hyeog-Jin son; Kyoung sik Moon; Joon Kyum kim; Jong-Gwan kim; Hyoung-Sik Chun; Soon Kil Ahn; Chung Il Hong, *J. Antibio.,* 2002, 55, 462-466

47. Arshag D.; Mooradian; Jerome E. Thurman, *Drugs*, 1999, 57, 19-29

48. Chao Tan; Qunxing Wang; Chunhua Luo; Sai Chen; Qianyuan Li; Peng Li, *Int. J. Mol. Sci*., 2013, 14, 2551-2558

49. Azam, S.; Uddin, R.; Wadood, A., *J. Mole. Liq.,* 2012, 174, 58-62.

50. Larner, J.; Lardy, H.; Myrback, K., Other Glucosidases. 2nd ed., New York: Academic Press. 1960, pp. 369-378.

51. Voet, D.; Voet, J. G.; Pratt, C. W. Fundamentals of Biochemistry: Life at the Molecular Level, 5th ed.; Wiley: Chichester, 2016. pp. 232

52. Wardrop, D. J.; Waidyarachchi, S. L. *Nat. Product Rep.*, 2010, 1431-1468.

53. Hatem A. Abuelizz; Nor Azman N. I. Iwana; Rohaya Ahmad; El-Hassane Anouar; Mohamed Marzouk; Rashad Al-Salahi, *BMC chem.* 2019, 1-14

CHAPTER 2

Phytochemical Investigation of *Macaranga capensis*

2.1 Introduction

The genus *Macaranga* is the largest genus of family Euphorbiaceae that consists of more than 250 plant species.[1] Plants of this genus *Macaranga* are found in West Africa, South Pacific Islands and Malaysia.[2] These plants are used in folk medicines. For instance, the fresh or dried leaves of *M. sampsonii* are used to treat swelling, bruises, sore and minor cuts. Whereas, *M. harveyana* locally known as loupata has been reportedly used for infertility in women in Veitnam.[3-4] In Thailand, the root decoction of *M. tanarius* is used as an antipyretic and antitussive agent.[5] Only 25 plants of this genus have been phytochemically investigated and these studies revealed the presence of diterpenoids, flavonoids, prenyl flavanones, and steroids in them.[6] These compounds have been reported to exhibit various biological activities including anti-α-glucosidase, anti-malarial, anti-xanthine oxidase, anti-cancer, and anti-microbial activities. All these studies are summarized as follows.

Phytochemical studies on *M. tanarius* have afforded lignin compounds namely, mallotinic acid (**60**), corilagin (**61**), chebulagic acid (**62**), macatanninn A (**63**) andmacatannin B (**64**). All of these compounds showed good to moderate activities against α-glucosidase and xanthine oxidase.[7] Compounds **60**-**62** have also been isolated from *Cunonia macrophylla* exhibiting anti-microbial and anti-viral activities.[8] Their bioactivity data are listed in **Table 2.1**

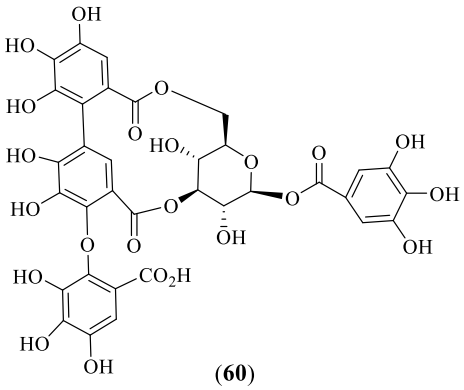

(**60**)

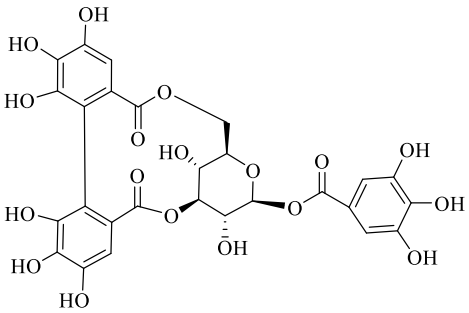

(**61**)

Table 2.1: Anti α-glucosidase, anti-xanthine oxidase and anti-microbial activities against *E. caratovora* of compounds **60-64**.

Compounds	**IC_{50} (µM)** α-Glucosidase inhibitory activity	**IC_{50} (µg/ml)** xanthine oxidase inhibitory activity	Antimicrobial activities (zone of inhibition in diameter (mm)
Mallotinic acid (**60**)	> 500	>100	13
Corilagin (**61**)	263	72.9	20
Macatanninn A (**62**)	80	-	-
Chebulagic acid (**63**)	100	46.3	19
Macatannin B (**64**)	55	-	-
1,2,3,4,6-Penta-*O*-galloyl-β-D-glucose (PGG) (**65**) (+ve control)	140	-	-
Quercetin (**66**) (+ve control)	-	3.4	-
Gentamycinsulphate (**67**) (+ve control)	-	-	21

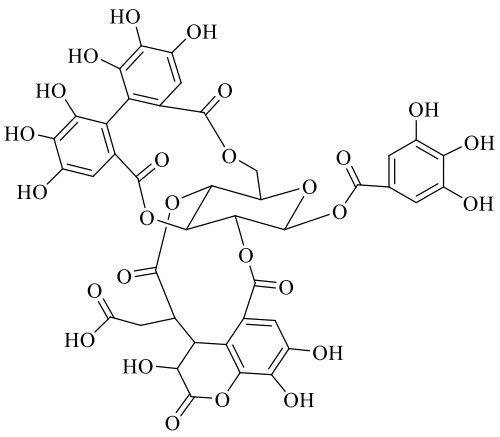

(**62**)

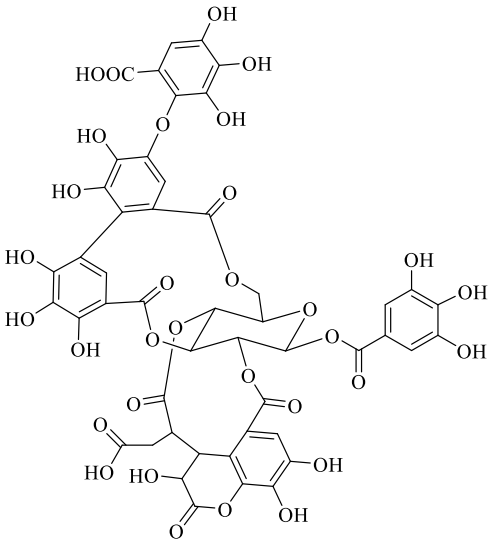

(**63**)

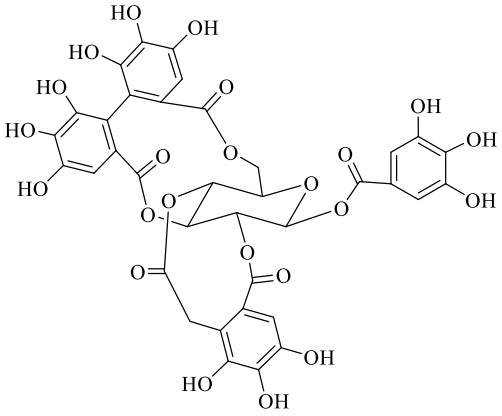

(**64**)

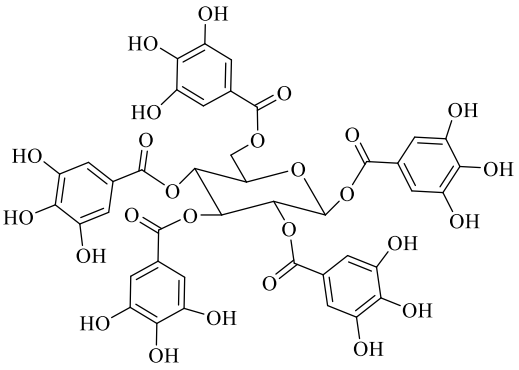

(**65**)

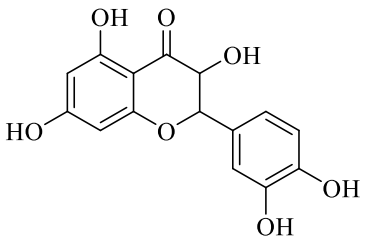

(**66**)

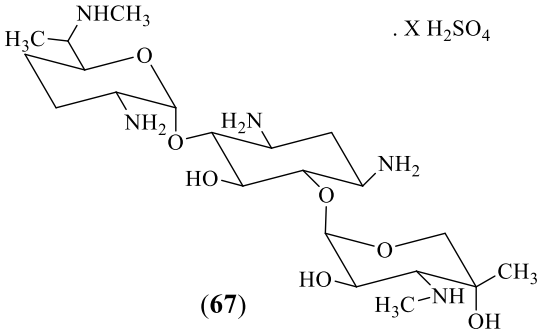

(**67**)

Compounds **62-64** showed better α-glucosidase inhibitory activity compared to the standard 1,2,3,4,6-Penta-*O*-galloyl-β-D-glucose (PGG) (**65**), a known potent inhibitor.[9] Whereas, compounds **60**, **61** and **63** exhibited moderate xanthine oxidase inhibitory activity compared to quercetin (**66**) and comparable anti-microbial activity with the standard gentamycin sulphate (**67**).

Similarly, chemical investigation of *M. kurzii* afforded kurzphenol A (**68**), kurzphenol C (**69**), 8-prenylnaringenin (**70**), acetyl-atractylodinol (**71**) and blumenol A (**72**). Compounds **69-72** inhibited the growth of human lung carcinoma (A-549) cell line with the IC_{50} values of 17.11, 9.76, 18.22 and 18.23μg/mL, respectively. These values are comparable with their positive control, an anti-cancer, 5-fluorouracil (5-FU) (IC_{50} = 13.60μg/mL). Whereas, Compound (**68**) exhibited modest cytotoxicity against human hepato cellular (Hep G2) cell line with IC_{50} value of 30.14 μg/mL.[10]

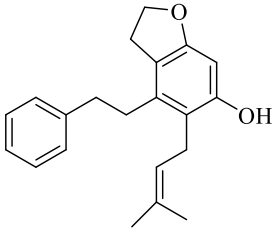

(**68**)

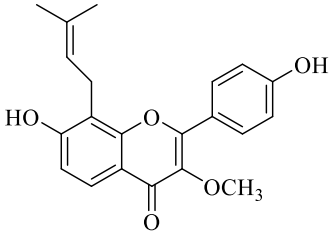

(**69**)

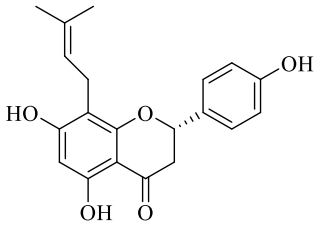

(**70**)

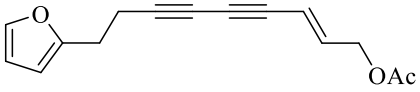

(**71**)

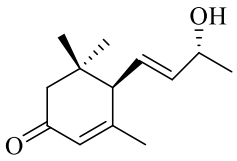

(**72**)

Chemical studies on *M. triloba* has yielded methoxyeriodictyol (**73**), nymphaeol B (**74**), nymphaeol C (**75**), malaysianone A (**76**) and nymphaeol A (**77**).[11] Compounds **74-75** and **77** showed anti-malarial activity against a parasite called *plasmodium falciparum* with the IC_{50} values of 4.02, 2.04 and 0.06 μM. This activity was moderate compared with chloroquine diphosphate with IC_{50} value of 0.0063 μM. These compounds (**74-75** and **77**) also exhibited acetyl cholinesterase (AChE) inhibitory activity with the IC_{50} value of 15.09, 15.70 and 7.77 μM, respectively. Compound **77** showed strong bioactivity compared to standard drug donepezil (IC_{50} = 8.13μM).[12] Compound (**77**) also showed cytotoxic activity against different human cancer cell lines; HL-60 (Human Leukemia,), MCF-7 (Human Breast Cancer) and HeLa (Human Cervical Cancer) with the IC_{50} values of 3.3, 5.6 and 1.3 μM respectively.[11]

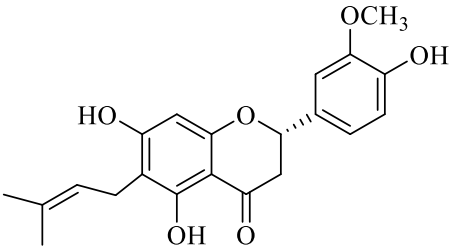

(**73**)

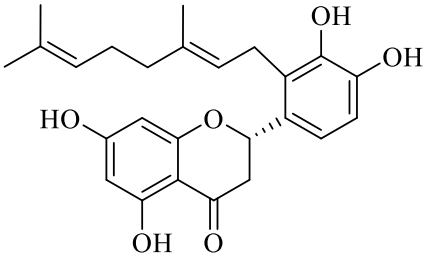

(**74**)

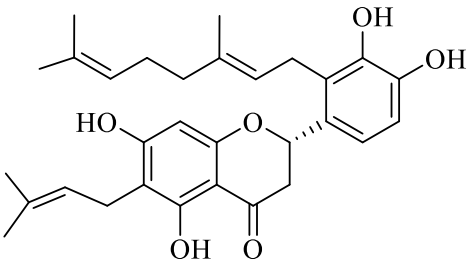

(**75**)

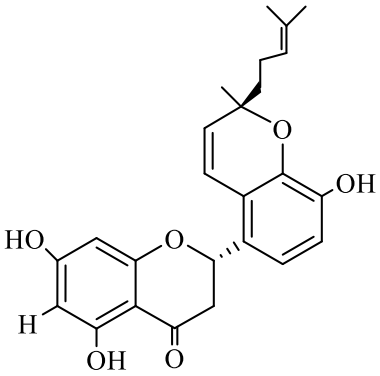

(**76**)

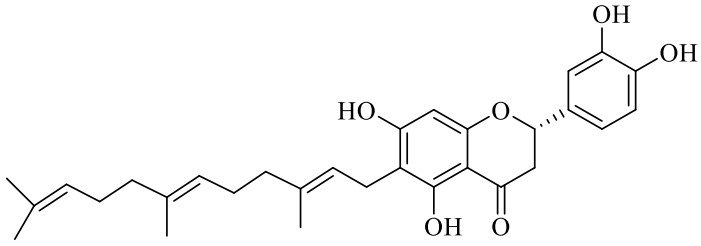

(**77**)

Macasiamenene A (**78**), macasiamenene B (**79**), macasiamenenes M (**80**), macasiamenenes G (**81**), (2*S*)-5,7-dihydroxy-2-(4-methoxyphenyl)-8-(3-methylbut-2-enyl)-2,3-dihydrochromen-4-one (**82**), macasiamenene R (**83**), macasiamenone A (**84**)

and macasiamenol B(**85**) were purified from *M. siamensis*. Compounds **79**-**81** and **85** exhibited radical scavenging activity of 1,1-diphenyl-2-picrylhydrazyl (DPPH) free radicals with the IC_{50} values of 26.2, 24.3, 96.2 62.5 and 46.6 μM, respectively.[13] The DPPH activity of compounds **79**-**81** and **85** were moderate compared to ascorbic acid (IC_{50} = 21.2 μM).Compounds **80**-**81** also showed oxygen radical absorbance capacity (ORAC) antioxidant activity 2.0±0.3, 2.5±0.3 expressed as relative trolox equivalents (1.0 unit).Moreover, compound (**82**) exhibited aromatase inhibiting activity with IC_{50} values of 0.5 μM is very strong activity compared with its standard ketoconazole (IC_{50} = 2.4 μM). Aromatase inhibiting activity is important for the treatment of breast cancer and cancer chemoprevention.

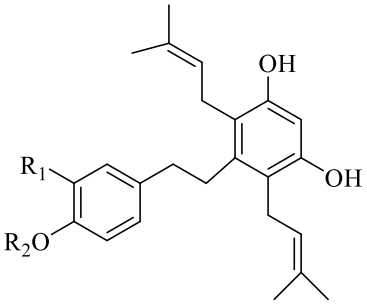

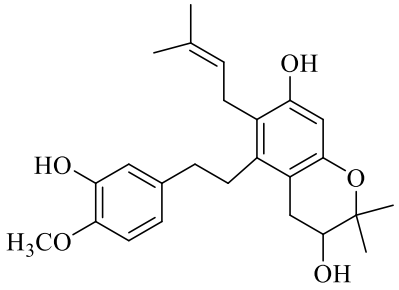

(**80**)

(**78**) R_1= H, R_2=CH_3

(**79**) R_1= OH, R_2=CH_3

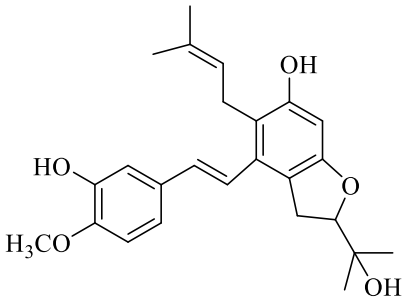

(**81**)

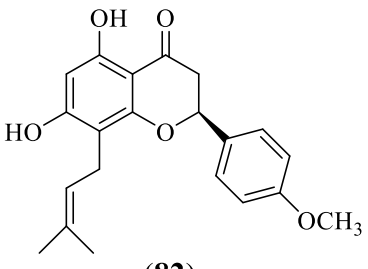

(**82**)

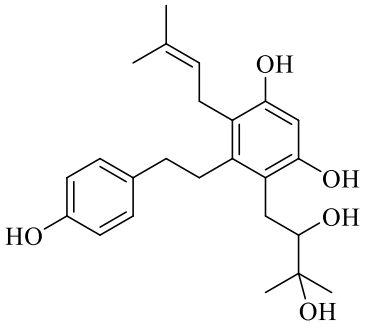

(**83**)

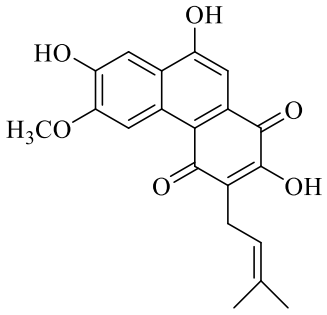

(**84**)

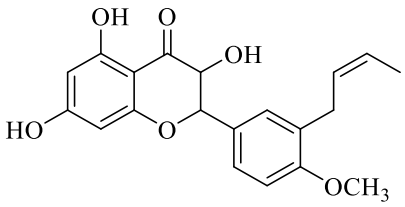

(**85**)

According to the traditional healers of Veitnam and Thailand, *M. capensis* is used as a medicinal plant to treat different diseases including diabetes. The methanolic extract of this plant was active against α-glucosidase inhibitory assay. This chapter describes the isolation, structure elucidation, bioactivity data and molecular docking of two triterpenoids, 3α-hydroxyaleuritolic acid 2-*p*-hydroxybenzoate (**86**) and 3-acetoxyoleanolic acid (**87**) isolated during the course of the study.

2.2 RESULTS AND DISCUSSION

The barks of *M. capensis* were collected from South Africa in 2007 and extracted with methanol. It was fractionated using solvent-solvent extraction. The defated extract and isolation of compounds **86-87** are described in the experimental section of this chapter (Sec. 2.3.3, p.46). Its acetone extract was found to be active against α-

glucosidase (IC_{50} = 30μg/ml) and our phytochemical investigation of bioactive fraction afforded two known triterpenoids (**86-87**). Their structural elucidation with the aid of UV, IR and NMR spectroscopic studies is described as follows.

2.2.1 Structure Elucidation of Compounds (86-87)

2.2.1.1 3α-Hydroxyaleuritolic acid 2-*p*-hydroxybenzoate (86)

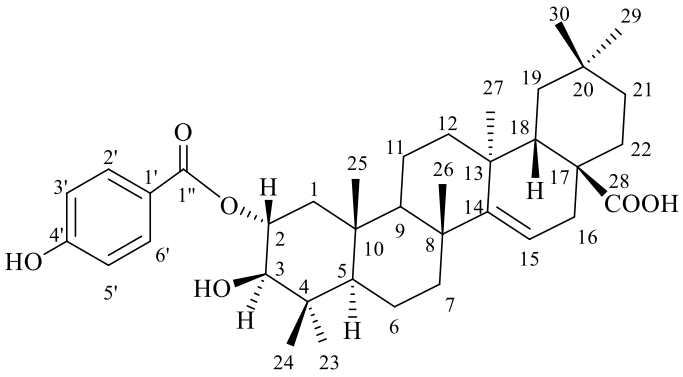

(**86**)

Compound (**86**) was isolated as a white amorphous solid. Its UV spectrum showed maximum absorption at 256 nm indicating the presence of *p*-hydroxybenzoyl moiety.[14] The IR spectrum of **86** showed intense absorption bands at 3339 (OH), 1452 (C=C) and 1708 (C=O) cm^{-1}.The ^{1}H-NMR spectrum (acetone-d_6, 400 MHz) of **86** showed the resonance of seven methyl groups at δ1.01, 1.0, 0.87, 1.03, 0.98, 0.97 and 0.87 due to H_3-23, H_3-24, H_3-25, H_3-26, H_3-27, H_3-29 and H_3-30, respectively. A double triplet, integrating for one proton, resonated at δ5.29 (J = 4.6, 10.4, 11.4 Hz) was assigned to H-2 proton. A one proton doublet appeared at δ4.94 (J = 10.4) was due to H-3 proton. The downfield chemical shift values of H-2 and H-3 were indicative of the presence of germinal oxygen functionalities. The coupling constants ($J_{2\alpha,3\beta}$= 10.4) indicated the *trans* diaxial orientation of H-2 and H-3. Based on the J value, α-

orientation of H-2 and β-orientation of H-3 was assumed. A double doublet, integrating for one proton, centered at δ5.60 (J = 3.5, 7.9 Hz) was ascribed to H-15.A one-proton multiplet at δ2.03 was due to H-18. Two, two-proton AB doublet, appeared at δ7.89 (J = 8.4 Hz) and 6.93 (J = 8.4 Hz) were ascribed to H-2'/H-6' and H-3'/H-5' of benzene moiety, respectively.

The COSY-45° spectrum of **86** was used to assign ^{1}H-NMR chemical shift values, H-2 (δ 5.29) showed vicinal couplings with H_2-1 (δ 2.42, 2.01) and H-3 (δ 4.94). Aromatic protons H2'/H-6' (δ 7.89) showed ^{1}H-^{1}H spin correlations with H-3'/H-5' (δ 6.93). The vinylic H-15 (δ 5.60) showed cross peaks with H_2-16 (δ 2.08, 1.33).

The ^{13}C-APT-NMR spectrum (acetone-d_6, 100 MHz) of **86** showed the signals for all thirty seven carbons. A combination of APT and DEPT spectra showed the presence of seven methyl, nine methylene, eleven methine and ten quaternary carbons in **86**. Two signals at δ 178.2 and δ 169.2 were due to C-28 and C-1''carbonyl carbons, respectively. C-2'/6' and C-3'/5' appeared at δ 131.6 and 115.2, respectively. Two downfield aliphatic signals at δ 69.6 and 80.4 were ascribed to C-2 and C-3, respectively. Vinylic C-15 appeared at δ 116.4.

The heteronuclear single quantum coherence (HSQC) spectrum of **86** was acquired in order to establish ^{1}H/^{13}C one-bond shift correlations of all the hydrogen bearing carbons. H-2' (δ 7.89) showed cross peak with C-2' (δ 131.6). H-3 (δ 4.94) exhibited ^{1}H/^{13}C one-bond shift correlations with C-3 (80.4). Complete ^{13}C-NMR chemical shift values and ^{1}H/^{13}C one-bond shift correlations of all hydrogen bearing carbons, as determined from HSQC spectrum, are shown in **Table 2.2.**

The heteronuclear multiple bond correlation (HMBC) spectrum of **86** showed long-range couplings of H-3'/H-5' (δ 6.93) with C-4' (δ 160.5). H-3 (δ 4.94) showed coupling with C-2 (69.6) indicated that C-2 is *ortho* to C-3. A combination of 1D and 2D-NMR spectroscopic data led us to the proposed structure **86** to this compound. ^{1}H and ^{13}C-NMR spectroscopic data were similar to those of 3α-hydroxyaleuritolic acid 2-p-hydroxybenzoate reported in the literature.[15] Based on these spectroscopic data, compound **86** was identified as reported triterpenoid (3α-hydroxyaleuritolic acid 2-*p*-hydroxybenzoate). All of the chemical shift values and the coupling constants of **86** were similar to those of the reported 3α-hydroxyaleuritolic acid 2-*p*-hydroxybenzoate. These spectroscopic studies led us to assume that compound **86** has the same stereochemistry at all chiral centres as those reported for 3α-hydroxyaleuritolic acid 2-*p*-hydroxybenzoate.[15] This compound was previously reported from *Maprounea africana*,[15] and has been isolated for the first time from this plant.

Table 2.2 ^{1}H and ^{13}C NMR spectroscopic data for **86** and $^{1}H/^{13}C$ one-bond shift correlations, as determined by HSQC.

Position	δH (*J* in Hz)	δC (multiplicity†)
1	2.42, 2.01, m	42.9 (-CH_2-)
2	5.29, dt, (4.6, 10.8)	69.5(-CH-)
3	4.94, d, (10.4)	80.4(-CH-)
4	-	39.5 (-C-)
5	1.2, 1.38, m	54.9 (-CH-)
6	1.78, 1.53, m	19.5 (-CH_2-)
7	1.2, 1.14, m	43.0 (-CH_2-)
8	-	35.5 (-C-)
9	1.5, d (5.7)	48.7 (-CH-)
10	-	39.5 (-C-)
11	1.06, 1.32, m	17.3 (-CH_2-)
12	1.30, 1.01, m	32.0 (-CH_2-)
13	-	38.9 (-C-)
14	-	165.3 (-C-)
15	5.29 dd,(4.6, 10.8)	116.4 (-CH-)
16	2.08, 1.33,m	29.2 (-CH_2-)
17	-	69.4 (-C-)
18	2.03, m	42.8(-CH-)
19	1.3, 1.01,m	35.3 (-CH_2-)
20	-	30.6 (-C-)
21	1.28,1.79, m	33.6 (-CH_2-)
22	1.29, 2.04,m	31.8 (-CH_2-)
23	1.01, s	28.7 (-CH_3-)
24	1.0, s	17.0 (-CH_3-)
25	0.87, s	13.3(-CH_3-)
26	1.03, s	25.5 (-CH_3-)
27	0.98, s	13.6 (-CH_3-)
28	-	178.2 (-C-)
29	0.97, s	31.8 (-CH_3-)
30	0.87, s	25.0 (-CH_3-)
1''	-	169.5 (-C-)
1'	-	121.6 (-C-)
2',6'	7.89, d, (8.4)	131.6 (-CH-)
3',5'	6.93, d, (8.4)	115.2 (-CH-)
4'	-	160.5 (-C-)

†Multiplicity was determined with the help of ^{13}C-APT and DEPT spectral data.

2.2.1.2 3-Acetoxyoleanolic acid (**87**)

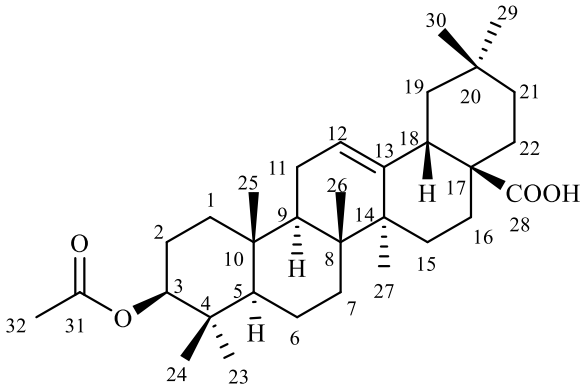

(**87**)

The second compound (**87**) was isolated as white crystals. Its UV spectrum showed terminal absorption indicating the lack of a conjugated π system. The IR spectrum showed absorption bands at 1241 (C-O), 1720 (C=O) and 1620 (C=C) cm^{-1}. The ^{1}H-NMR spectrum ($CDCl_3$, 400 MHz) of **87** showed the resonances of eight methyl signals at δ 2.06, 1.15, 0.96, 0.95, 0.93, 0.88, 0.87, and 0.77 that were attributed to H_3-32, H_3-27, H_3-24, H_3-30, H_3-29 H_3-25, H_3-23, and H_3-26, respectively.

A one proton signal at δ5.30 was ascribed to H-12. A one proton doublet, resonated at δ 2.84 was due to H-18; both of these peaks suggested that compound **87** was an olea12-ene type triterpene. A triplet, integrated for one proton, appeared at δ 4.52 (*J*= 9.2 Hz) was assigned to H-3. Its downfield chemical shift value suggested the presence of acetoxy group at C-3.

The COSY-45° spectrum of **87** showed vicinal couplings of H-2 (δ 1.73) with H_2-1 (δ 1.08, 1.65) and H-3 (δ 4.52). Similarly, H-5 (δ 0.87) showed vicinal couplings with H_2-6 (δ 1.40, 1.57) which in turn showed cross peaks with H_2-7 (δ 1.31, 1.47).

Vinylic H-12 (δ 5.30) showed vicinal coupling peak with H-11 (δ 1.97).H-12 (δ 5.30) also showed allylic coupling with H-18 (δ 2.84).

The ^{13}C-APT-NMR spectrum ($CDCl_3$, 100 MHz) of **87** exhibited the resonances of all the thirty two carbons. This spectrum also revealed the presence of eight methyls, ten methylene, six methine and eight quaternary carbons in this compound. Two carbonyl carbons, C-28 and C-31 appeared at δ183.2 and171.2, respectively. Vinylic C-12 appeared at δ 122.7. The downfield aliphatic signal at δ 80.8 was ascribed to C-3, suggesting the presence of a geminal acetyl functional group at C-3. Signals at δ21.2, 25.6, 16.3, 23.6, 33.0, 16.1, 28.3 and 16.9 were due to C-32, C-27, C-24, C-30, C-29, C-25, C-23 and C-26, respectively.

The HSQC spectrum of **87** showed the ^{1}H/^{13}C one-bond shift correlation of H-3 (δ 4.52) with C-3 (80.8). H-12 (5.30) showed cross peaks with C-12 (122.7). Complete ^{13}C-NMR chemical shift values and ^{1}H/^{13}C one-bond shift correlations of all hydrogen bearing carbons, as detrmined from HSQC spectrum, are shown in **Table 2.3**. A combination of 1D-NMR and 2D-NMR spectroscopic data led us to propose structure **87** to 3-acetoxyoleanolic acid. The ^{1}H and ^{13}C-NMR spectroscopic data of **87** were distinctly similar to those of 3-acetoxyoleanolic acid, reported in the literature.[16,17] Based on these spectroscopic data, compound **87** was identified as 3-acetoxyoleanolic acid. This compound was previously isolated from *Hibiscus syriacus,*[18] *Vigna sinensis* (Cowpea seed)[19] and *Neoboutonia macrocalyx.*[20] This is the first time report of this compound from *M. capensis*.

Table 2.3 ^{1}H and ^{13}C NMR chemical shift assignments for **87** and $^{1}H/^{13}C$ one-bond shift correlations of hydrogen bearing carbons, as determined by HSQC.

Position	δH (J in Hz)	δC (multiplicity†)
1	1.08, 1.65,m	38.4 (-CH_2-)
2	1.73, 1.15,m	27.7 (-CH_2-)
3	4.52,d, (9.2)	80.8(-CH-)
4	-	39.4 (-C-)
5	0.87, m	55.8 (-CH-)
6	1.40, 1.56, m	18.3(-CH_2-)
7	1.31, 1.47, m	32.6 (-CH_2-)
8	-	39.2 (-C-)
9	1.57, m	47.8 (-CH-)
10	-	37.5 (-C-)
11	1.65, 1.92, dd (1.8, 8.0)	23.7 (-CH_2-)
12	5.30, s	122.7(-CH-)
13	-	143.8 (-C-)
14	-	41.1(-CH-)
15	1.64, 1.90, t	30.8(-CH_2-)
16	1.66, 0.93, m	23.0 (-CH_2-)
17	-	46.7 (-C-)
18	2.84, d (7.8)	37.1 (-CH-)
19	1.17, 1.65, m	46.3 (-CH_2-)
20	-	34.0 (-C-)
21	1.24, 1.37, m	33.7 (-CH_2-)
22	1.62, 1.71, m	33.8 (-CH_2-)
23	0.87, s	28.3 (-CH_3-)
24	0.96, s	16.3 (-CH_3-)
25	0.88, s	16.9 (-CH_3-)
26	0.77, s	25.6 (-CH_3-)
27	1.15, s	25.6 (-CH_3-)
28	-	183.2 (-C-)
29	0.97, s	31.8 (-CH_3-)
30	0.87, s	25.0 (-CH_3-)
31	-	171.2 (-C-)
32	2.05, s	21.3 (-CH_3-)

†Multiplicity was determined with the aid of, ^{13}C-APT and HSQC spectral data.

2.2.1.3 α-Glucosidase Inhibitory Activity of Compound (**86**)

Compound (**86**) was evaluated for α-glucosidase inhibitory activity. It was active in our assay with the IC_{50} value of 2.17 mM, compared to the acarbose, used as a positive control (IC_{50} = 0.45 mM). The activity might be due to the presence of ester carbonyl carbon. We were unable to evaluate compound (**87**) in this bioassay as it was only soluble in chloroform and precipitate out in buffer solution. To avoid precipitation in buffer solution this kind of non-polar compounds (**87**) could be dissolved in DMSO.

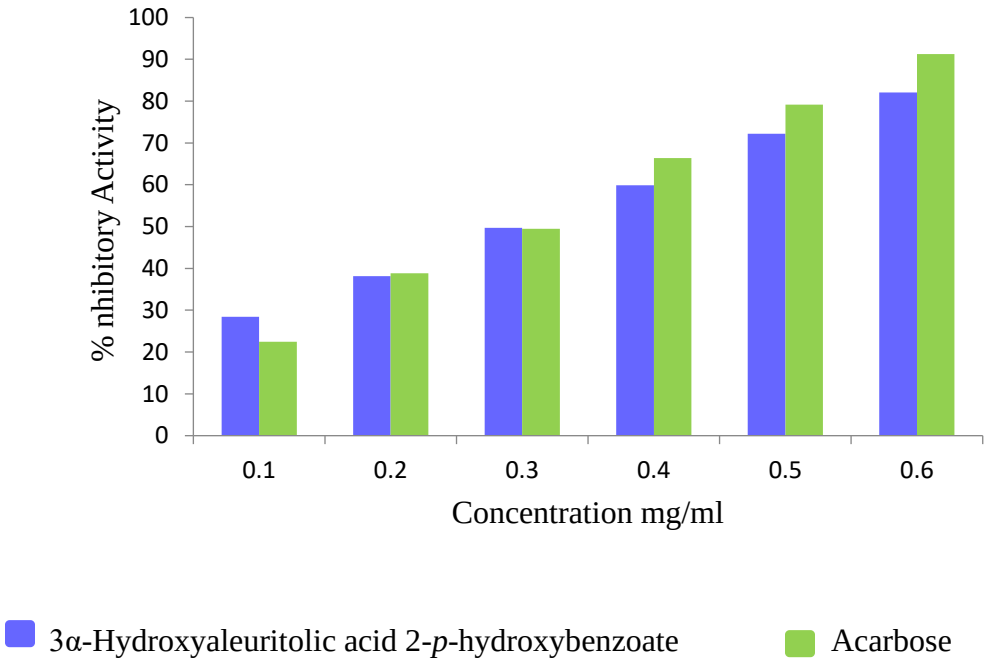

Figure: 2.1 % Inhibitory activity of compound (**86**) and acarbose.

The bioactivity of compound (**86**) suggested its in-vitro potency to inhibit α-glucosidase is moderate compared to acarbose.

2.2.1.4 Molecular Docking

In order to determine the mode of interaction of compound **86**, the docking studies were carried out. These studies indicated the interaction of C-2 ester carbonyl with 531-histidine via hydrogen bonding with the distance of 3.3 Å. The Gibbs free energy binding (ΔG), obtained from the results of molecular docking, showed that the compound **86** has moderate affinity to the histidine subunit of the enzyme with free binding energy of –5.8 kcal/mol shown in **Figure: 2.2.**

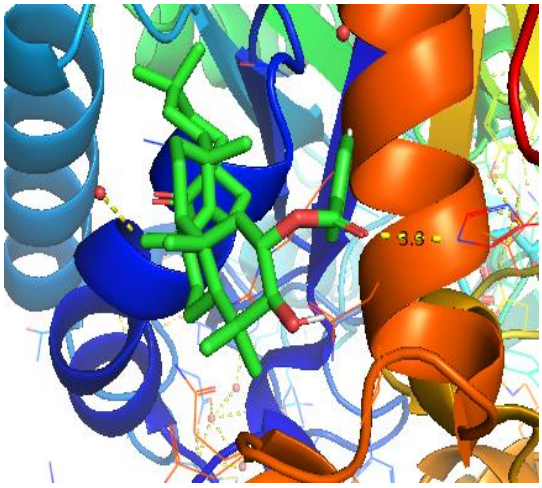

Figure: 2.2 Binding of compounds **86** in the binding sites of α-glucosidase enzyme.

2.3 Experimental

2.3.1 General Experimental Conditions

2.3.1.1 Spectroscopy

The UV spectra were recorded in methanol on a Shimadzu UV-2501 PC spectrophotometer. IR spectra were acquired on a Varian 1000 FT-IR (Scimitar Series). 1D-NMR (^{1}H, ^{13}C-APT, DEPT spectrum) and 2D-NMR (COSY-45°, HSQC, HMBC) spectra were acquired on a Bruker Avance-3 400MHz spectrometer; chemical shifts are expressed in ppm (δ). Coupling constants (*J*) are reported in Hz. All of the above mentioned NMR spectroscopic data were obtained using deuterated solvents including $CDCl_3$ and acetone-d_6. These solvents were purchased from CDN Isotopes, Canada.

2.3.1.2 Chromatographic Supplies

Column chromatography was carried out using 60 Å silica gel (230-400 mesh) as the stationary phase; purchased from Caledon Laboratory Chemicals, Canada. All solvents used as a mobile phase during fractionation of crude extract, isolation and purification of compounds were ACS grade and were purchased from Caledon Laboratory Chemicals, Canada. Thin layer chromatography (TLC) was performed on silica gel 60 F_{254} aluminum-backed TLC plates (Machery-Nagel, Germany; Merck, Germany) were purchased from EMD. These plates were visualized by using UV light Entela model UVGL-58.

2.3.1.3 Bioassay Supplies

α-Glucosidase inhibitory bioassays were carried out spectrophotometrically using Synergu HT multidetection Biotek microplate reader. The enzyme (100 units) and acarbose (as a standard) were purchased from Sigma-Aldrich Canada.

2.3.2 Plant Material

The barks of *M. capensis* were collected on 20th April 2007 at a riveine forest in Dewede, South Africa by Dr. R.M. Gengan and Mr. Abin James. The plant was then identified by Mr. M. Khipheni A. Ngwenya, Scientific Officers, at the South Africa National Biodiversity Institute. A voucher specimen was deposited there. The methanolic extract of the barks was shipped to the University of Winnipeg for further investigation.

2.3.3 Extraction and Isolation

The barks (12.3 Kg) of *M. capensis* were dried and ground into a powder. This was extracted with 23L of methanol and was dried under vacuum (below 40°C) to yield a crimson residue. Then 3.8 Kg of the methanolic extract was extracted again with dichloromethane for four times. The extract was concentrated under vacuum to yield 31g of crude. This crude was then loaded onto a silica gel column and eluted with hexane and increasing polarity with acetone. Fractions in the volume of 50 ml each were collected and pooled them together based on the analytical TLCs. The aforementioned procedures were done by Mr. Abin James. All the fractions were checked against α-glucosidase inhibitory activities. Fractions **35-55** showed good activities with IC_{50}=30 μg/ml whereas the other fractions exhibited moderate to no activity.

For the isolation of (**86**) and (**87**) the acetone extract (32g) was loaded onto a silica gel column (230-400 mesh, Merk) and was eluted with hexane-chloroform (0-100%) and chloroform-methanol (0-100%). This afforded 309 fractions which were pooled on the basis of similar R_f values into 23 fractions. These 23 fractions were subjected to α-glucosidase bioassay, among which MC-9 and MC-10 showed good

activity. Based on bioassay information MC-9 and MC-10 were selected for further fractionation as they also contained major products different from one another. MC-9 eluted at 98% $CHCl_3$: 2% MeOH was subjected to secondary column chromatography and it was further eluted with hexane: acetone (0-100%) and the fraction eluted at 85% hexane: 15% acetone (167.9 mg) further loaded onto the column, eluted with hexane: ethyl acetate (0-100%), collected 5 fractions after scaling up the column fractions. The fraction at 70% ethylacetate was purified by preparative TLC using hexane: chloroform: MeOH (4.7:5:0.2) to afford 3-acetoxyoleanolic acid (**87**) (5.1mg). Fraction MC-10 (230.8 mg) collected at 96% $CHCl_3$: 4% MeOH subjected to secondary column as well, and eluted with hexane: acetone (0-100%) afforded 4 sub-fractions after pooling up the eluted fractions. The fraction eluted at 70% hexane: 30% acetone (90.7 mg) was further loaded onto the column, eluted once again with the solvent system hexane: acetone (0-100%). The fraction (MC-10-4) (8.2 mg) was further purified by preparative TLC using hexane-ethyl acetate (4.4:5.6) to yield (3α-hydroxyaleuritolic acid 2-*p*-hydroxybenzoate (**86**) (2.3 mg).

3α-hydroxyaleuritolic acid 2-*p*-hydroxybenzoate (**86**); White amorphous solid, 2.3 mg; UV ($CHCl_3$): λmax 259 nm; IR ($CHCl_3$): vmax3339, 2932, 2959, 1708, 1598, 1516, 1614 cm^{-1}; ^{1}H-NMR (*acetone-d6*, 400 MHz) = see Table 2.2; ^{13}C-NMR (*acetone-d6*, 100 MHz) = see Table 2.2.

3-acetoxyoleanolic acid (**87**); White crystals, 5.1 mg; IR ($CHCl_3$): vmax 2936, 1714, 1708, 1452 cm^{-1}; ^{1}H-NMR (*acetone-d6*, 400 MHz) = see Table 2.3; ^{13}C-NMR (*acetone-d6*, 100 MHz) = see Table 2.3.

2.3.4 Assay for α-Glucosidase Inhibition

The inhibitory activity of *M. Capensis* fractions and isolated compounds were tested against α-glucosidase. This assay measures the inhibitory activity of the enzyme by measuring the presence of *para* nitro phenol as the by-product of the hydrolysis of *para*-nitrophenyl-α D-glucopyranoside (*p*-NPG substrate). Various concentrations (0.1, 0.2, 0.3, 0.4 and 0.5) of the compounds were incubated with an enzyme at 37°C for 15 minutes in the 96-well microtiter plate. The assay mixture containing 50 µL of phosphate buffer (100 mM, pH = 6.8), 10 µL of α-glucosidase (1 U/ml) and 20 µL of varying concentrations of the test compounds. This was first pre-incubated and then 20 µL of *p*-NPG substrate was added and incubated further 37°C for 20 minutes. The reaction was stopped by adding 50 µL Na_2CO_3 (0.1M). The absorbance of the released *para* nitro phenol was measured at 405 nm using the *Synergu HT multidetection BioTek* microplate reader. Acarbose at various concentrations (0.1-0.5 mg/ml) was used as a standard. Without adding the test compounds were set up as a blank and each experiment was performed as a triplicates. The results were expressed as percent inhibition by using **Formula 1**. The effects of the compounds as inhibitors of α-glucosidase was calculated as an IC_{50} value, which is the concentration of the inhibitor required to reduce enzyme activity to 50%.

Formula 1: % Inhibition= (Ac – As)/Ac× 100

Where, Ac is the absorbance of the blank with no test compound and As is the absorbance value for each concentration tested.

2.3.5 Molecular Docking

In order to verify the α-glucosidase inhibitory activity results of the isolated compounds; 3α-hydroxyaleuritolic acid 2-*p*-hydroxybenzoate (**86**) and 3-acetoxyoleanolic acid (**87**), molecular docking was performed. The autodock-vina program was used to explore the different binding modes of the target enzyme and the docked isolated compounds. Docking results were used to show the possible hydrogen bonding and hydrophilic interactions of the studied compounds and the target receptor. The crystal structure of α-glucosidase was downloaded from Protein Data Bank (PDB) www.rcsb.org (with the code 3WY1 Biological Assembly 1 as a PDB file) used as a template.[21]

2.4 References

1. Dae S. Jang; Muriel Cuendet; Alison D. pawlus; Leonardus B. S. Kardono; Kazoko Kawanishi; Norman R. Farnsworth; Harry H.S. Fong; John M. Pezzato; A. Douglas Kinghorn, *Phytochem*. 2004, 65, 345-350
2. Lin J.H.; Ishimatsu M.; Tanaka T.; Nonaka G.I.; Nishioka I., *Chem. Pharm. Bull*.,1990, 38, 1844–1851
3. D.S. Jang; M. Cuendet; M. Hawthorn; L.B. Kardono; K. Kawanishi, H.H.; Fong, R.G. Mehta; J.M. Pezzuto; A.D. Kinghorn; *Phytochem*., 2002, 61, 867–872
4. Do Thi Quynh; Le Tran Nguyen Vu; Doan Thi Mai Huong; Truong Bich Ngan; Nguyen Thi Hue; Tran Dang Thach; Pham Van Cuong, *Vietnam J. Chem.*, 2018, 56, 587-590
5. Suporn Phommart; Pakawadee Sutthivaiyakit; Nitirat Chimnoi; Somsak Ruchirawat; Somyote Sutthivaiyakit; *J. Nat. Prod.* 2005, 68, 927-930
6. Yana M. Syah; Emilio I. Ghisalberti; *Biochem. Syst. and Ecol*., 2015, 62, 151-154
7. Maria D.P.T.; Gunawan-Puteri; Jun Kawabata; *Food Chem*., 2010, 123, 384-389
8. Bruno Fogliani; Phila Raharivelomanana; Jean-Pierre Bianchini; Saliou Bouraima-Madjebi; Edouard Hnawia, *Phytochem*., 2005, 66, 241-247
9. Gao; H. Huang; Y. N. Xu; P. Y. Kawabata, *J. Food Chem*., 2007, 105, 628–634.
10. Da-SongYang; Jian-Guo Wei; Wei-Bing Peng; Shuang-Mei Wang; Chen Sun; Yong-Ping Yang; Ke-Chun Liu; Xiao-Li Li, *Fitoterapia*, 2014, 99, 261-266
11. Ishak Zakaria; Norizan Ahmat; Faridahanim M. jaafar; Aty Widya waruyanti, *Fitoterapia*, 2012, 83, 968-972

12. M. Shahinozzaman; Nozomi Taira; Takahiro Ishii; Mohammad A. Halim; M. Amzad Hossain; Shinkichi Tawata, *Molecules*, 2018, 23, 2479
13. Phanruethai Pailee; Suwannee Sangpetsiripan; Chulabhorn Mahidol; Somsak Ruchirawat; Vilailak Prachyawarakorn, *Tetrahedron*, 2015, 71, 5562-5571
14. Swapan K. Chaudhuri; Fekadu Fullas; Daniel M. Brown; Mansukh C. Wani; Monroe E. Wal; *J. Nat. Prod*., 1995, 58, 1-9
15. John A. Beutler; Yoel Kashman; Mark Tischler; John H. Cardellina; Glenn N. Gray; Michael J. Currens; Monroe E. Wall; Mansukh C. Wani; Michael R. Boyd, *J. Nat. Prod*, 1995, 58, 1039-1046
16. M. Maillard; C. O. Adewunmi; K. Hostettmann, *Phytochem.*, 1992, 31, 1321 -1323
17. Gohari A.R.; Saeidnia S.; Hadjiakhoondi A.; Abdoullahi M.; Nezafati M., *Med. Plants*, 2009, 8, 65-69.
18. Li-Shian Shi; Chao-Hsuan Wu; Te-Chun Yang; Chen-Wen Yao; Hang-Ching Lin; Wen-Liang Chang, *Fitoterapia*, 2014, 97, 184-191
19. En-Ji Cui; Jeon H. wang-Bo; Jong-Hwa; Park; Nam-In Baek; Jiyoung Kim; Seong Gil Hong; In Sik Chung, *Biotech. Lett*., 2013, 35, 1807-1815
20. Timoleon Maffo; Pascal Wafo; Ramsay Soup; Teoua Kamdem; Raduis Melong; Philip F. Uzor; Pierre Mkounga; Zulfiqar Ali; Bonavenature Tchaleu Ngadjui, *Phytochem. Lett*., 2015, 12, 328-331
21. Shen X.; Saburi W.; Gai Z.; Kato K.; Ojima-Kato T.; Yu J.; Komoda K.; Kido Y.; Matsui H.; Mori H.; Yao M., Acta Crystallogr. D Biol. *Crystallog*., 2015, 71, 1382-1391

CHAPTER 3

Phytochemical investigation of *Sapium integerrimum*

3.1 Introduction

Sapium integerrimum, (family Euphorbiaceae) commonly known as leonard, dulkerberry and dulkerbessie, is found in the areas of South Africa and Zimbabwe. This plant is a small tree nearly seven meter in height and consists of 120 species;[1] including *S. insigne,*[2] *S. japonicum,*[3] *S. indicum,*[4] *S. sebiferum,*[5] *S. glandulosum,*[6], *S. baccatum,*[14] *S. chihsianum*[7] and *S. discolor*.[7]

Plants of genus *Sapium* are reported to be used as ethnomedicines in various parts of Africa. For instance, the roots of *S. integerrimum* are used to treat gynaecological and obstetric disorders in women in Zulu and diabetes like symptoms by traditional healers.[8] Similarly, the barks and the seeds of *S. sebiferum* are used to cure digestive and excretory ailments.[9] The resin of *S. glandulosum* is to treat hernia by the traditional healers of Bolivia.[6] The fruits of *S. baccatum* have folk medicinal application in treating ulcer in Pahang.[11] *S. ellipticum* is used to cure cough, headache, pain in the chest, wounds anaemia, fever, guinea worms elephantiasis and rheumatic problems in Kenya, Tanzania and Burundi.[12] *S. integerrimum* has not been phytochemically investigated and based on the ethnomedicinal uses, this plant was evaluated for anti α- glucosidase activity in our lab. This was found to be active in this bioassay with the IC_{50} values of 31 ug/ml. It was decided to carry out phytochemical studies on the crude extract of this plant.

Previous phytochemical reports on genus *sapium* resulted in the isolation of diverse bioactive natural products. These natural products are phorbol esters,

di/triterpenoids, flavonoids and steroids.[13] For instance, chemical studies on *S. baccatum* yielded four triterpenoids, malaytaraxerate (**88**), taraxerol (**89**), taraxerone (**90**) lupeol (**91**);[10] a steroid, *β*-sitosterol (**92**); two coumarins baccatune A (**93**)[14] baccatune G (**94**), five tannins corilagin (**95**), 3,7-dimethyl-1-octen-3,6,7-triol-7-*O*-β-D-2,6-digalloylglucopyranoside (**96**), tercatain (**97**), chebulagic acid (**98**) and chebulinic acid (**99**).[15] Compounds (**90**-**92**) showed cytotoxicity against two kinds of cancer cell lines; human colorectal cancer (HT-29) and mammary breast cancer (MDA-MB) with the LC_{50} values of 2.99, 1.58 and 4.22 µg/mL. vincristine sulphate used as a positive control with the LC_{50} of 2.51 µg/mL.[12] Compound (**92**) exhibited stronger TNF-α inhibitory effect with the IC_{50} value 1503.51 pg/mL, whereas, compound (**93**) moderate activity (2165 pg/mL) compared to positive control quercetin which was 1674.44 pg/mL.

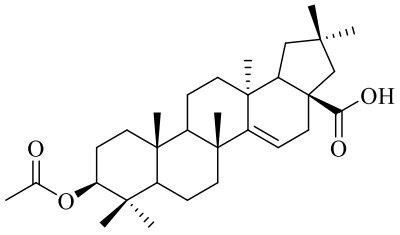

(**88**)

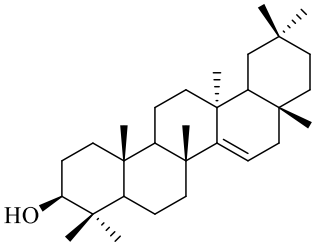

(**89**)

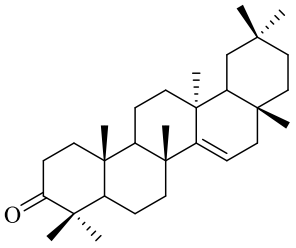

(**90**)

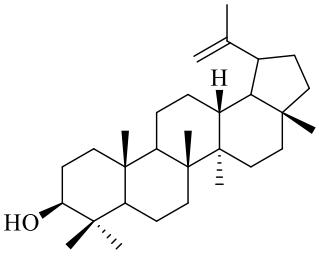

(**91**)

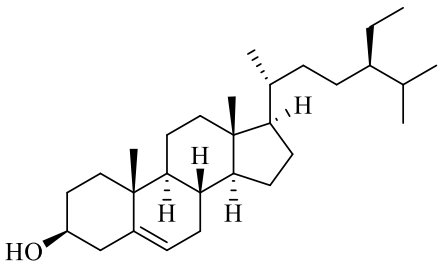

(**92**)

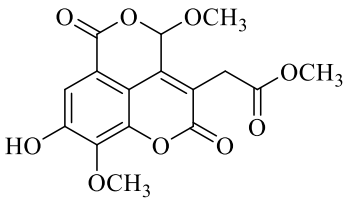

(**93**)

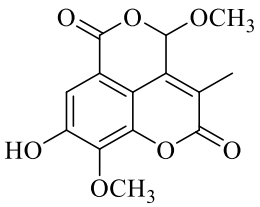

(**94**)

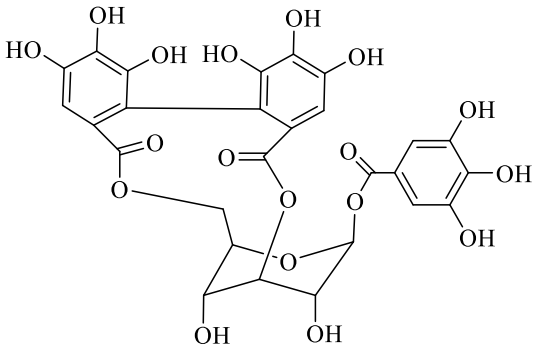

(**95**)

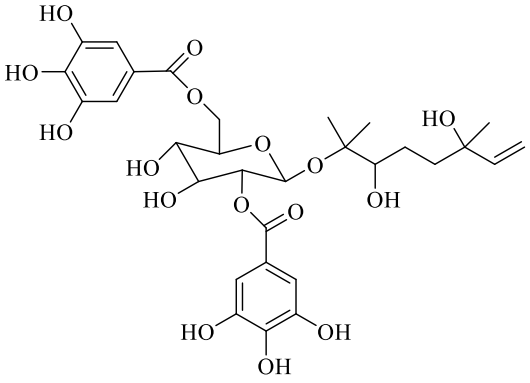

(**96**)

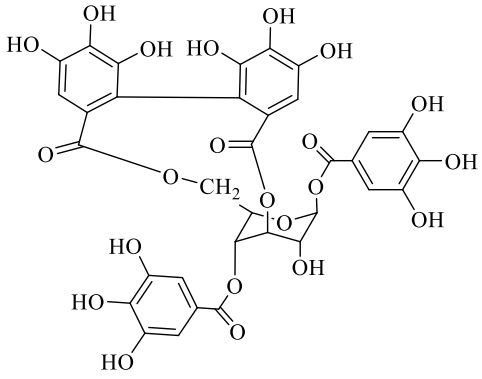

(**97**)

Compound (**95**) exhibited cytotoxicity against SMMC-7721, Bel-7402 and MHCC97-H cell lines with the values of 38.12, 39.7 and 37.05 µM. Compound (**95-99**) also showed anti-bacterial activity against different bacteria; it showed good activity against *Ralstonia solanacearum* with the MIC value of 52.1 µg/mL Whereas, compounds (**88**), (**95)**, (**98)** and (**99**) also showed moderate activity against *Xanthomonas arboricola* with MIC values of 88.3[14] 88.3, 52.1 and 53.1 µg/mL.[16] Compound (**98**) also exhibited weak antifungal activity against *Candida albicans* with the MIC value of 64 µg/mL.[15]

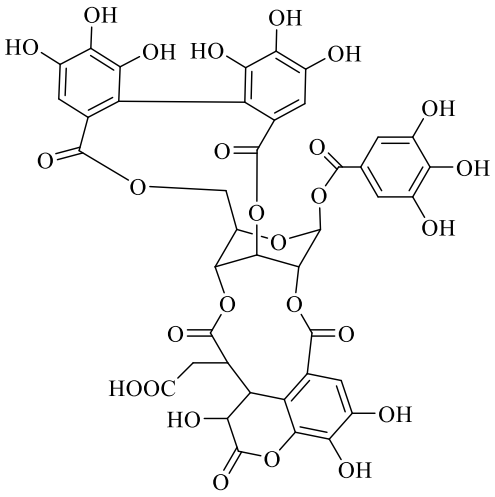

(**98**)

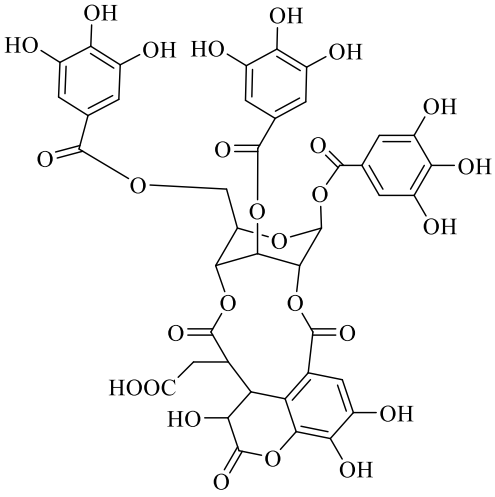

(**99**)

Similarly, chemical studies on *S. discolour* afforded four lignins, cleomiscosin A (**100**), balanophonin (**101**), americanin A (**102**), isoamericanin A (**103**);[17] a coumarin, (7′S,8′S)-sapiumin B (**104**); three triterpenoids, sapiumic acid C (**105**), Sapiumic acid E (**106**) and sapiumic acid F (**107**). These compounds exhibited inhibition of the

production of nitric oxide (NO) in lipopolysaccharide (LPS)-stimulated BV-2 microglial cells with the IC_{50} values of 4.74, 8.62, 11.37 2.13 , 4.2, 14.0, 2.7, and 1.7 μM respectively. Compared with minocycline (IC_{50}=1.51 μM) as a positive control.[17]

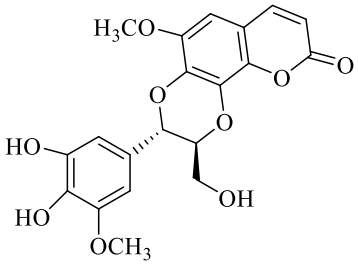

(**100**)

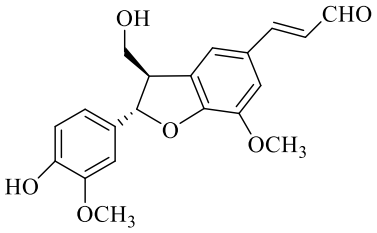

(**101**)

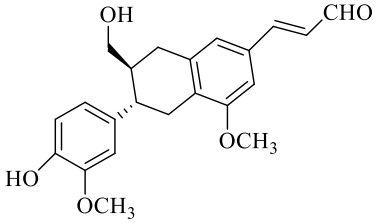

(**102**)

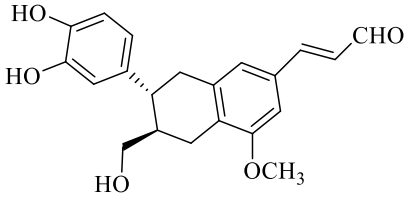

(**103**)

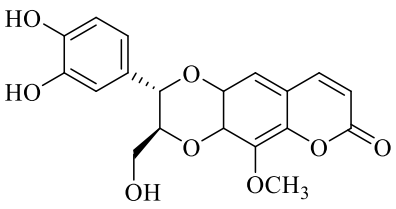

(**104**)

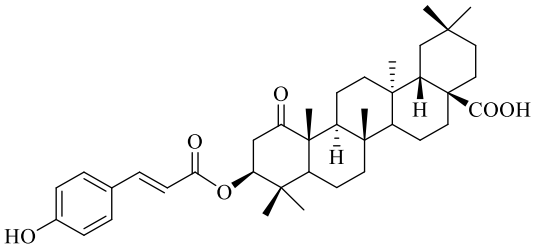

(**105**)

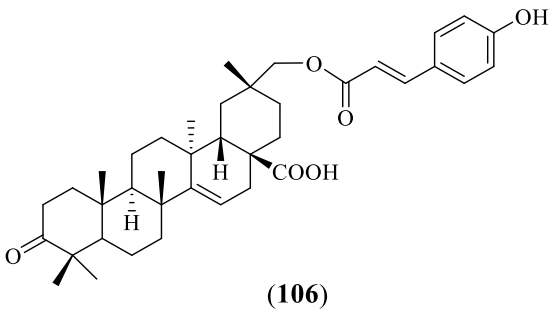

(**106**)

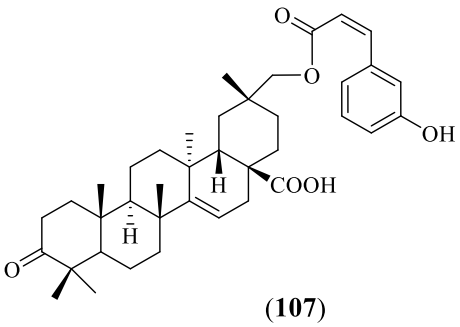

(**107**)

Similarly, chemical investigation on *S. haematospermum* yielded one flavanol glycosides, quercetin-3-O-β -D-glucopyranoside (**108**) and four terpenes, 3α hydroxylup-20 (29)-ene (**109**), cycloartanol (**110**), lecheronol A (**111**) and 3α -hydroxyolean-12-ene (**112**). These compounds exhibited cytotoxicity in vero cells and anti-mycobacterial activity against *Mycobacterium tuberculosis* H37Rv.[18] Their bioactivity data are listed in **Table 3.1** as follow.

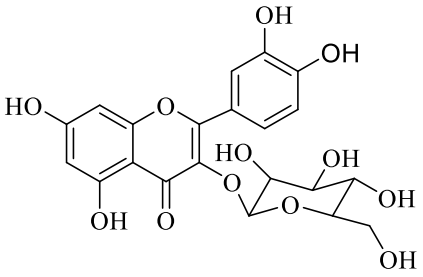

(**108**)

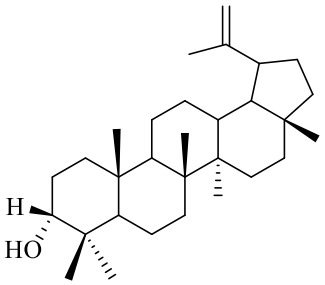

(**109**)

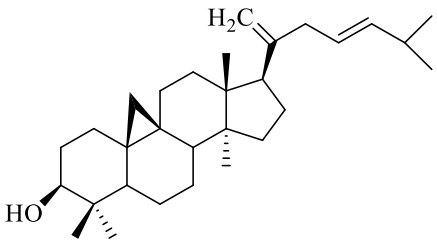

(**110**)

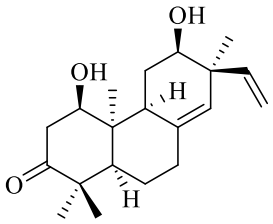

(**111**)

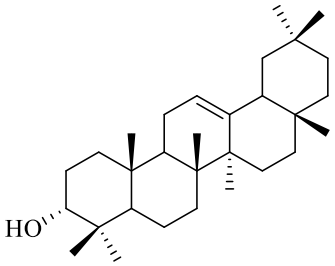

(**112**)

Table 3.1: Cytotoxicity and anti-mycobacterial inhibitory activities of compounds (**108-112**).

Compounds	Anti-mycobacterial activity (H37Rv) MIC=(µg/mL)	Cytotoxicity against vero cells IC_{50}=(µg/mL)
108	-	127.2
109	94	-
110	8	102.4
111	4	104.8
112	12.2	127.2
Refampin(+ve control)	0.06	
E coli K12(-ve control)		100

Although different species of genus *Sapium* have been phytochemically investigated, but the plant *Sapium integerrimum* is still unexplored. We have phytochemically investigated this plant against α-glucosidase. The ethyl acetate extract of this plant was active against α-glucosidase inhibitory assay. In this chapter, isolation,

characterization, bioactivity data and molecular docking results of compounds **113-115** will be described.

3.2 RESULTS AND DISCUSSION

The barks of *S. integerrimum* were collected from South Africa in 2007 and were shipped to the Department of Chemistry, University of Winnipeg, Winnipeg, Manitoba. The extraction procedure was the same as discussed in chapter **2** section: **2.3** (For details see experimental section). Its EtOAc extract was found to be active in α-glucosidase inhibition assay with an IC_{50} value of 31μg/ml. Our phytochemical investigation of bioactive fractions afforded three known compounds 12-(2'-*N*-methylaminobenzoyl)-4*β*,5,20-trideoxyphorbol-13-acetate (**113**), quercetin-3-*O*-α-rhamnopyranoside**(114)** and scpoletin (**115**). Compounds, **113-115** were evaluated for their anti α-glucosidase activity. Their structural elucidation with the aid of UV, IR and NMR spectroscopic studies and bioactivity data are described as follows.

3.2.1 Structure Elucidation of Compounds (113-115)

3.2.1.1 12-(2'-*N*-methylaminobenzoyl)-4*β*,5,20-trideoxyphorbol-13-acetate (113)

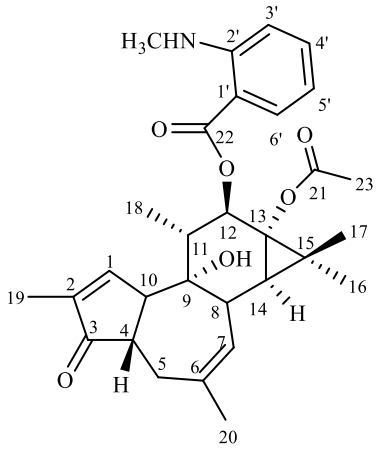

(**113**)

Compound (**113**) was isolated as colourless solid. Its UV spectrum showed maximum absorption at 247 and 360 nm indicating the presence of conjugated enone and benzoyl chromophores respectively.[19] The IR spectrum of **113** showed intense absorption at 1724 (ester C=O), 1685 (enone C=O) and 1452 (C=C) cm^{-1}.

The ^{1}H-NMR spectrum ($CDCl_3$, 400 MHz) of **113** showed the resonance of seven methyl groups at δ 1.24, 1.42, 1.15, 1.76 1.81, 2.13 and 2.96 due to H_3-16, H_3-17, H_3-18, H_3-19 H_3-20, C-13 acetyl methyl and N-CH_3 protons respectively. The chemical shifts of H_3-19 and H_3-20 were indicative of their allylic protons. A one-proton broad singlet resonated at δ 7.52 attributed to H-1. A doublet, integrating for one proton, observed at δ 5.74 (J = 10.3) was due to H-12. A doublet, integrating for one proton, appeared at δ 1.02 (J = 6.3) was ascribed to H-14. Whereas, H-3' and H-5', integrating for one protons

each, centered at δ 6.73 (J = 8.4) and 6.64 (J = 1.5, 8.5), respectively. Another double doublet resonated at δ 7.45 assigned to H-4'.

The COSY-45° spectrum of **113** showed vicinal couplings of H-1 (δ 7.53) with H-10 (δ 3.14) and allylic coupling with H-19 (δ 1.76). H-10 exhibited cross peak with H-4 (δ 3.06). H-11 (δ 2.17) exhibited vicinal coupling with H-12 (δ 5.74). Aromatic protons H-6' (δ 8.11) and H-3' (δ 6.73) showed ^{1}H-^{1}H spin correlations with H-4' (δ 7.45).

The ^{13}C-NMR spectrum ($CDCl_3$, 100 MHz) of **113** showed the resonances of all thirty carbons. Three carbonyl signals at δ 206.5, 174.0 and 166.2 were attributed to C-3, C-21 and C-22, respectively. Two allylic methyl carbons C-19 and C-20 resonated at δ 9.4 and 27.0, respectively. Whereas, C-16, C-17, C-18, $COCH_3$ and N-CH_3 methyls observed at δ 24.1, 15.9, 11.7, 21.1 and 28.6 respectively. C-3', C-4', C-5'and C-6' appeared at δ 110.9, 135.4, 114.2 and 131.7, respectively. A combination of APT and DEPT-135 spectra showed the presence of seven methyls, one methylene, twelve methines and ten quaternary carbons.

The heteronuclear single quantum coherence (HSQC) spectrum of **113** was recorded in order to establish ^{1}H/^{13}C one-bond shift correlations of all the hydrogen bearing carbons. H-1 (δ 7.09) showed cross peak with C-1 (δ 155.7). H-12 (δ 5.78) exhibited ^{1}H/^{13}C one-bond shift correlations with C-12 (δ 75.9). Complete ^{13}C-NMR chemical shift assignments and ^{1}H/ ^{13}C for one-bond shift correlations of all the hydrogen bearing carbons, determined from HSQC spectrum, are shown in **Table 3.2**.

The heteronuclear multiple bond correlation (HMBC) spectrum of **113** showed long-range ^{1}H/^{13}C couplings of H-2'/H-6' (δ 8.08) with C-4' (δ 132.7). H_3-20 (δ 1.81)

exhibited coupling with C-7 (δ 125.8) and C-6 (δ 142.9). A combination of UV, IR, 1D and 2D-NMR spectroscopic data led us to propose structure **113** to this compound. The $^{1}H/^{13}C$-NMR spectra were similar to those of reported 12-(2'-*N*-methylaminobenzoyl)-4*β*,5,20-trideoxyphorbol-13-acetate, reported in the literature.[19] Based on these spectroscopic data compound **113** was identified as 12-(2'-*N*-methylaminobenzoyl)-4*β*,5,20-trideoxyphorbol-13-acetate. This compound was previously reported from *Sapium indicum.*[19] This is the first time we have identified compound **113** from *S. integerrimum*.

Table 3.2 ^{1}H and ^{13}C NMR data for **113** and $^{1}H/^{13}C$ one-bond shift correlations as determined by HSQC.

Position	δH (J in Hz)	δC (multiplicity†)
1	7.52, br s	155.7(-CH-)
2	-	136.8 (-C-)
3	-	206.5 (-C-)
4	2.13, m	40.3 (-CH-)
5	2.30, 1.96, m	29.3 ($-CH_2-$)
6	-	142.9 (-C-)
7	4.94, br s	126.1 (-CH-)
8	2.14, m	42.9 (-CH-)
9	-	78.4 (-C-)
10	3.62, m	56.1 (-CH-)
11	2.17, m	43.2 (-CH-)
12	5.74, d (10.3)	75.9 (-CH-)
13	-	65.0 (-C-)
14	1.02, d (6.3)	37.5 (-CH-)
15	-	25.5 (-C-)
16	1.24, s	24.1 ($-CH_{3-}$)
17	1.34, s	15.9 (CH_{3-})
18	1.15, d (5.8)	11.7 ($-CH_{3-}$)
19	1.76, s	9.4 ($-CH_{3-}$)
20	1.81,s	27.0 ($-CH_{3-}$)
21	-	174.0 (-C-)
22	-	168.2 (-C-)
1’	-	152.3 (-C-)
3’	6.73, d (8.4)	110.9 (-CH-)
4’	7.45, dd (1.4, 8.3)	135.0 (-CH-)
5’	6.64, m	114.2 (-CH-)
6’	8.11, dd (1.6, 8.0)	131.7 (-CH-)
$COCH_3$	2.13, s	20.1 ($-CH_3-$)
$N-CH_3$	2.96, d (5.1)	28.6 ($-CH_3-$)

†Multiplicity was determined with the help of the ^{13}C-APT and DEPT-135 spectra

3.2.1.2 Quercetin-3-*O*-α-rhamnopyranoside (114)

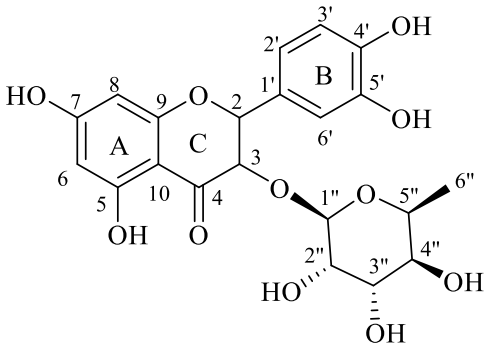

(**114**)

Compound (**114**) was isolated as a dark yellow solid. Its UV spectrum showed absorption at 259, 361 nm indicating the presence of conjugated enone and aromatic moiety.[20] The IR spectrum of **114** showed intense absorption bands at 1760 (C=O) and 3334 (OH) cm^{-1}.

The ^{1}H-NMR spectrum (acetone-*d6*, 400 MHz) of **114** exhibited two one-proton doublets at δ 6.48 (*J* = 2.2) and 6.28 (*J* = 2.2) due to H-8 and H-6, respectively. A downfield doublet, integrating for one proton, appeared at δ 7.53 (*J* = 2.0) and was assigned to H-2'. A one-proton double doublet at δ 7.40 (*J* = 8.2, 2.1), was attributed to H-6'. A one-proton doublet of ring B resonating at δ 6.99 (*J* = 8.2) was due to H-5', indicating tri-substituted benzene ring. Anomeric proton (H-1'') appeared, as a doublet at δ 5.53 (*J* = 1.3). The remaining sugar protons appeared as three separate peaks in the region of δ 3.33-4.24. The up-field doublet, integrating for three protons, resonated at δ 0.93 (*J* = 5.9), was attributed to H-6'' of the rhamnose moiety.

The COSY-45° spectrum of **114** was used to assign ^{1}H-NMR chemical shift assignments.H-6' (δ 7.40) showed cross peak with H-5' (δ 6.99). H-6 (δ 6.48) of ring A showed ^{1}H-^{1}H *meta* coupling with H-8 (δ 6.28). H-1'' (anomeric proton) (δ 5.53) exhibited vicinal coupling to H-2'' (δ 4.42) which in turn showed cross peak with H-3'' (δ 3.78). H-4''(δ 3.37) exhibited cross peaks with H-3'' (δ 3.78) and H-5'' (δ 3.45), which in turn exhibited ^{1}H-^{1}H spin correlations with H-6''(δ 0.93).

The ^{13}C-APT-NMR spectrum (acetone-*d6*, 100 MHz) of **114** displayed resonances for all twenty-one carbons. ^{13}C-APT spectra showed ten quaternary carbons, one methyl and ten methine carbons in **114**. The carbonyl signal appeared at δ 178.6. The ^{13}C signals at δ 164.7, 161.9, 158.1, 157.2, 148.6, 145.1, 135.0, 121.7 and 104.6 attributed to C-7, C-5, C-9, C-2, C-4', C-3', C-3, C-1' and C-10, respectively. C-6', C-5', C-2', C-6 and C-8 methine carbons resonated at δ 121.7, 115.7, 115.0, 98.5 and 93.4, respectively. The C-5'', C-4'', C-2'', C-3'' and C-1'' of rhamnose moiety resonated at δ 70.5, 70.6, 70.7, 71.9, 102.3, respectively.

The heteronuclear single quantum coherence (HSQC) spectrum of **114** showed ^{1}H/^{13}Cone-bond shift correlation of H-6 (δ 6.28) with C-6 (δ 98.6). H-8 (δ 6.48) exhibited cross peak with C-8 (δ 93.4). Complete ^{1}H- and ^{13}C-NMR chemical shift assignments and ^{1}H/^{13}C one-bond shift correlations of all the hydrogen bearing carbons, determined from HSQC spectrum, are shown for **114** in **Table 3.3**.

The heteronuclear multiple bond correlation (HMBC) spectrum of **114** showed long-range ^{1}H/^{13}C couplings of H-6' (δ 7.40) with C-4' (δ 148.6). H-8 (δ 6.48) exhibited coupling with C-10 (δ 104.6) and C-6 (δ 98.6) indicated that C-8 was *ortho* to C-10 and *meta* to C-6. A combination of UV, IR and NMR spectroscopic data led us to identify

compound (**114)** as quercetin-3-*O*-α-rhamnopyranoside. This was further confirmed by comparing the ^{1}H and ^{13}C-NMR spectroscopic data of 37 with those of quercetin-3-*O*-α-rhamnopyranoside reported in the literature.[20-21] This compound was previously reported from *Bladhia japonica*[22] and *Dendrophthoe falcate.*[23] This is the first time we have identified compound **114** from *S. integerrimum*.

Table 3.3 ^{1}H and ^{13}C NMR data for **114** and $^{1}H/^{13}C$ one-bond shift correlations as determined by HSQC.

Position	δH (J in Hz)	δC (multiplicity†)
1	-	-
2	-	157.2 (-C-)
3	-	135.0 (-C-)
4	-	178.6 (-C-)
5	-	161.9 (-C-)
6	6.28, d (2.2)	98.6 (-CH-)
7	-	164.7 (-C-)
8	6.48, d (2.2)	93.4 (-CH-)
9	-	158.1 (-C-)
10	-	104.6 (-C-)
1’	-	121.7 (-C-)
2’	7.53, d (2.2)	115.0 (-CH-)
3’	-	145.1 (-C-)
4’	-	148.6 (-C-)
5’	6.99, d (8.2)	115.7 (-CH-)
6’	7.40, dd (8.2, 2.1)	121.7 (-CH-)
1’’	5.53, d (1.3)	102.3 (-CH-)
2’’	4.42,dd (4.28, 1.56)	70.9 (-CH-)
3’’	3.78, dd (9.6, 3.6)	71.9 (-CH-)
4’’	3.37, m	70.6 (-CH-)
5’’	3.45, m	72.2 (-CH-)
6’’	0.93, d (5.9)	16.9 ($-CH_3-$)

†Multiplicity was determined with the help of the ^{13}C-APT spectra.

3.2.1.3 Scopoletin (115)

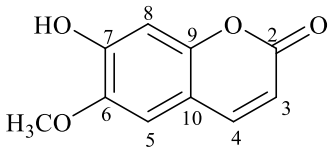

(**115**)

Compound (**115**) was isolated as white yellowish crystals. Its UV spectrum absorptions at 229, 255, 296 and 344 nm indicated that compound **115** contained coumarin-type chromophore[24] (α, *β* unsaturated carbonyl and aromatic ring). The IR spectrum of this compound showed intense absorption at 3335 (OH) and 1708 (C=O) cm^{-1}.

The ^{1}H-NMR spectrum ($CDCl_3$, 400MHz) of (**115**) showed two one-proton AB doublets at δ 7.63 (*J* = 9.6 Hz) and 6.29 (*J* = 9.6 Hz) due to H-4 and H-3, respectively. Two singlets, integrating for one proton each, at δ 6.94 and 6.87, were assigned to H-8 and H-5, respectively. The multiplicity of these signals suggested the *para* position of these protons. A three proton singlet centered at δ 3.97 was due to the C-6/*O*-methyl protons.

The COSY-45° spectrum of **115** showed vicinal coupling of H-3 (δ 6.29) with H-4 (δ 7.63). H-5 (δ 6.94) exhibited *para* coupling with H-8 (δ 6.87).

The ^{13}C-APT-NMR spectrum ($CDCl_3$, 100MHz) of **115** showed resonances of all ten carbons. A signal at δ161.5 was due to C-2 carbonyl carbon. Four quaternary carbons appeared at δ111.6, 150.9, 149.7 and 144.0 were ascribed to C-10, C-9, C-7 and C-6, respectively. C-4, C-3, C-8 and C-5 methine carbons resonated at δ 143.3, 113.5, 107.6

and 103.3, respectively. Previously, the two isomers; scopoletin and isoscopoletin were distinguished by melting points,[21] which could be unreliable. The position of C-6 - methoxy group was determined with the aid of C-6/O-methyl protons (δ 3.97) showed cross- peak with H-5 (δ 6.87). The latter proton exhibited spatial coupling with H-4 (δ 7.63). The ROESY spectroscopic data helped to identify compound (**115**) as scopoletin. The heteronuclear single quantum coherence (HSQC) spectrum of **115** was acquired in order to establish $^{1}H/^{13}C$ one-bond shift correlations of all the hydrogen bearing carbons. H-3 (δ 6.29) exhibited $^{1}H/^{13}C$ one bond shift correlation with C-3 (δ 113.7). H-4 (δ 7.63) showed cross peak with C-4 (δ 143.3). Complete ^{1}H- and ^{13}C-NMR chemical shift assignments and $^{1}H/^{13}C$ one-bond shift correlations of all the hydrogen bearing carbons, determined from HSQC spectrum, are shown for **115** in **Table 3.4**.

The heteronuclear multiple bond correlation (HMBC) spectrum of **115** showed long-range $^{1}H/^{13}C$ couplings of H-4 (δ 7.63) with C-10 (δ111.6) and C-5 (δ 103.3). H-5 (δ 6.94) exhibited coupling with C-9 (δ 150.9) and C-4 (δ 143.3). A combination of UV, IR, 1D and 2D-NMR spectroscopic data led us to propose structure **115** to this compound. The ^{1}H and ^{13}C-NMR spectra were similar to those of reported scopoletin reported in the literature.[24] Based on these spectroscopic data compound **115** was identified as scopoletin. This compound was previously reported from *Senecio nutans*,[25] *Artemisia argyi*,[26] *Sinomonium acutum*,[27] *Hevea brasiliensis*,[28] *and Sopgora mollis.*[29] This is the first time we have identified compound **115** from *S. integerrimum*.

Table 3.4 ^{1}H and ^{13}C NMR data for **115** and $^{1}H/^{13}C$ one-bond shift correlations as determined by HSQC.

Position	δH (J in Hz)	δC (multiplicity†)
1	-	-
2	-	161.5 (-C-)
3	6.29, d (9.6)	113.7 (-C-)
4	7.63, d (9.6)	143.3 (-CH-)
5	6.94, s	103.3 (-CH-)
6	-	144.0 (-C-)
7	-	149.7 (-C-)
8	6.87, s	107.6 (-CH-)
9	-	150.9 (-C-)
10	-	111.6 (-C-)
$-OCH_3$	3.96, s	56.7 ($-CH_3$-)

†Multiplicity was determined with the help of ^{13}C-APT spectra.

3.2.1.4 α-Glucosidase Inhibitory Activity of Compounds (113-115)

α-Glucosidase inhibitory potencies of compounds (**113-115**) was determined and these compounds were found to be active with IC_{50} values of 0.57, 0.74 and 1.124 mM, respectively. The reported IC_{50} value for compound **114** is 0.151 mM,[30] which is comparable to the determined IC_{50}value. Acarbose, was used as a positive control in this assay with the IC_{50} value of 0.45 mM. The % inhibitory activities of all the compounds (**113-115**) are given in **Figure: 3.1**

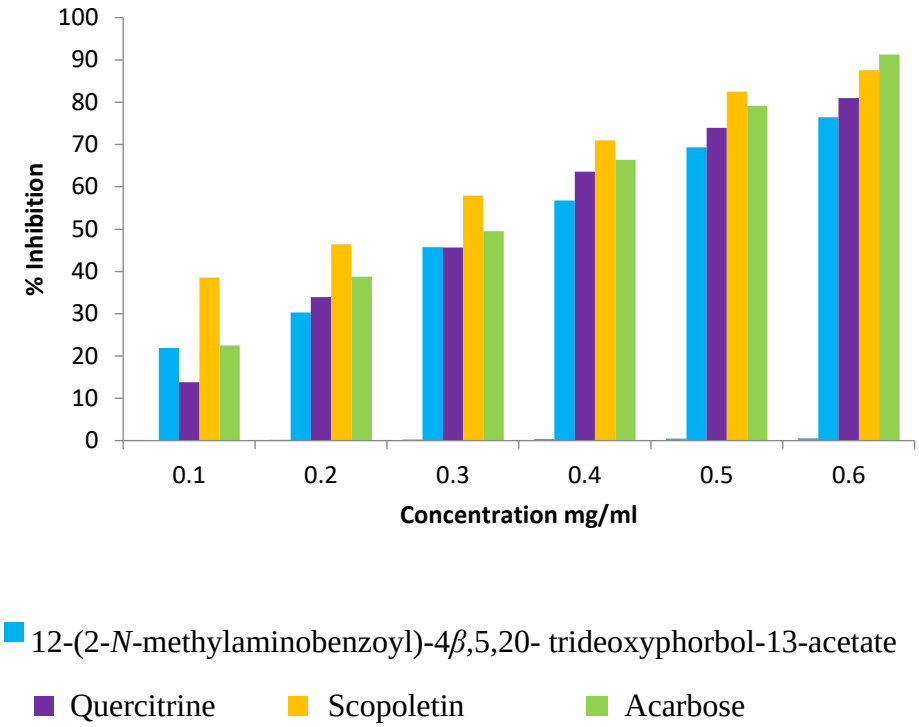

Figure: 3.1 % Inhibitory activity of compounds **113-115** and acarbose.

3.2.1.5 Molecular Docking

Molecular docking studies were also conducted to understand the interactions of compounds **113-115** with α-glucosidase enzyme. Compound **113** showed the interaction of C-16 and C-23 methyl with the 236-tryptophan and 217-proline via hydrophobic interaction. The Gibbs free energy binding (ΔG) (–5.5 kcal/mol) favours the compound **113** enzyme-complex interaction. Compound **114** exhibited highest binding energy (ΔG) of –7.2 kcal/mol. The molecular docking scores, the key interactions and the types of bonding of all three compounds **113-115** are given in **Table 3.5.**

Table 3.5 Docking scores (kcal/mol) and key interactions of compound **113-115** and acarbose in the α-glucosidase enzyme.

Ligands	**Docking score (ΔG)** kcal/mol	**Key interactions**	**Types of Bonds**
113	–5.5	236-tryptophan, 217-proline	Hydrophobic bonding
114	–7.2	439-aspartic acid, 444-threonine, 46-asparagine	Hydrogen bonding
115	–6.2	48-aspartic acid	Hydrogen bonding
Acarbose (positive control)	–6.0	514-histidine, 446-asparagine, 449-arginine, 46-asparagine, 439-aspartic acid	Hydrogen bonding

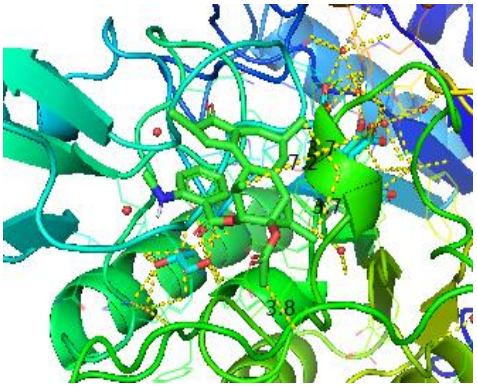

(**A**)

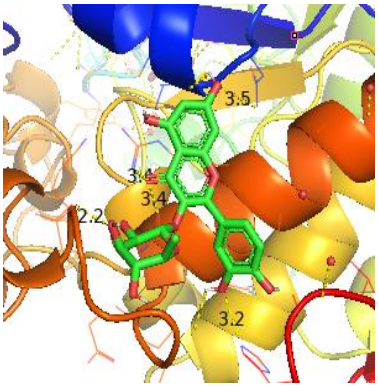

(**B**)

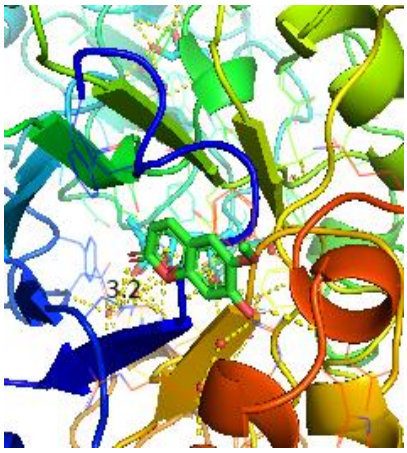

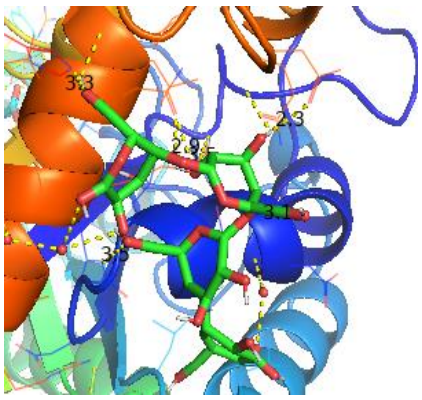

(**C**) (**D**)

Figure: 3.2 Binding interactions of compounds **113** (**A**), **114** (**B**), **115** (**C**) and acarbose (**D**) in α-glucosidase enzyme.

Compound **114** showed three different interactions with the enzyme. These are with subunits 439-aspartic acid, 444-threonine and 46-asparagine, with the distance of 2.2, 3.4 and 3.5 Ǻ. The Gibbs free energy compound **114** and enzyme complex interaction showed binding energy (ΔG) –7.2 kcal/mol. Compound **115** also showed interaction with subunit 48-aspartic acid with the distance of 3.2 Ǻ. The maxium Gibbs free energy binding (ΔG) for this compound is –6.2 kcal/mol shown in **Figure 3.1**. **Table 3.4** summarized all the docking scores, key interactions and types of bonding of compound **113-115.**

3.3 EXPERIMENTAL

3.3.1 General Experimental Conditions

The general experimental procedures of chromatography and spectroscopy were the same as discussed in chapter 2 (section 2.3.1)

3.3.2 Plant Material

The barks of *Sapium integerrimum* were collected from Umbalanga Rocks Nature Reserve, in Natal Kawa Zulu, the Republic of South Africa. Specimen was collected and identified by M. Khipheni A. Ngwenya, on Feb. 14, 2007. The voucher specimen (132294) was deposited in the Kawa Zulu-Natal Herbarium. The plant was dried and grounded for use in this experiment.

3.3.3 Extraction and Isolation

The barks of *S. integerrimum* (10 kg) were crushed into powder and extracted with methanol (10L) three times for two days each time. The extract was separated using column chromatography which was carried out by graduate MSC student (Department of Chemistry, University of Manitoba) Abin James and April McElrea. The crude extract of *S. integerrimum* was then chromatographed over silica gel using hexane-chloroform-methanol (0-100%) and chloroform-methanol (0-100%) as a mobile phase. This produced several fractions that were combined together based on TLC results to yield 15 fractions.

S. integerrimum crude was extracted with ethyl acetate and run the primary column was done by April McElrea. All those primary column fractions were tested against different solvent system and selected SIF15 loaded onto a silica gel column

(230-400 mesh, Merk), eluted with hexane-ethyl acetate (0-100%) and ethyl acetate: methanol (0-100%). That yielded several fractions and pooled together on the bases of analytical TLC results. SIF8 again loaded onto the silica column run with ethyl acetate: methanol (0-100%) yielded several fractions once again, pooled on the bases of TLC results. A fraction (55.4 mg) eluted at 8% methanol had the major compound which was separated by preparative TLC using $CHCl_3$: MeOH: acetic acid (9.3:0.7:0.1) as a mobile phase to afford quercetin-3-*O*-α-rhamnopyranoside (**114)** (8.2mg). Another fraction (SIF7) from the primary column was eluted with hexane: dichloromethane (0-100%) and dichloromethane: methanol (0-100%) afforded several fractions, pooled together. SIF4 was again loaded onto the column and afforded 9 fractions. One of the fraction SIF2 showed a major compound which were separated by preparative TLC using hexane-ethyl acetate as a mobile phase to afford one phorbol ester; (12-(2'-*N*-methylaminobenzoyl)-4*β*,5,20- trideoxyphorbol-13-acetate (**113)** (2.9 mg). Scopoletin (**115)** (135 mg) was isolated from one of the frcation of SIF7 and was purified by preparative TLC using hexane: ethyl acetate (7.5:2.5) as a mobile phase.

(12-(2'-*N*-methylaminobenzoyl)-4*β*,5,20-trideoxyphorbol-13-acetate(**113**); colourless solid, 2.9 mg; UV ($CHCl_3$): λmax 247, 360 nm; IR ($CHCl_3$): vmax 3338, 1724, 11685 cm-^{1}; ^{1}H-NMR ($CDCl_3$, 400 MHz) = see Table 3.1. ^{13}C-NMR ($CDCl_3$, 100 MHz) = see Table 2.3.

Quercetin-3-*O*-α-rhamnopyranoside (**114**); dark yellow solid, 8.2 mg; UV (MeOH): λmax 259, 361 nm; IR ($CHCl_3$): vmax 3334, 1760 cm-^{1}; ^{1}H-NMR (*acetone-d6*, 400 MHz) = see Table 3.2; ^{13}C-NMR (*acetone-d6*, 100 MHz) = see Table 3.2.

Scopoletin (**115**); White yellowish crystals, 135 mg; UV ($CHCl_3$): λmax 229, 255, 296, 344 nm IR ($CHCl_3$): vmax 3335, 1708 cm^{-1}; ^{1}H-NMR (*acetone-d6*, 400 MHz) = see Table 3.3; ^{13}C-NMR (*acetone-d6*, 100 MHz) = see Table 3.3.

3.3.4 Assay for α-Glucosidase Inhibition

The procedure adapted for the bioassay of the isolated compounds (**113-115**) is the same as discussed in chapter 2 section: 2.3.4.

3.3.5 Molecular Docking

Molecular Docking is the same as discussed in chapter 2 section 2.3.5.

3.4 References:

1. Schmelzer, GH.; Gurib-Fakim; Medicinal Plants, Backhuys, CTA Wageningen, Netherlands, 2008, p 145
2. Hari Prasad Devkota; Purusotam Basnet; Shoji Yahara, *J. Natural Med.,* 2010, 64, 191-193
3. Omas G. Back; Brian P.Dyck, *Tetrahed. Lett.,* 1992, 33, 4725-4726
4. Stephen E. Taylor; Elizabeth M. Williamson; Fred J. Evans, *Phytochem*., 1983, 22, 1231-1233
5. Sumei Huang; Toshihiro Fujioka; Miyako Yoshida; Kanji Ishimaru, *J. Natural Med.,* 2007, 61, 339-341
6. Carlos Henrique Tabosa Pereira da Silva1; Tadeu José da Silva Peixoto Sobrinho1; Antônio Marcos Saraiva; Maria Nelly Caetano Pisciottano; Elba Lúcia Cavalcanti de Amorim, *J. Med. Plant Res.,* 2012, 6, 4766-4771
7. L.M.R. Al Muqarrabun; N. Ahmatn; S. Ruzaina S. Aris, *Ethnopharm*., 2014, 155, 9-20
8. X.Z. Lai; Y.B. Yang; X.L. Shan, *Economic Bot*., 2004, 307-320
9. Z. Hajdu; J. Hohmann, *Ethnopharm.,* 2012, 838-857
10. L.M. Ramadhan Al Muqarrabuna; Norizan Ahmad; S. Ruzaina S. Arisa; Norhazana Norizana; Nurdiana Shamsulrijala; Farida Z.M. Yusofa; M. Nazip Suratmana; M. Izwan M. Yusof; Fatimah Salim, *Natural pro. res*., 2014, 28, 1003-1009
11. Neuwinger H.D., African Ethnobotany Poison and Drugs: Chemistry Pharmacology Toxicology, Chapman Hall, London, 1994, p 645
12. Yunus Ahmad; Md. Hussain Sohrab; Sharif M.Al-Reza; Faqir Shahidulla Tareq; C.M. Hasan; M.A. Sattar, *Food and Chem. Toxicol.,* 2010,48, 549-552

13. Yuan Deng; Xudan Li; Xuan Li; Zfflzhong Zheng; Wen Huang; Lianghua Chen, *Oncology rep.*,39, 2018, 2545
14. Ting Li; Shanshan Wang; Peihong Fan; Hongxiang Lou, *Fitoterapia*, 134, 2019, 435-442
15. Thuy Thu Vu; Hun Kim; Vu Khac Tran; Hoang Dinh Vu; Tien Xuan Hoang; Jae Woo Han; Yong Ho Choi; Kyoung Soo Jang; Gyung Ja Choil; Jin-Cheol Kim, *PLoS ONE*, 7, 2017, 1-12
16. Gui-Jie Zhang; Qi-Ming Pan; Yong-Li Zhang; Hai-Bing Liao; Yan-Qiu Yang; Yue Hou; Dong Lian, *J. Nat. Prod.*, 2018, 81, 2251−2258
17. Yong-Li Zhang;Qi-Min Pan;Hai-Bing Liao;Jiang-Ke Qin;Ning Li;Dong Liang;Gui-Jie Zhang,*Fitoterapia*, 2018, 133, 17-22
18. Girma M. Woldemichael; Maria-Teresa Gutierrez-Lugo; Scott G. Franzblau;Yuehong Wang; Enrique Suarez; Barbara N. Timmermann, *J. Nat. Prod. Chem.*, 2004, 67, 598-603
19. Parinuch Chumkaew; Chatchanok Karalai; Chanita Ponglimanont; Kan Chantrapromma, *J. Nat. Prod*., 2003, 66, 540-543
20. Chung-Oui H.; Hyun Ah LEE; Chae Hong Rhee; Se-Young Choung; Kwang-Won Lee, *Biosci. Biotechnol. Biochem.*, 2013, 77, 58–64
21. Xiaofeng Ma; Weixi Tian; Linhuan Wu; Xueli Cao; Yoichiro Ito, *J. Chromato*., A, 2005, 1070, 211-214
22. M Aritomi, *Yakugaku Zasshi,* 1963, 83, 659-661

23. Md Shihab Hasan; Md Iqbal ahmed; Sukla Mondal; Shaikh Jamal Uddin; Mohammad Mededi Masud; Samir Kumar Sadhu; Masami Ishibashi, *Oriental Pharm. and Exp. Med*., 2006, 6, 355-360
24. Bayoumi S. A. L.; Rowan M. G.; Beeching J. R.; Blagbrough I. S., *Phytochem*., 2010, 71, 598-604
25. Claudio Parraa; Emilio Sotoa; Gloria Leonb; Cristian O. Salasc; Michael Heinrichd; Carlos Echiburu-Chaua, *J. Nat. Prod. Res.*, 2018, 32, 719–722
26. Michael Adams; Thomas Efferth; Rudolf Bauer, *Plant. Med*., 2006; 9, 862-864
27. Shaw CY; Chen CH.; Hsu CC.; Chen CC.; Tsai YC., *Phytother. Res.*, 2003, 17, 823-825
28. W.P.K. Silva; S. A. Deraniyagala; R. L. C. Wijesundera; E. H. Karunanayake; U. M. S. Priyanka, *Mycopatholo.*, 2002, 153, 199-202
29. Zhang, GP.; Xiao, ZY.; Rafique, J.; Arfan, M.; Smith, P. J.; Lategan, C. A.; Hu, LH. *J. Nat. Prod.*,2009, *72*, 1265-1268
30. Munjur Ali Sheliya; Begum Rayhana; Abuzer Ali; Krishna Kollapa Pillai; Vidhu Aeri; Manju Sharma Showkat R. Mir, *J. Ethnopharm*., 2015, 176, 1-8

4 Conclusion

During this study, we carried out phytochemical investigation of two medicinally important plants: *M. capensis* and *S. integerrimum.* Methanolic extracts of *M. capensis* resulted in the isolation of two known compounds; 3α-Hydroxyaleuritolic acid 2-*p*-hydroxybenzoate (**86**) and 3-acetoxyoleanolic acid (**87**). Chemical investigation of ethyl acetate extract of *S. integerrimum* afforded three known compounds; 12-(2'-*N*-methylaminobenzoyl)-4*β*,5,20-trideoxyphorbol-13-acetate (**113**), quercetin-3-*O*-α-rhamnopyranoside (**114**) and scopoletin (**115**).

All of these compounds exhibited strong to moderate α-glucosidase inhibition activity. The bioactivities of these compounds are listed in **Table 4.1.** Compound **113** was significantly active in this bioassay with the IC_{50} value of 0.57 mM. This activity is comparable with that of acarbose (IC_{50} = 0.45 mM). The higher potency was hypothesized due to the presence of amine or the ester functionalities in **113.** This was further supported by the docking experiment in which **113** showed interactions of amine and ester with 439-aspartic acid, 444-threonine and 46-asparagine, shown in **Table: 3.5**

Table 4.1. Results of the α-glucosidase inhibition assay on compounds **86** and **113-115** isolated from *M. capensis* and *S. integerrimum*, respectively.

Compounds	IC_{50} values (mM)
86	2.17
113	0.57
114	0.74
115	1.124
Acarbose	0.45

APPENDIX

3*α*-Hydroxyaleuritolic acid 2-*p*-hydroxybenzoate (86)

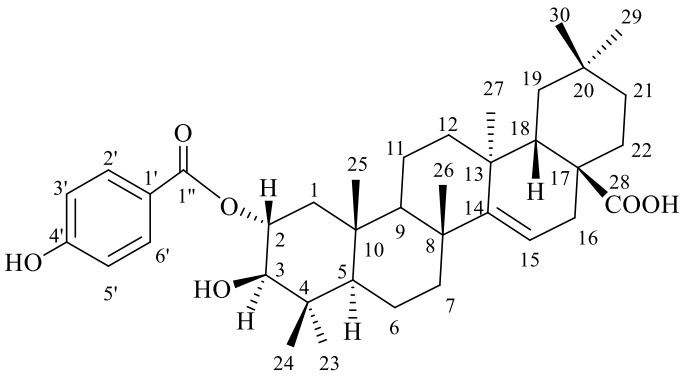

(**86**)

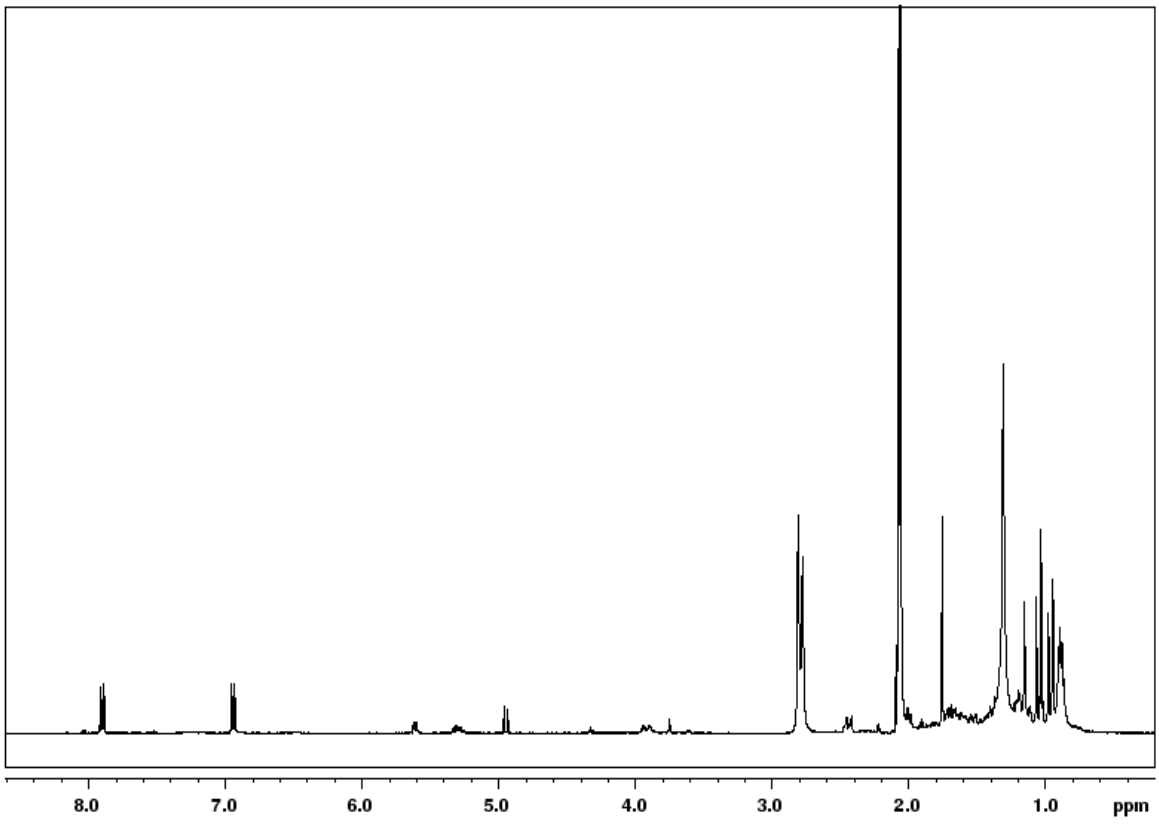

A1: ^{1}H-NMR spectrum of compound (**86**) in acetone-d_6.

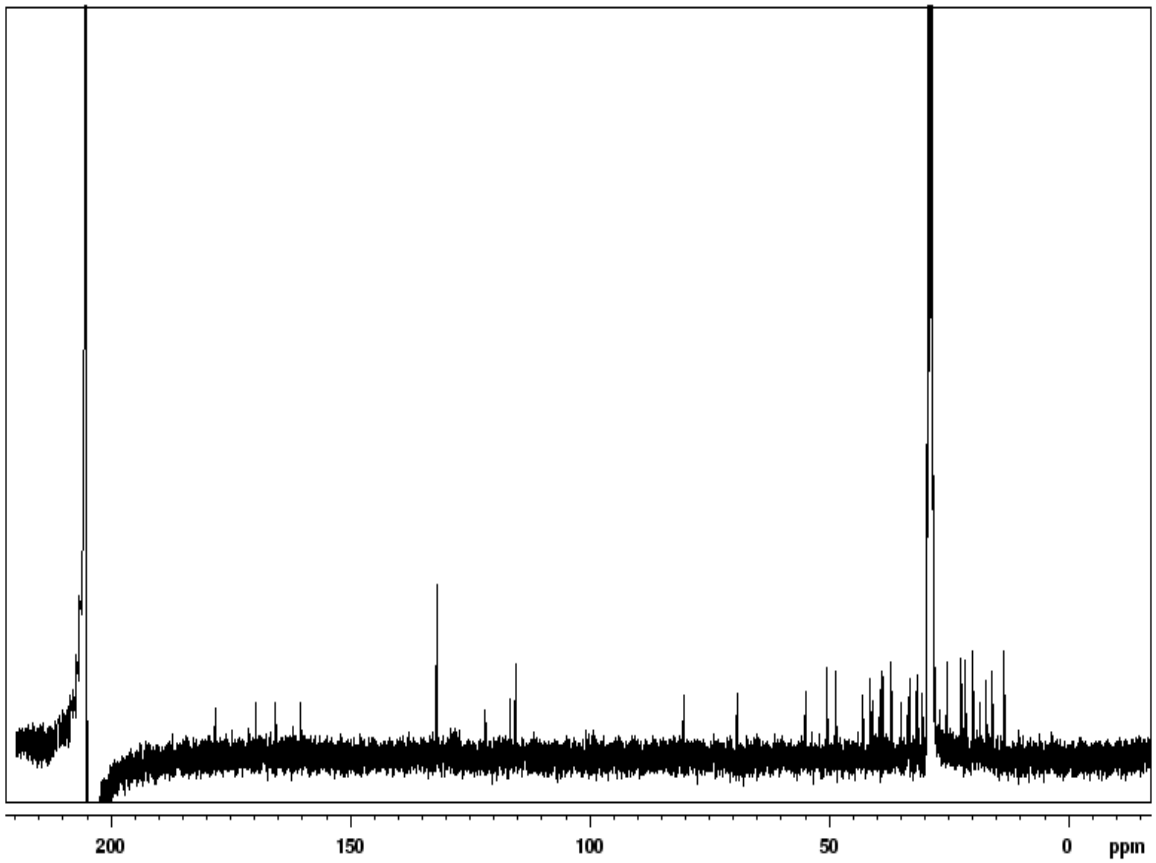

A2: ^{13}C-NMR spectrum of compound (**86**) in acetone-d_6.

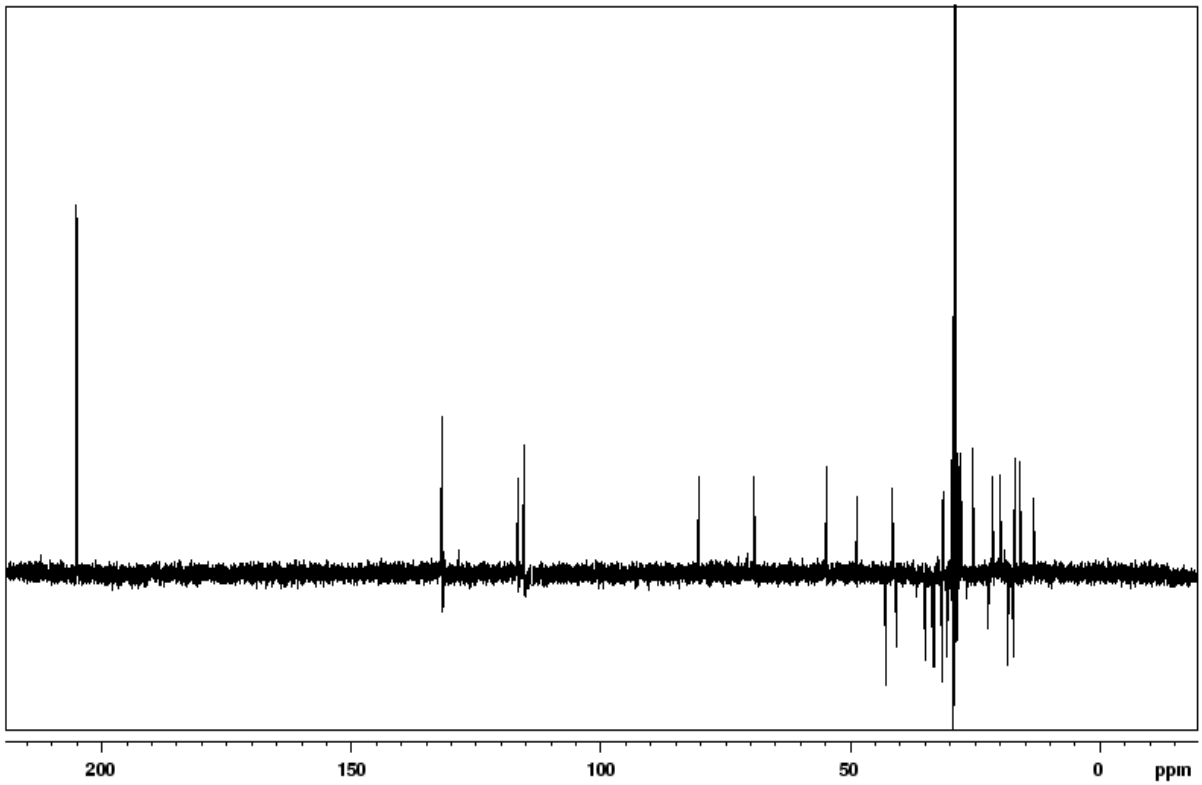

A3: DEPT 135 spectrum of compound (**86**) in acetone-d_6

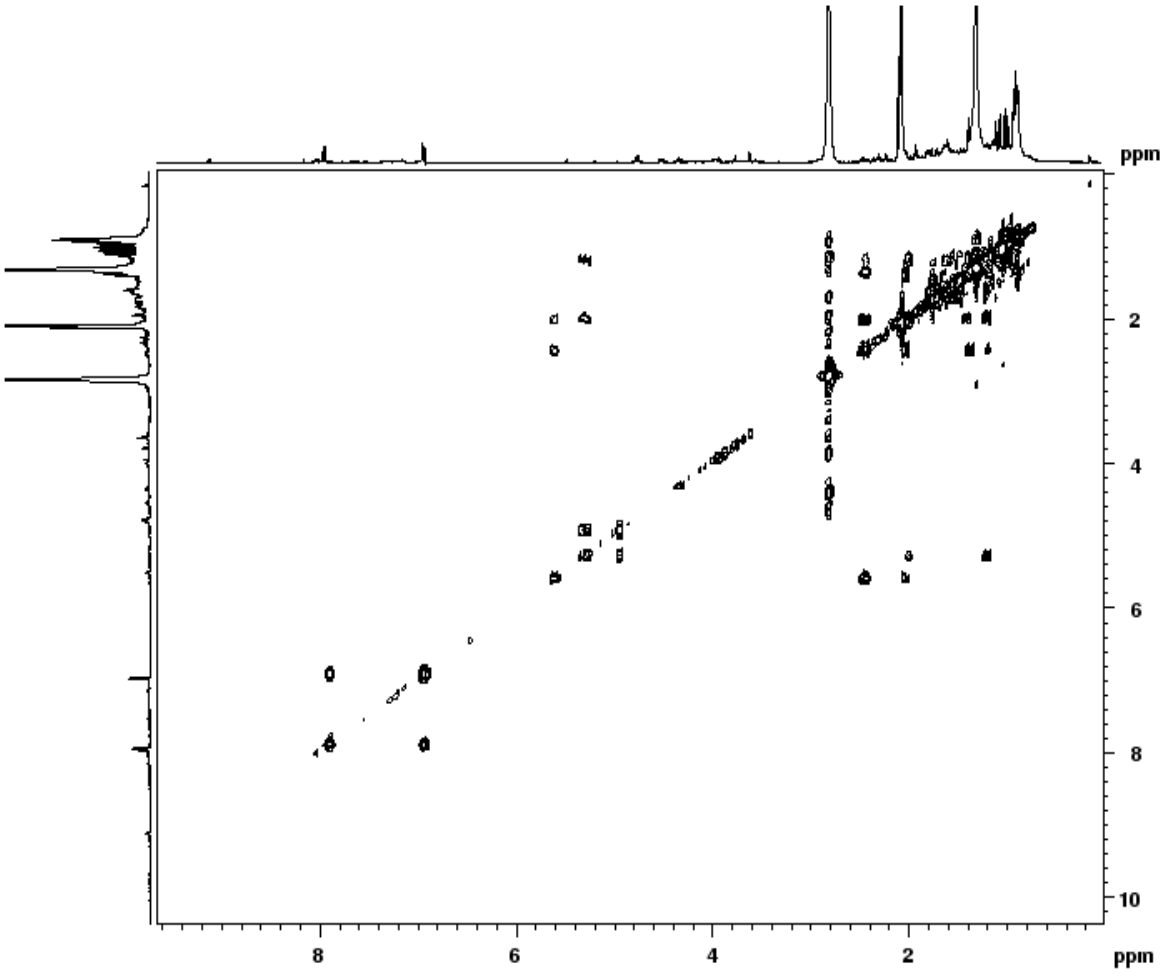

A4: COSY spectrum of compound (**86**) in acetone-d_6

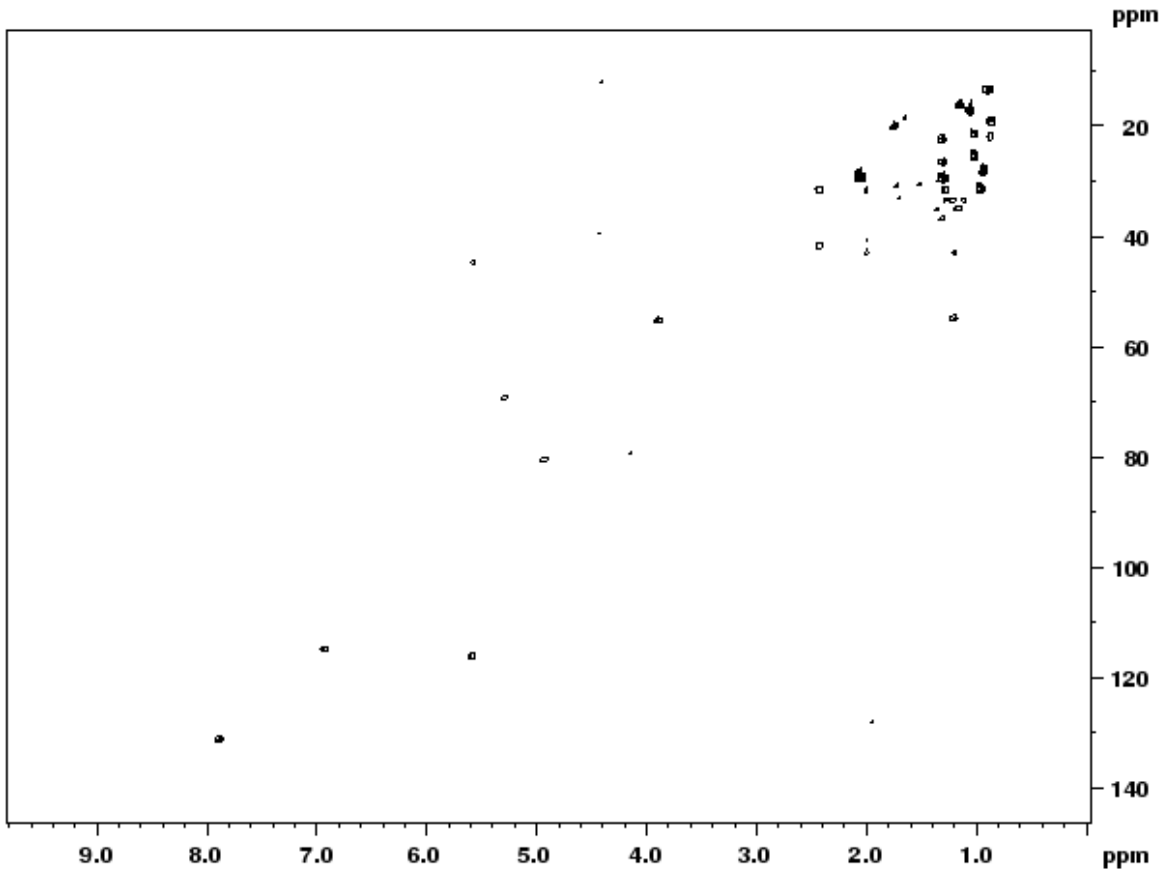

A5: HSQC spectrum of compound (**86**) in acetone-d_6

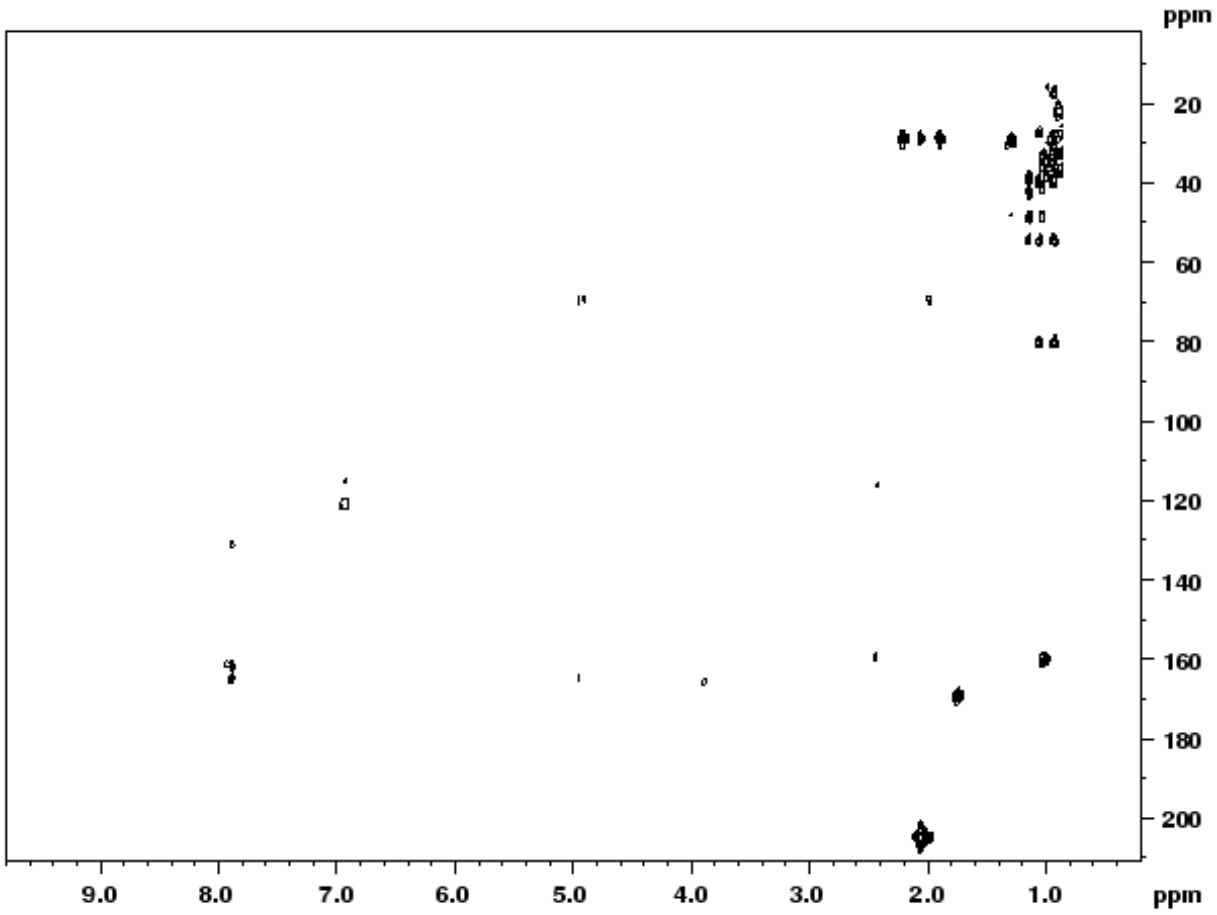

A6: HMBC spectrum of compound (**86**) in acetone-d_6

3-Acetoxyoleanolic acid (87)

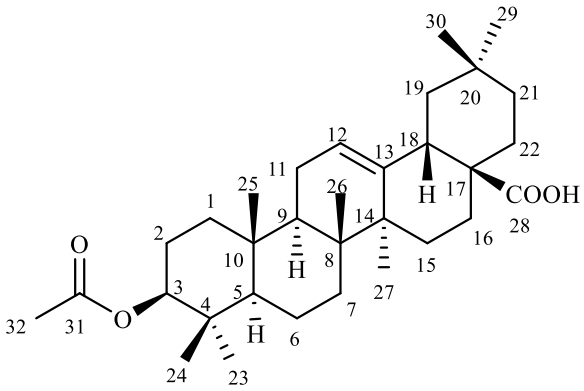

(**87**)

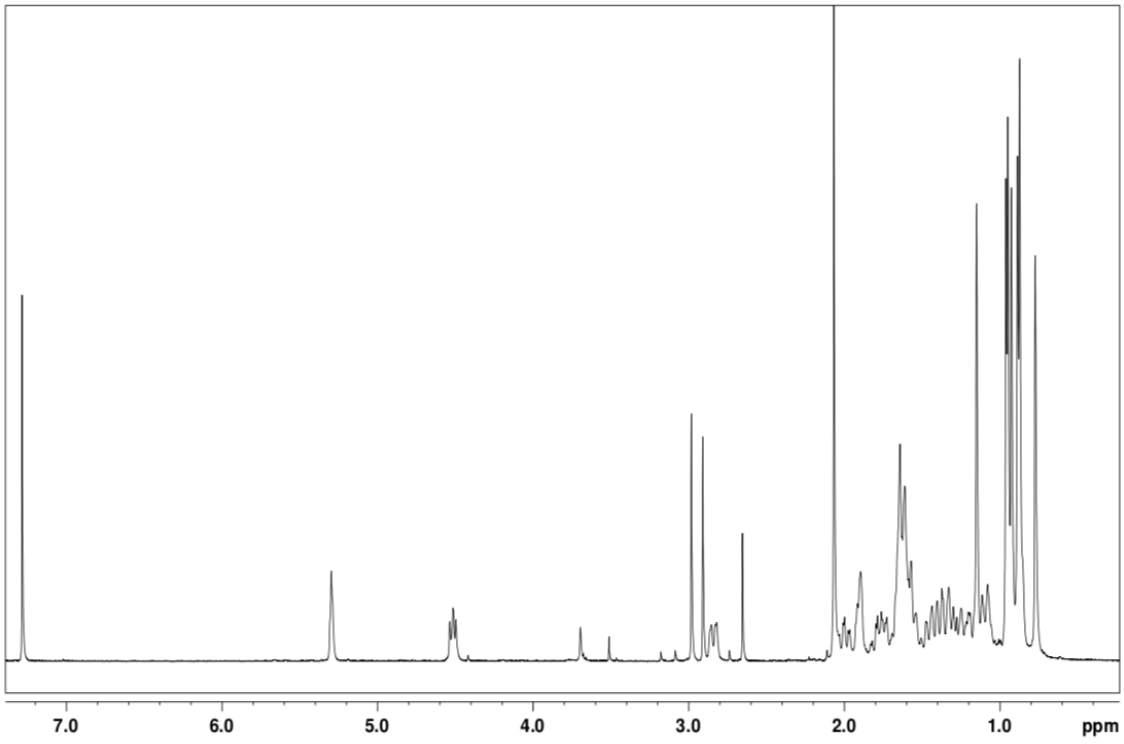

A7: ^{1}H-NMR spectrum of compound (**87**) in $CDCl_3$

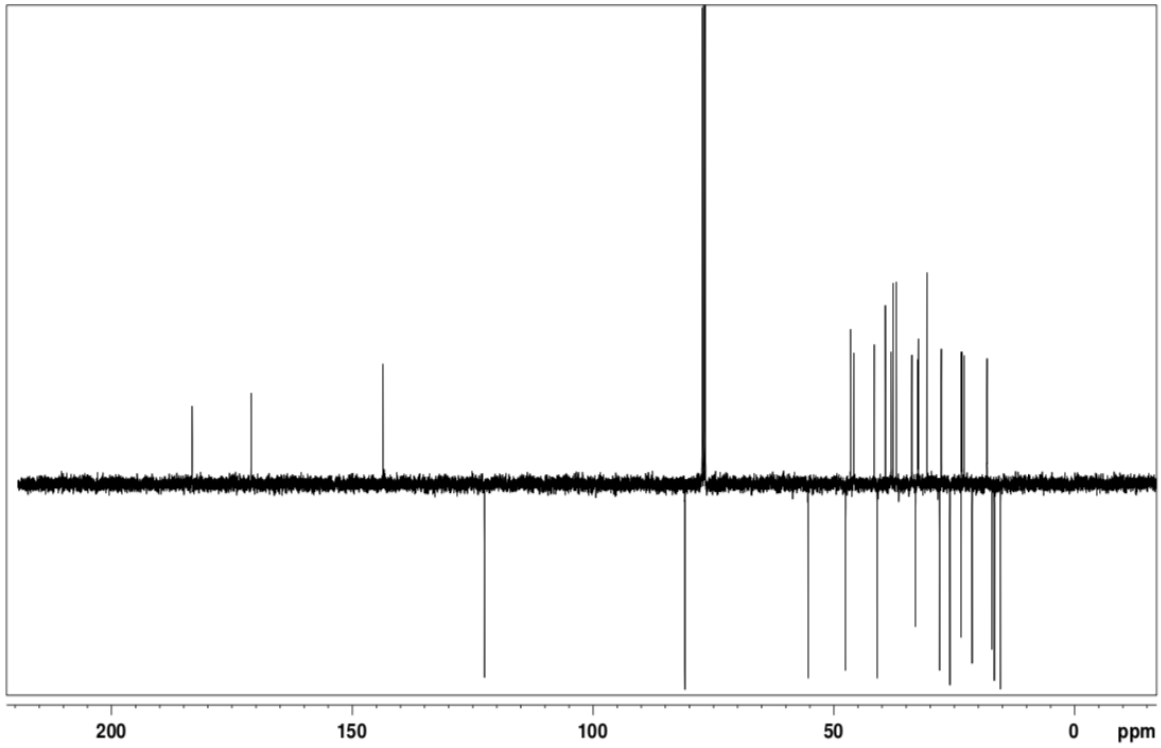

A8: ^{13}C-APT spectrum of compound (**87**) in $CDCl_3$

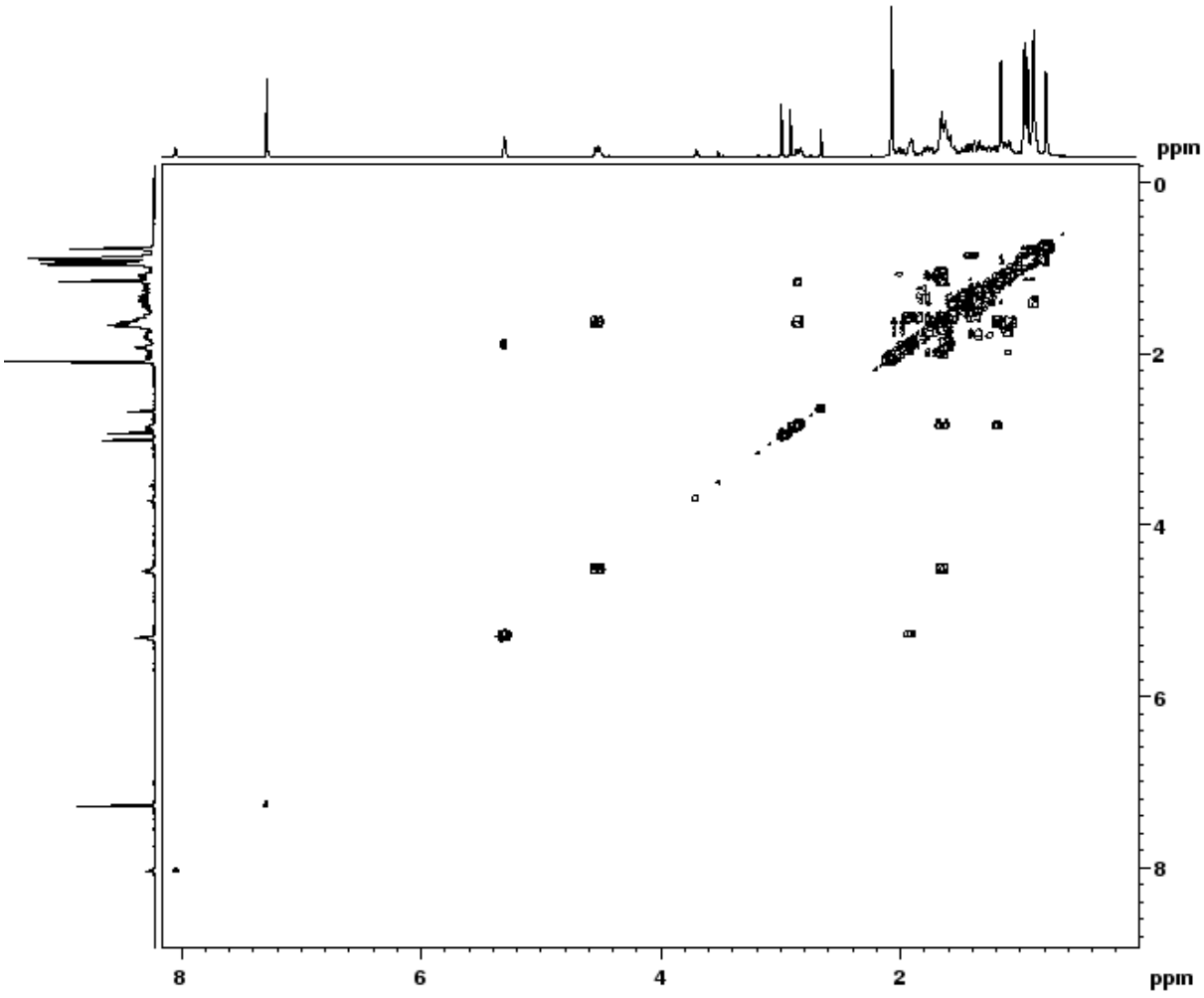

A9: COSY spectrum of compound (**87**) in $CDCl_3$

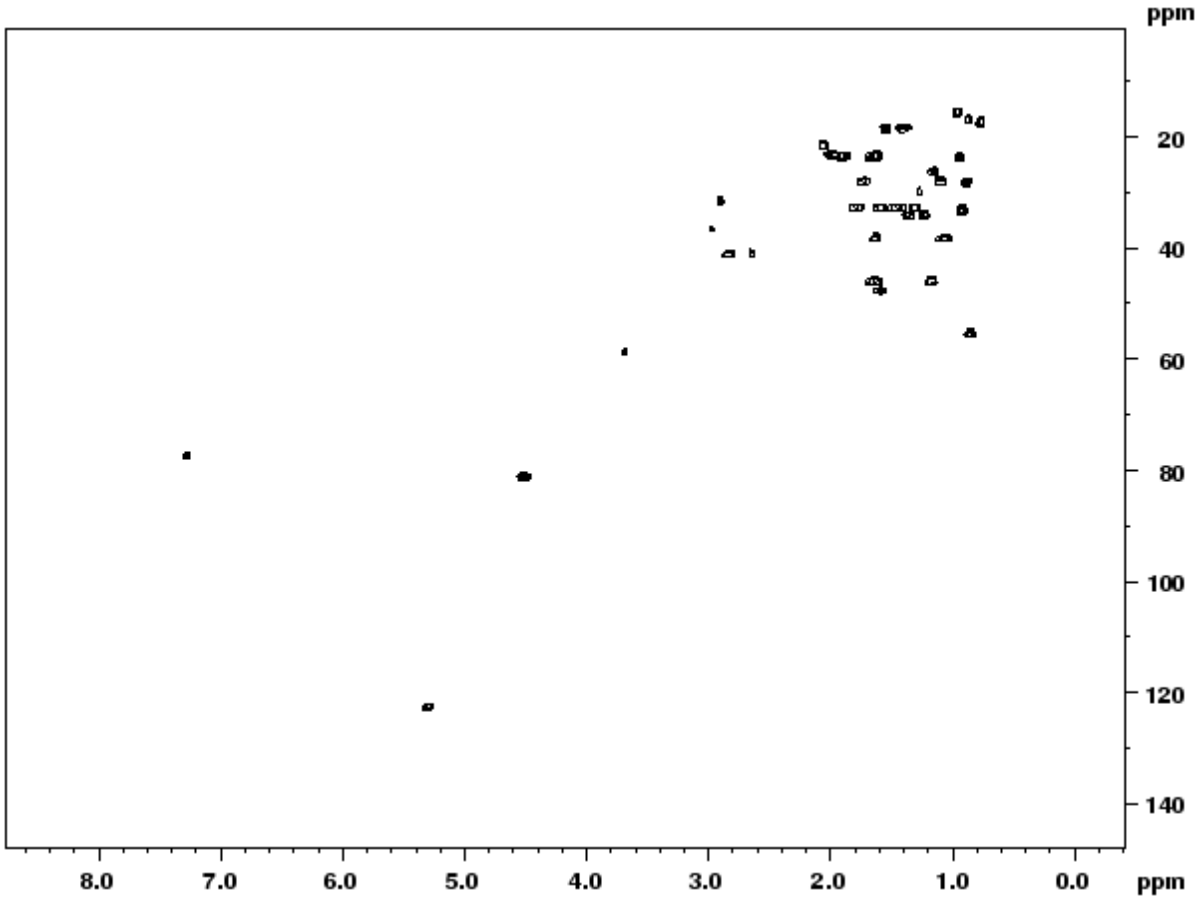

A10: HSQC spectrum of compound (**87**) in $CDCl_3$

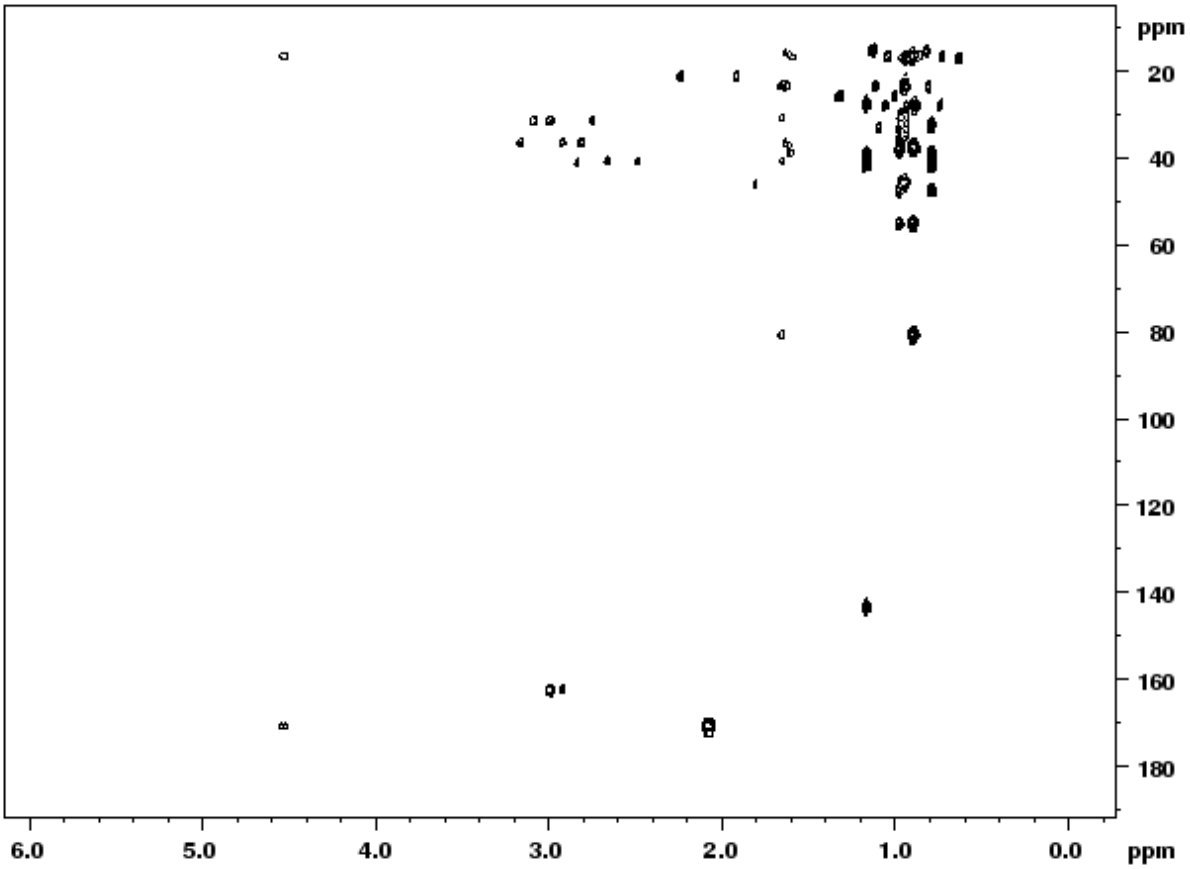

A11: HMBC spectrum of compound (**87**) in $CDCl_3$

12-(2'-*N*-methylaminobenzoyl)-4*β*,5,20-trideoxyphorbol-13-acetate (113)

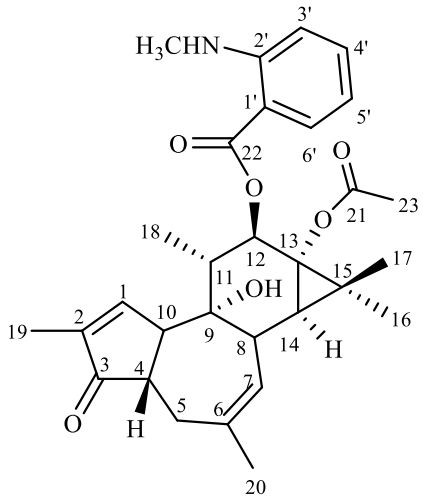

(**113**)

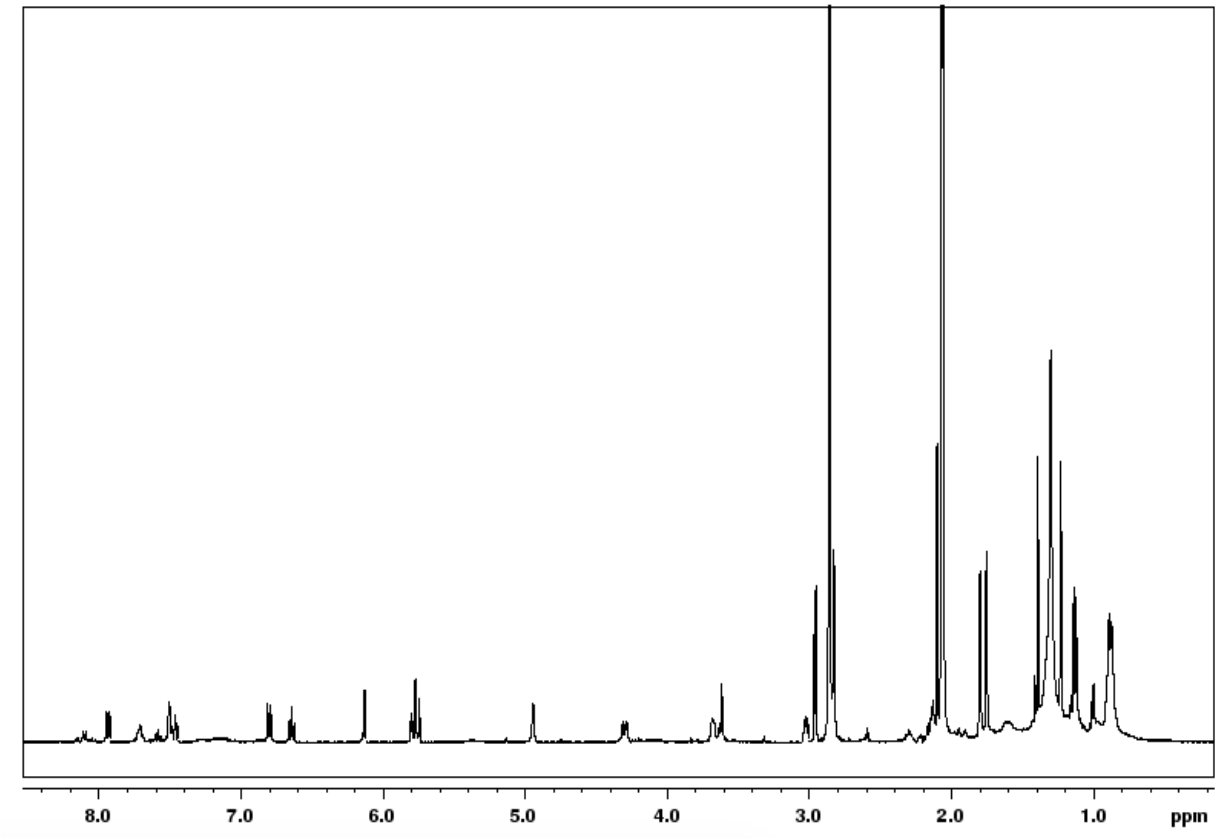

A12: ^{1}H-NMR spectrum of compound (**113**) in acetone-d_6.

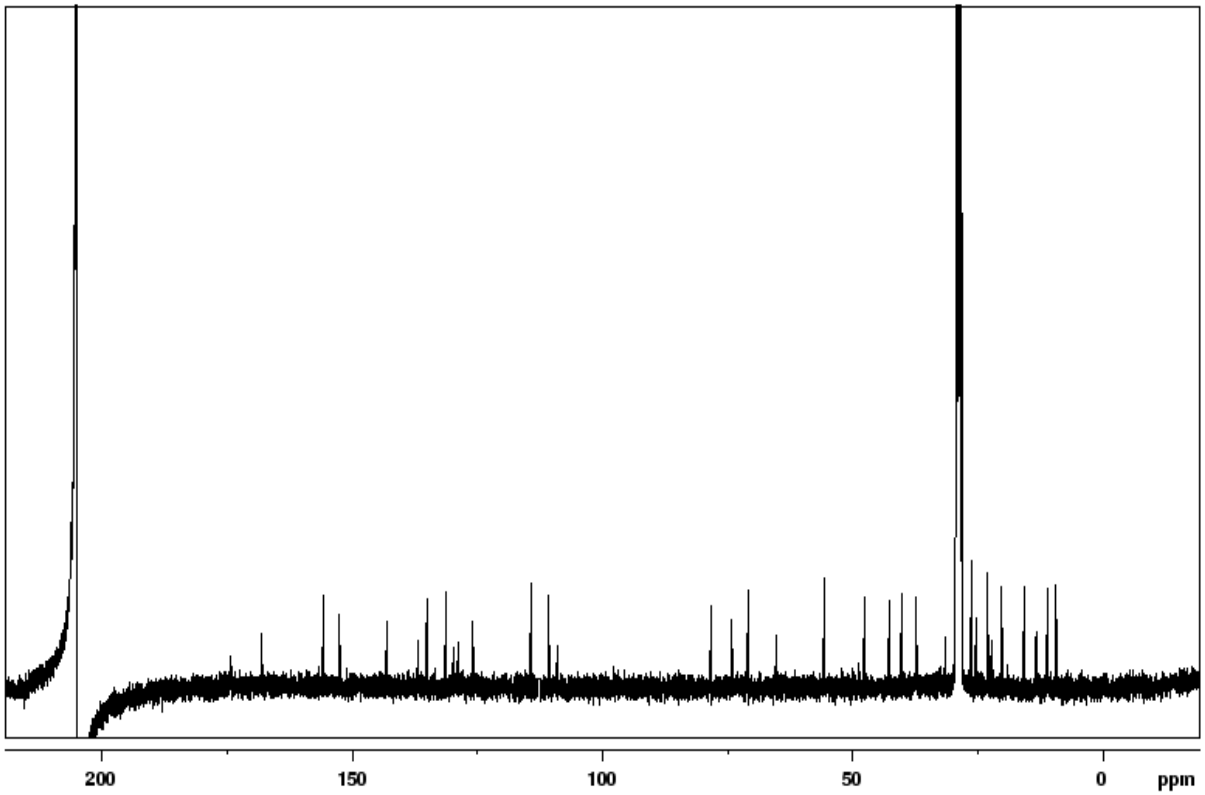

A13: ^{13}C-NMR spectrum of compound (**113**) in acetone-d_6.

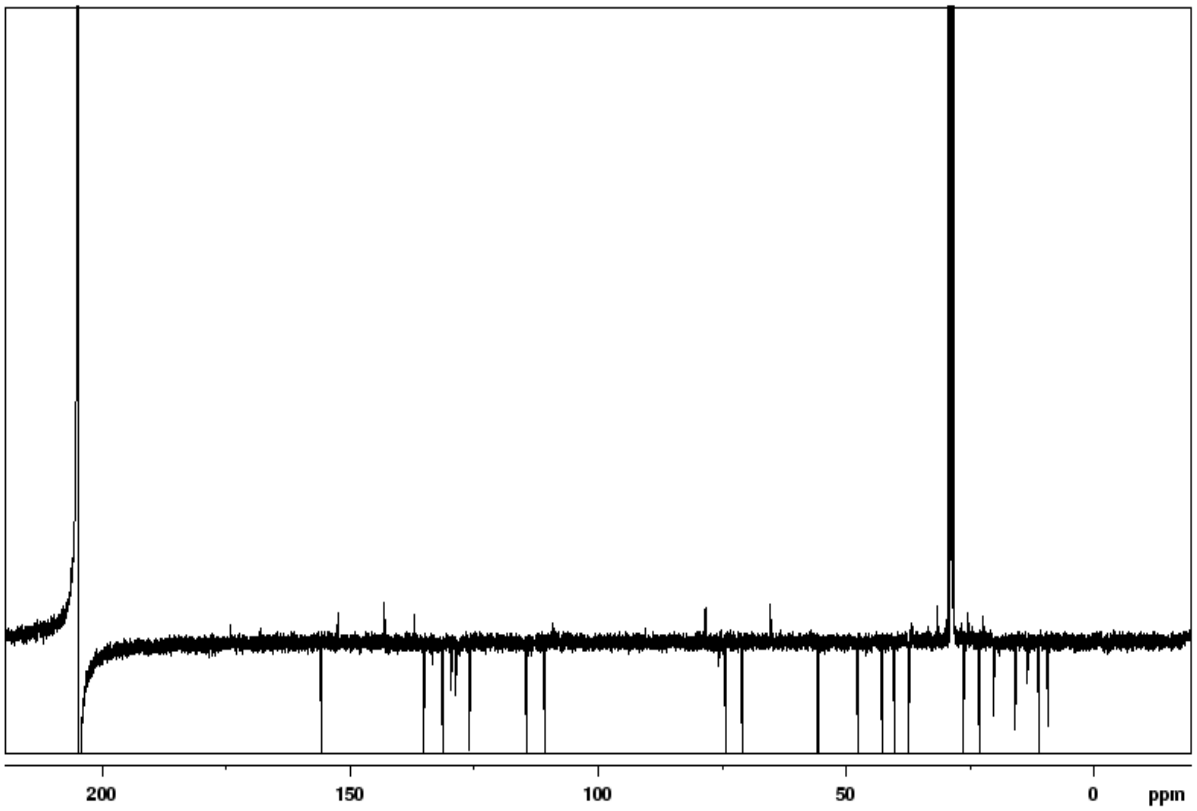

A14: ^{13}C-APT spectrum of compound (**113**) in acetone-d_6.

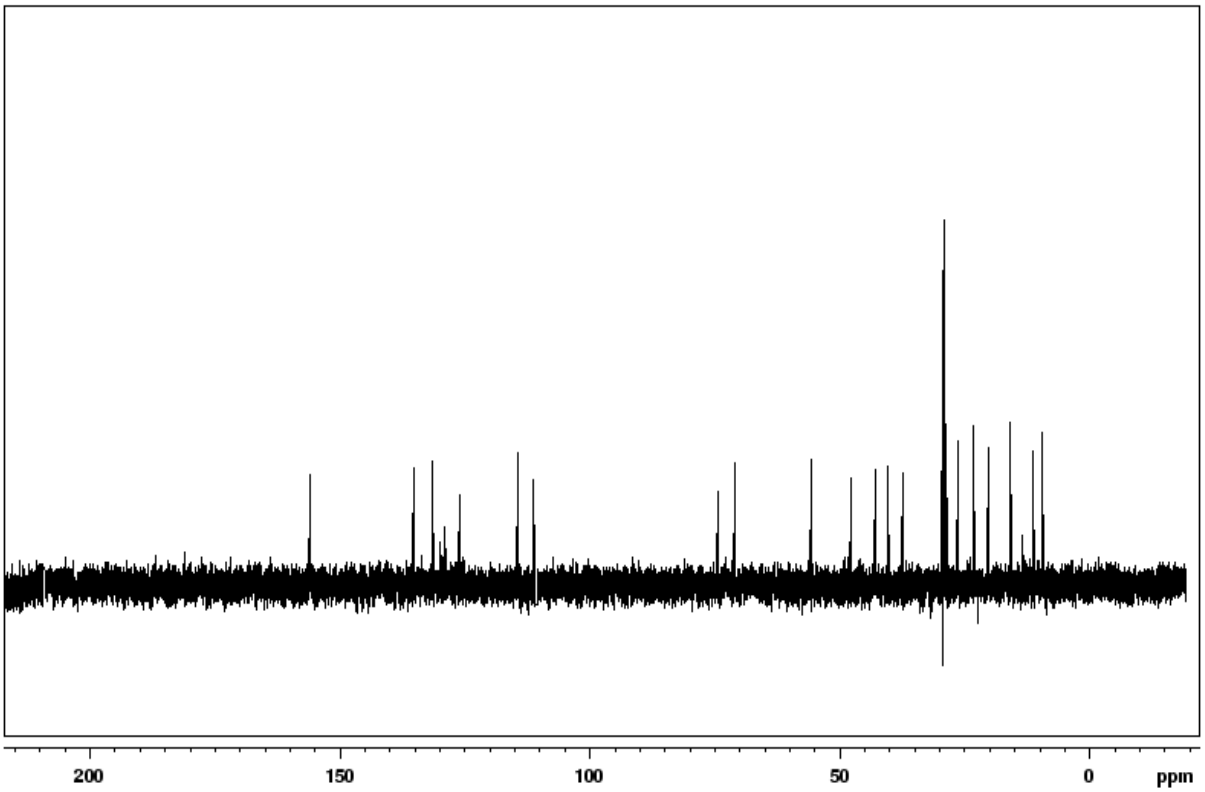

A15: DEPT-135 spectrum of compound (**113**) in acetone-d_6.

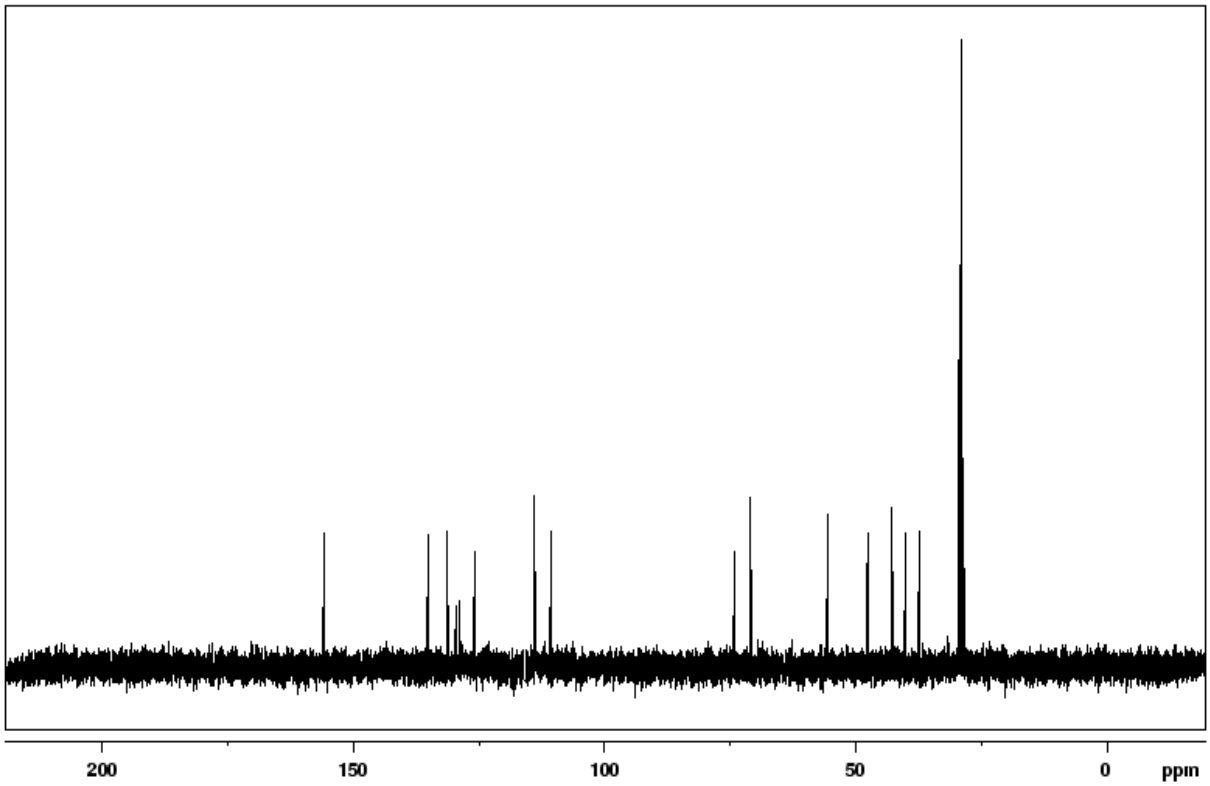

A16: DEPT-90 spectrum of compound (**113**) in acetone-d_6.

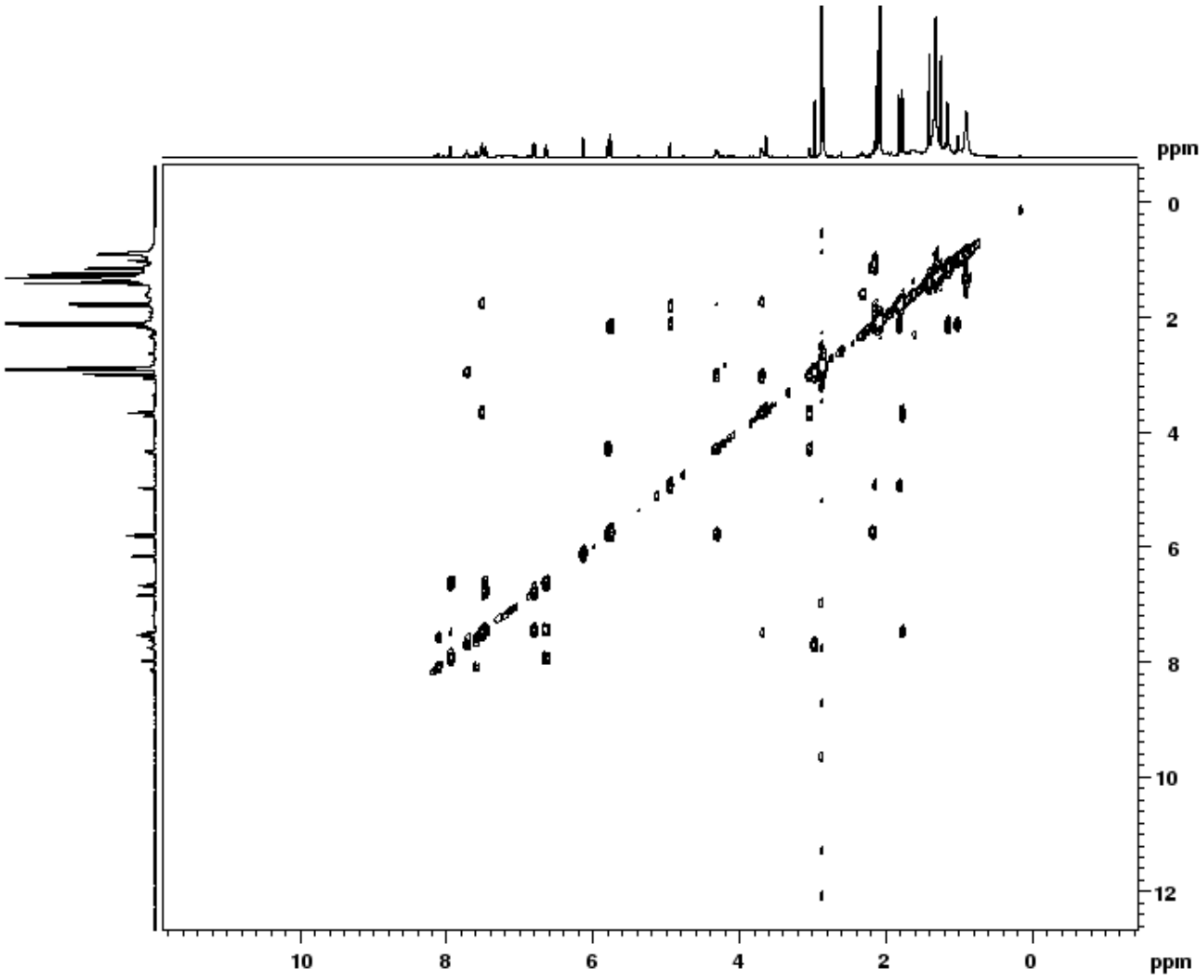

A17: COSY spectrum of compound (**113**) in acetone-d_6

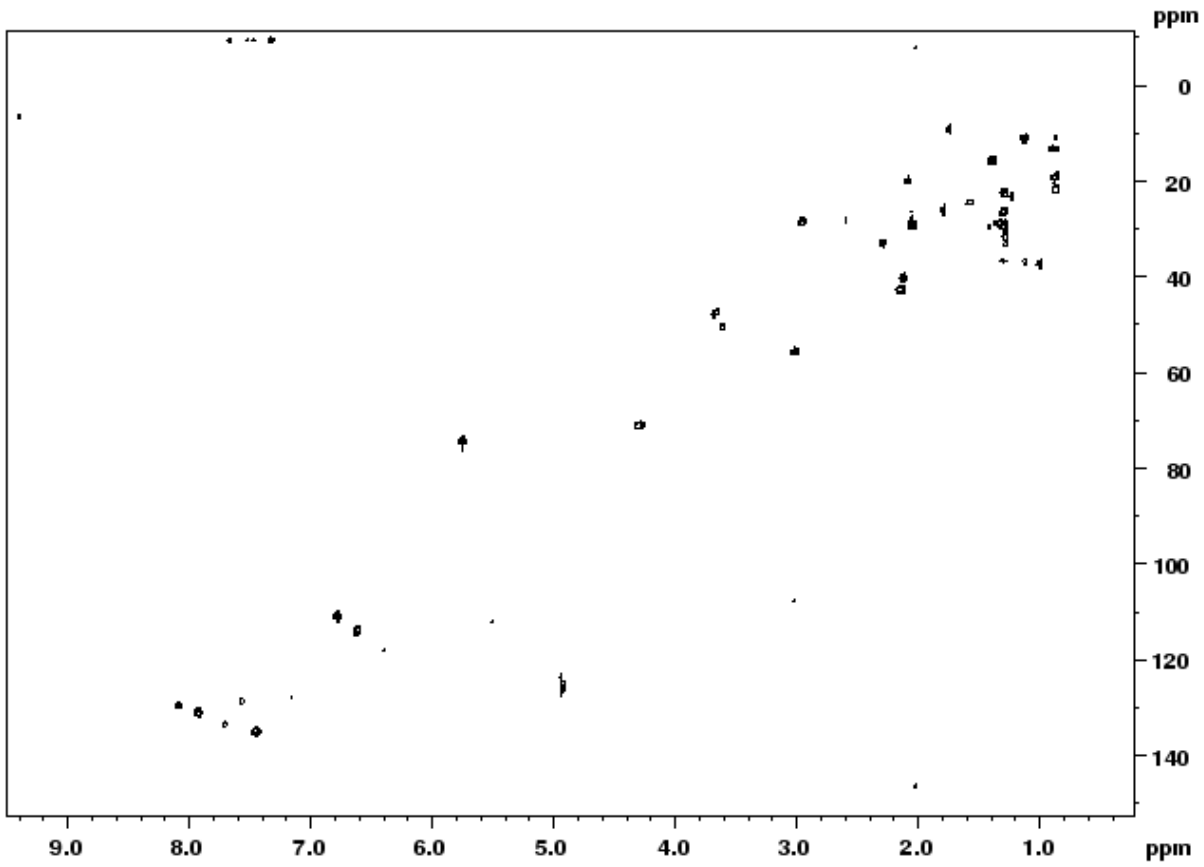

A18: HSQC spectrum of compound (**113**) in acetone-d_6.

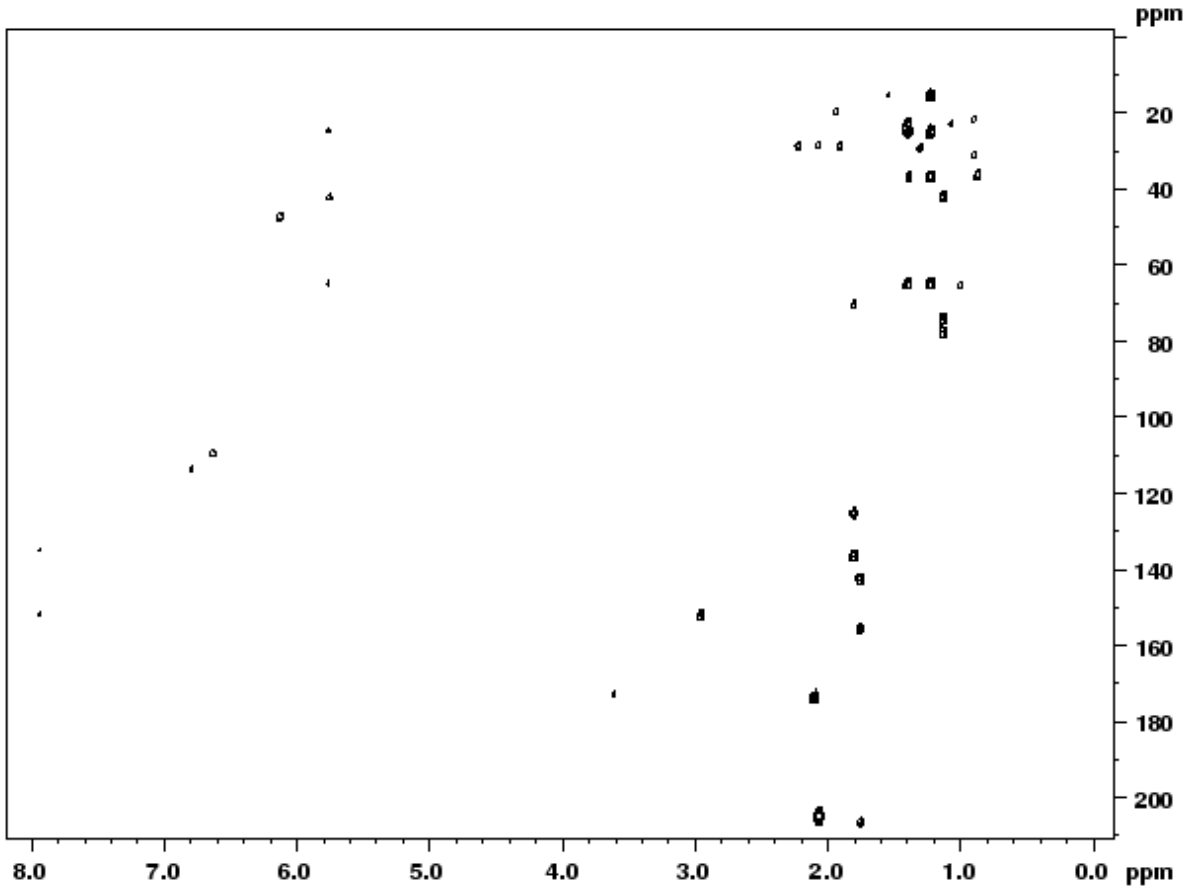

A19: HMBC spectrum of compound (**113**) in acetone-d_6.

Quercetin-3-*O*-α-rhamnopyranoside (114)

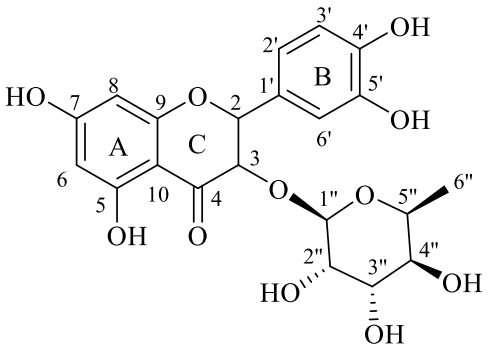

(**114**)

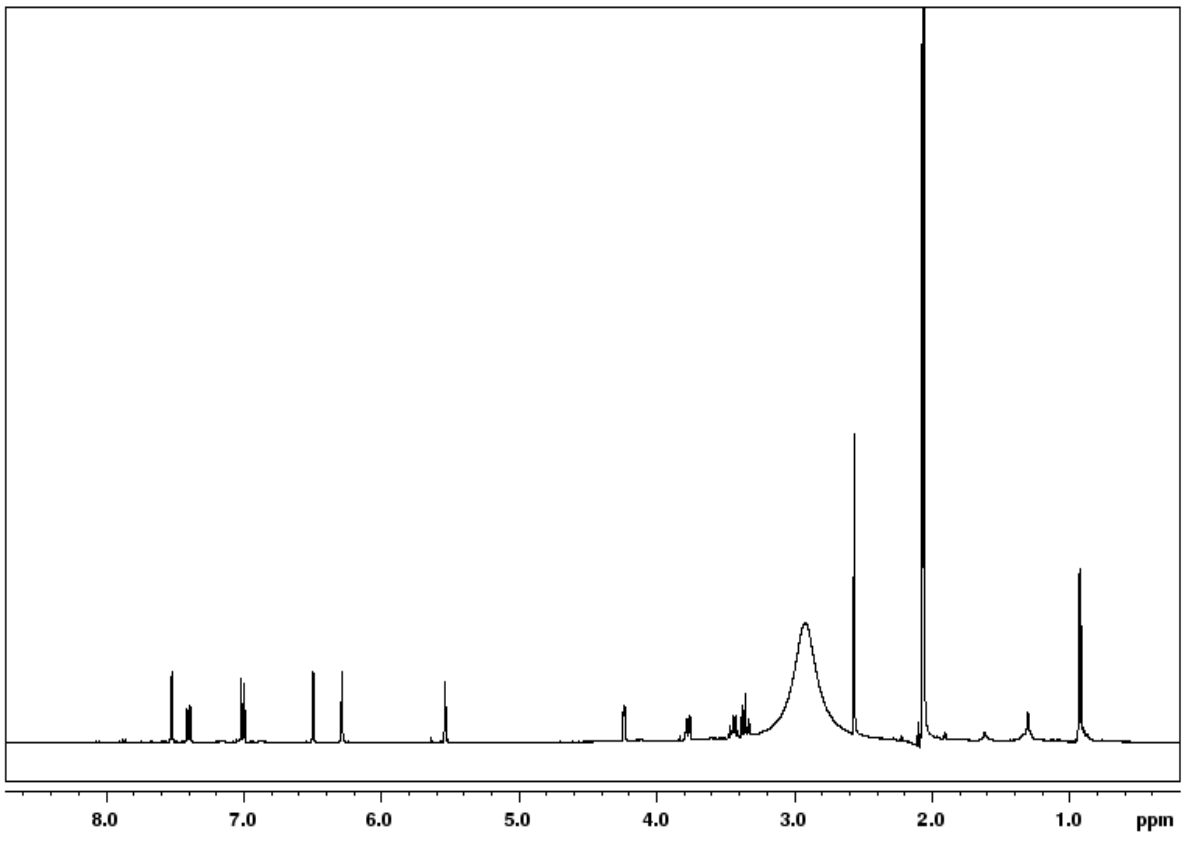

A20: ^{1}H spectrum of compound (**114**) in acetone-d_6.

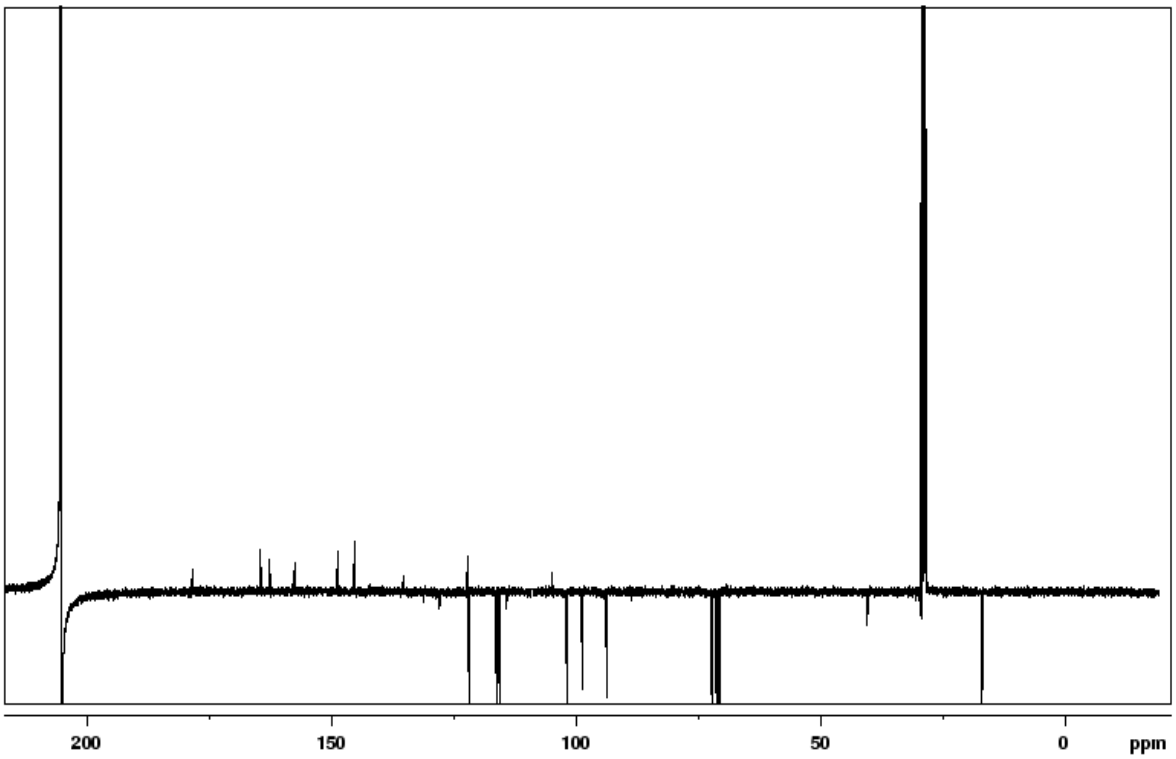

A21: ^{13}C-NMR spectrum of compound (**114**) in acetone-d_6.

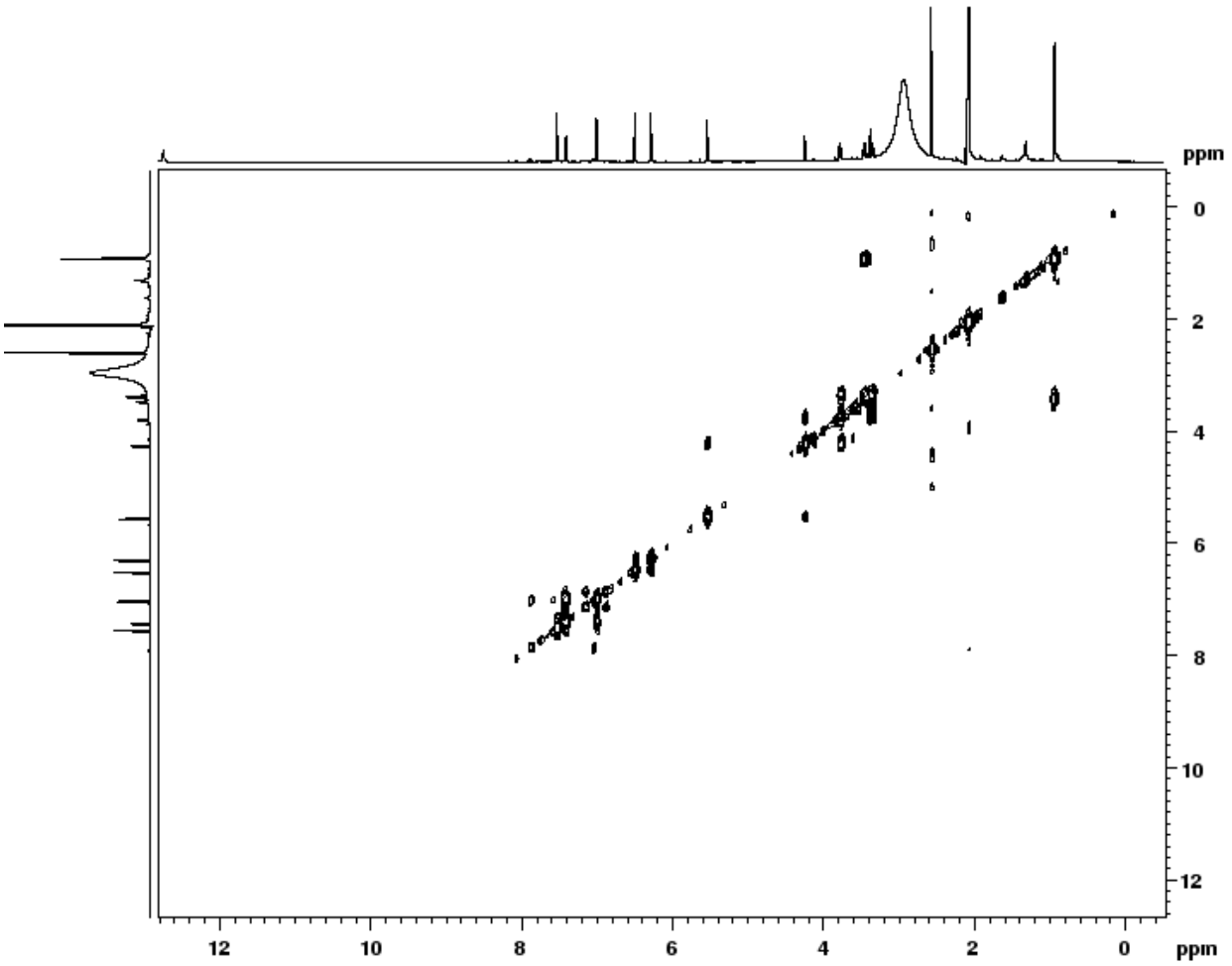

A22: COSY spectrum of compound (**114**) in acetone-d_6.

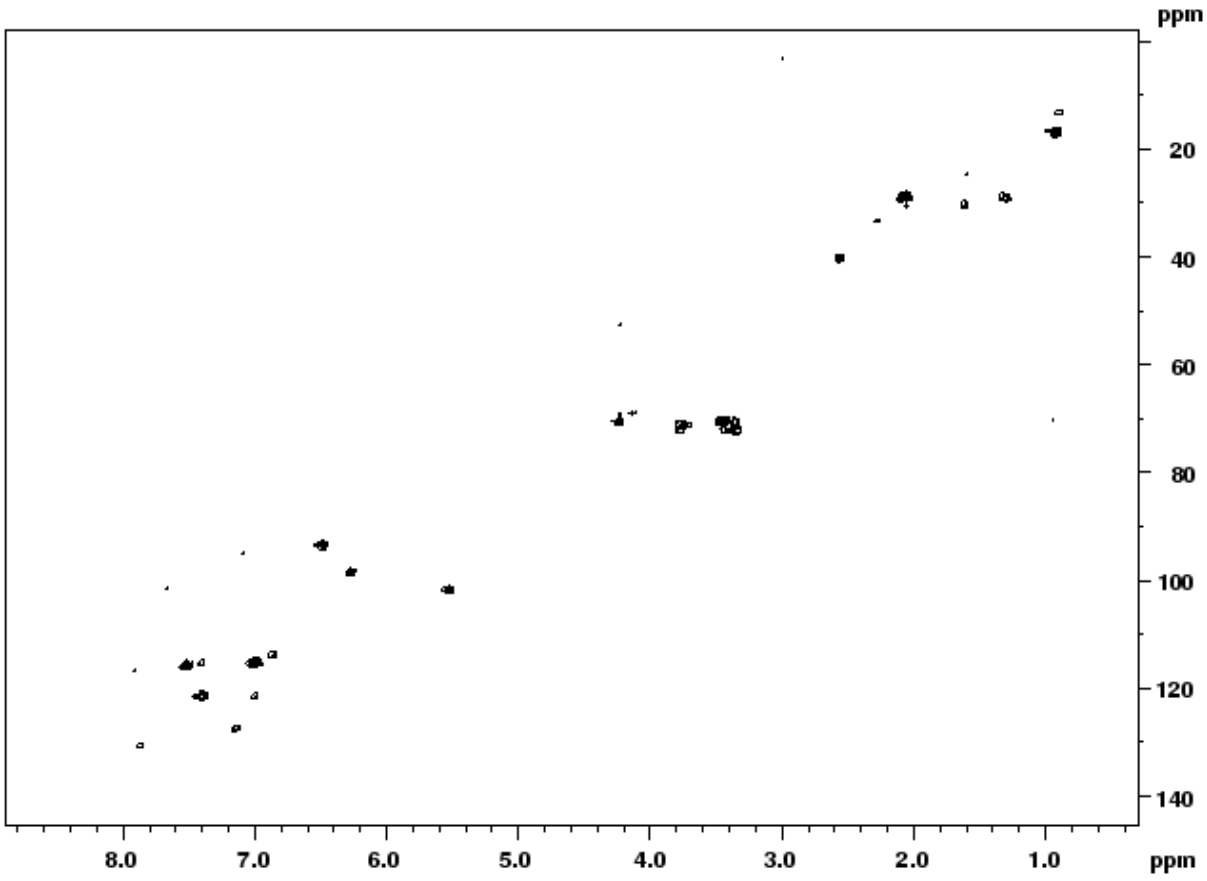

A23: HSQC spectrum of compound (**114**) in acetone-d_6.

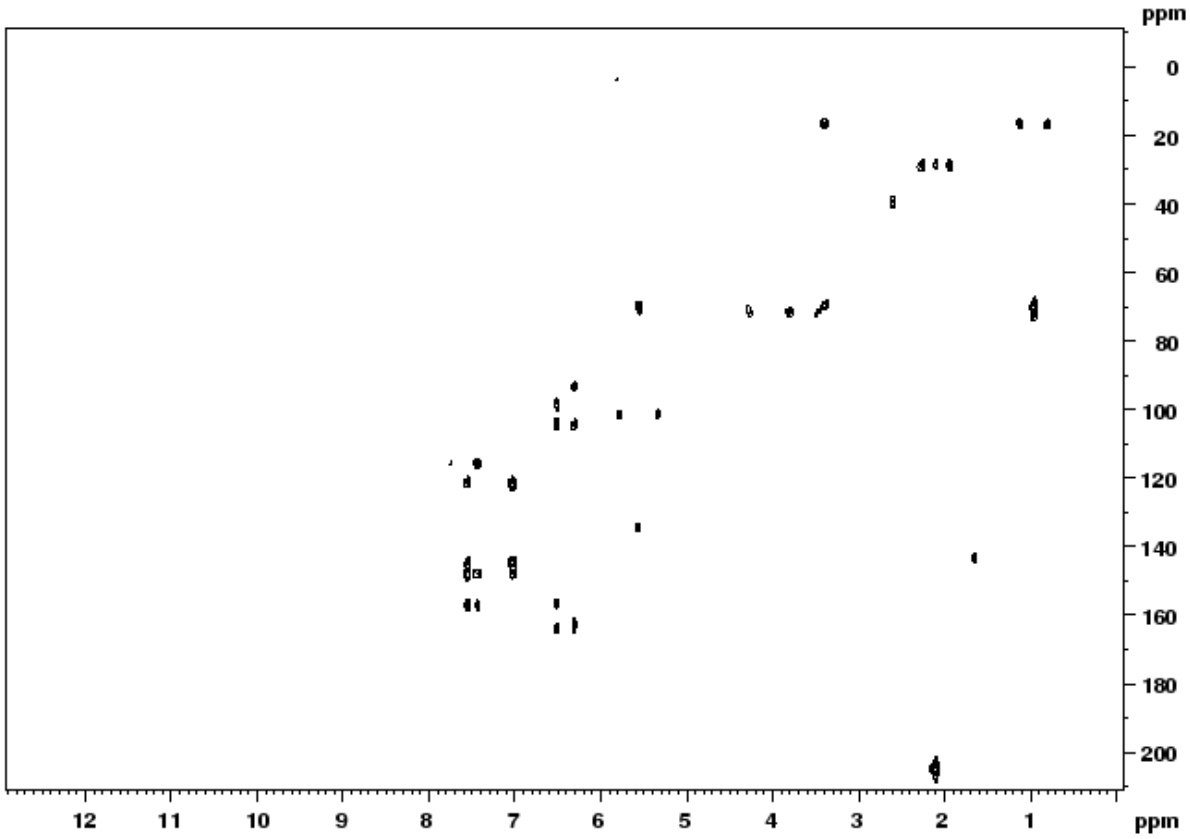

A24: HMBC spectrum of compound (**114**) in acetone-d_6.

Scopoletin (115)

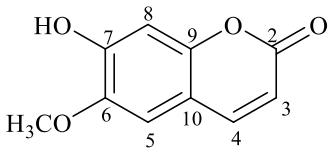

(**115**)

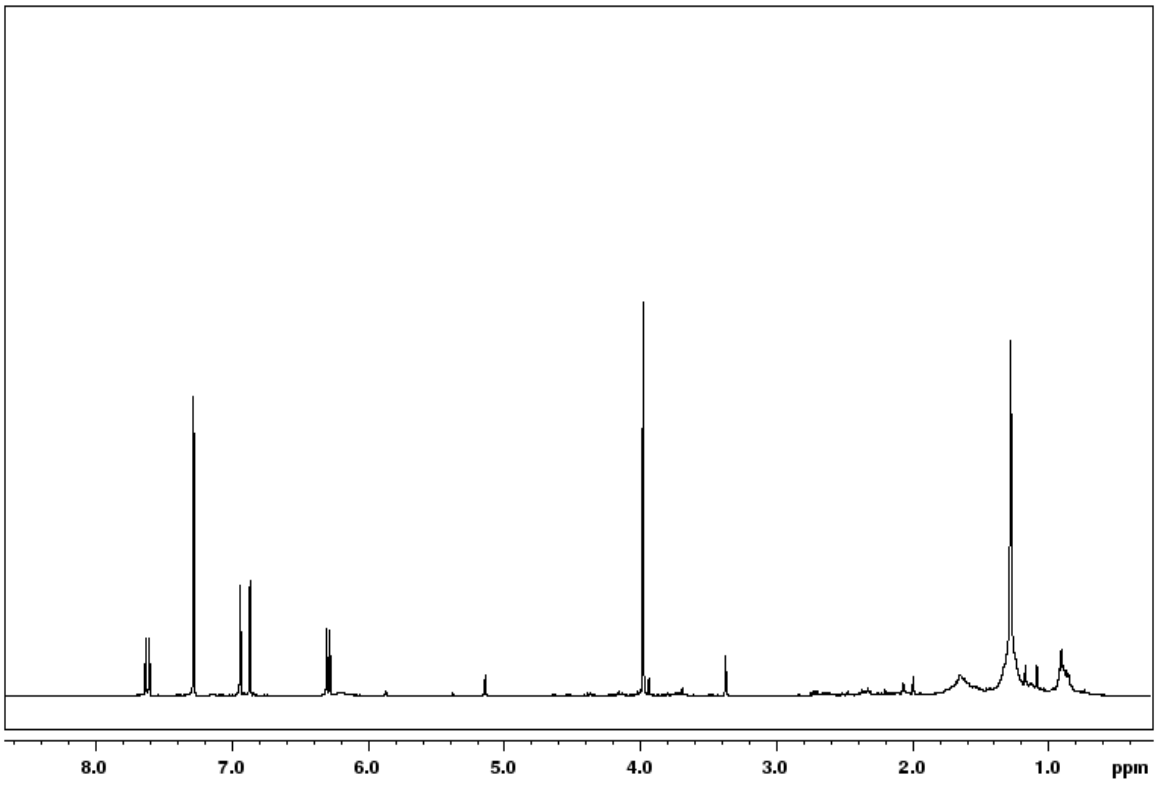

A25: ^{1}H spectrum of compound (**115**) in $CDCl_3$

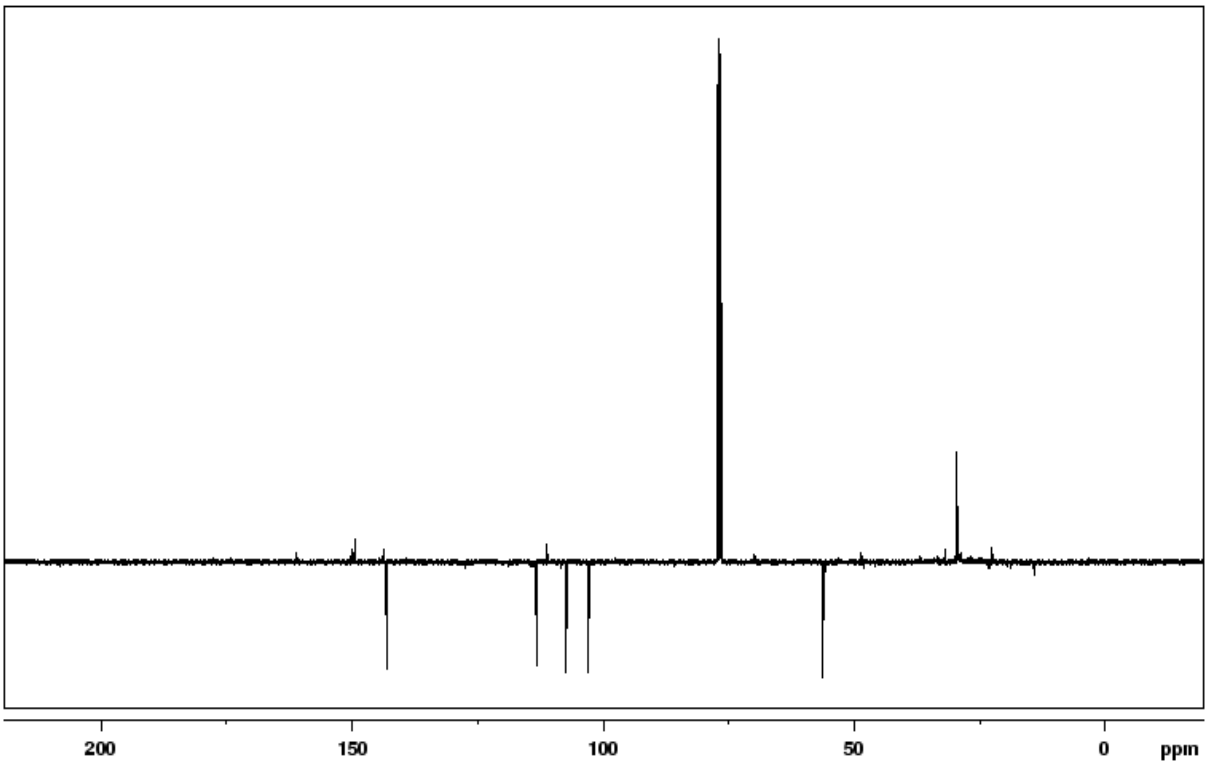

A26: ^{13}C-APT spectrum of compound (**115**) in $CDCl_3$

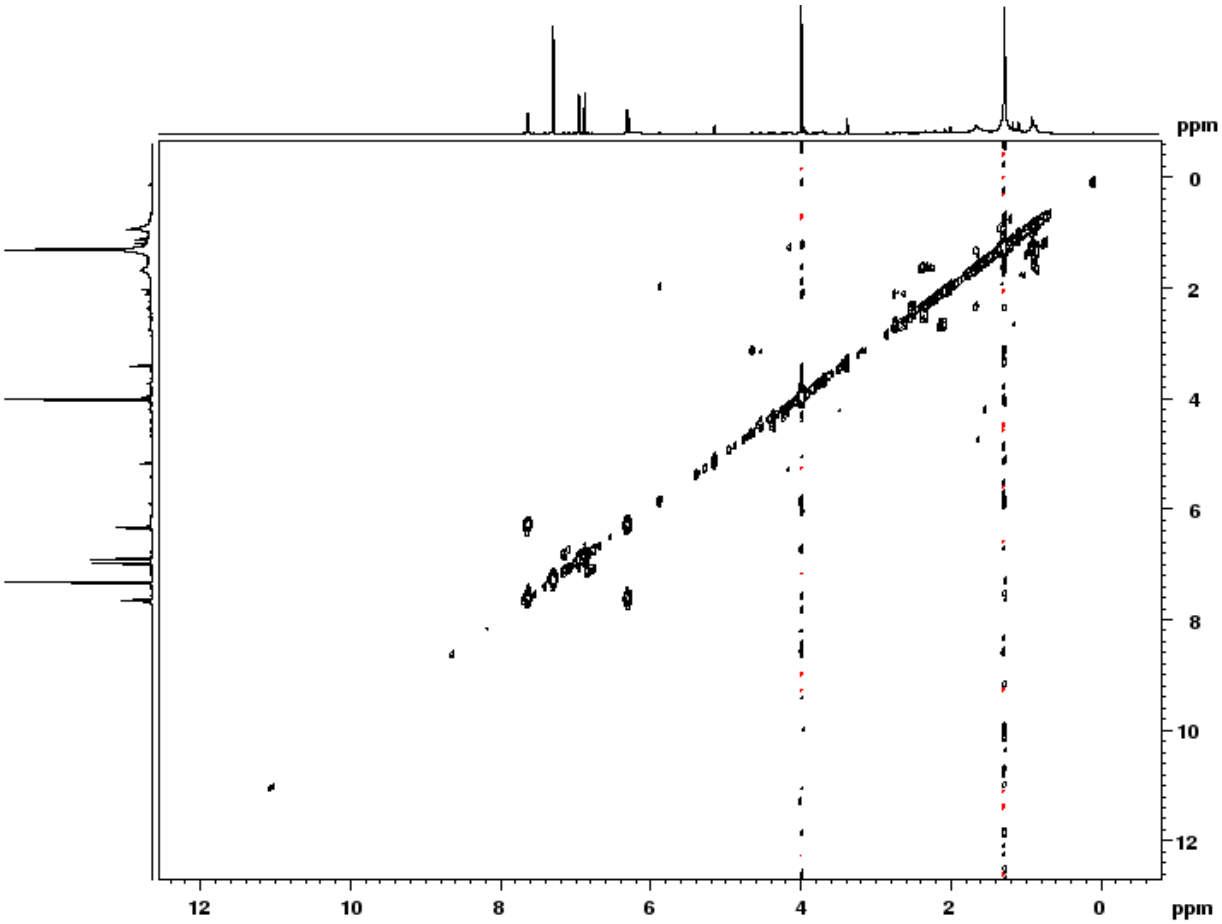

A27: COSY spectrum of compound (**115**) in $CDCl_3$

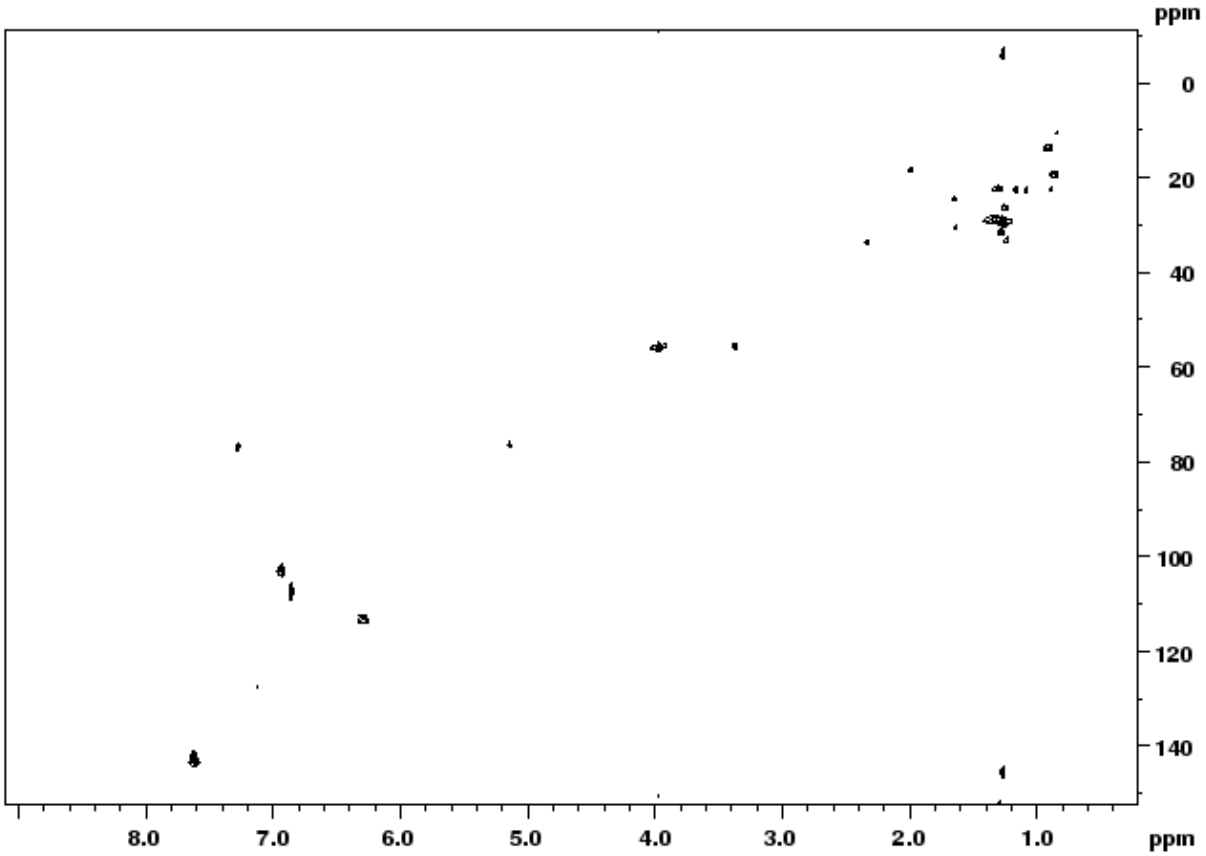

A28: HSQC spectrum of compound (**115**) in $CDCl_3$

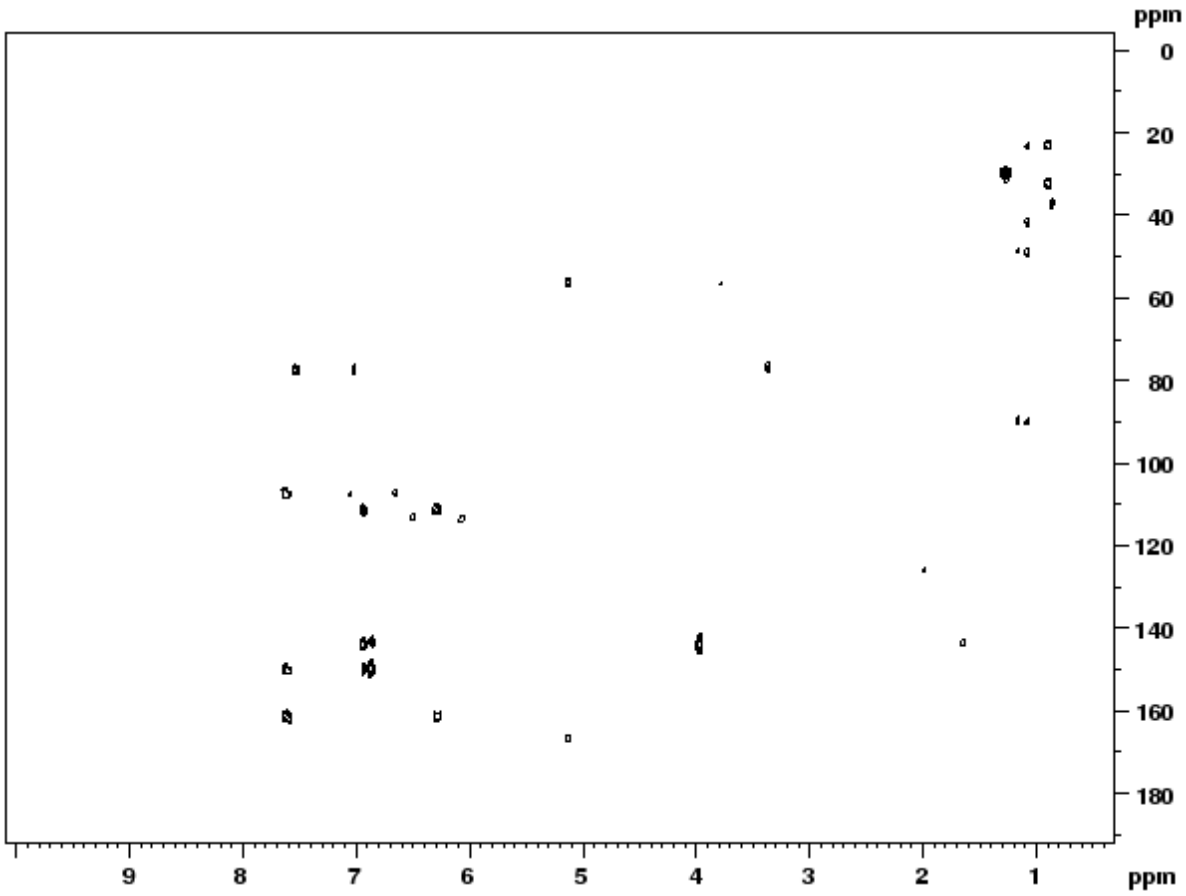

A29: HMBC spectrum of compound (**115**) in $CDCl_3$